UNIVERSITÀ DEGLI STUDI DI MILANO

PhD Course in

Biochemical Sciences

XXXIII cycle

Department of Pharmacological and Biomolecular Sciences

PhD Thesis

"*In silico* investigations of N-glycosylation role in modulating IgG1 conformational behavior and Fc effector functions"

SSD

BIO/10 - Biochimica

PhD candidate:

Simona SAPORITI

Matr. R11865

Supervisor: Prof. Ivano EBERINI

Coordinator: Prof. Alessandro PRINETTI

A.Y. 2019/2020

Summary

Chapter 1

Introduction *4*

1.1 Monoclonal antibodies: overview 5

1.2 Immunoglobulin G subclass 7

1.3 Fc effector functions 10

1.4 Fc receptors classification and functions 12

1.5 N-glycosylation 16

1.6 The role of fucosylation in regulating Fc effector functions 18

1.7 Structural and computational studies on the N-glycosylation role: state of the art 22

1.8 Quality by design 23

Chapter 2

Aim of the study *27*

Chapter 3

Materials and methods *30*

3.1 Homology modeling 31

3.2 Molecular dynamics simulations 32

3.3 Molecular dynamics analysis 34

Chapter 4

Results and Discussion: part I *35*

4.1 Force field validation for glycans description 37

4.2 Homology modeling and MD simulations of aglycosylated, G0 and G0F adalimumab 39

4.3 Principal component analysis (PCA) 48

4.4 Sugars analysis 51

4.5 Discussion 55

Chapter 5

Results and Discussion: part II *58*

5.1 Homology modeling and MD simulations of G0 and G0F adalimumab in complex with FcγRIIIa 60

5.2 Structural analysis of complexes 64

5.3 Hydrogen bonds analysis 70

5.4 MD simulations of Fc:: FcγRIIIa complexes 79

5.5 Mapping of Fc::FcγRIIIa complexes interaction network 83

5.6 ΔG binding free energy calculation 87

5.7 Discussion 90

Chapter 6

Conclusions *93*

Bibliography *96*

Chapter 1

Introduction

1.1 Monoclonal antibodies: overview

Since 2017, monoclonal antibodies (mAbs) have been taking an outstanding position in the global biopharmaceutical market with a value of $101 billion and an estimated growth rate of 8.5% in the forecast period 2019-2025[1]. The first therapeutic mAb, moronumab-CD3 (Orthoclone OKT3), has been approved by the United States Food and Drug Administration (US FDA) in 1986 and since that, the pharmaceutical development of mAbs for therapeutic purposes has been increased, leading to 79 approved antibodies currently on the market[2] and at least 550 molecules under clinical investigation[3]. The main advantage of using mAbs in therapy is due to their high target selectivity and specificity that may result in a lower risk of side effects. They can recognize specific epitopes on the target antigen by the portions called "complementarity determining regions (CDRs)", restraining the therapeutic response to specific tissues. Of note, even if not of interest in this thesis, it should be mentioned that there are second-generation products derived from mAbs, such as bispecific antibodies, antibody-drug conjugates (ADC), antibody fusion proteins, single chain fragment variable (scFv) and nanobodies (Nb) that are gradually taking a relevant place in the biopharmaceutical market.

Among the different classifications that could be used to describe the monoclonal antibodies, the most common one is connected to the origin organism. In fact, based on the primary sequence composition that depends on the genome expression system, mAbs can be classified in (Figure 1)[4]:

- murine, which are completely mice-derived;
- chimeric, which are made up of about 65% human genetic component and 35% mouse component;
- humanized, that are 95% near to the human origin;
- fully human.

The challenge to develop antibody species closer and closer to the human one has become a need over time, because of the urgency to reduce the immunogenic response in favor of the therapeutic action. In fact, the administration of non-human or not fully human antibodies often led to severe allergic reactions and anaphylactic shock, driven by antibodies recognizing epitopes located in the mouse component of the mAb (anti-mouse antibodies) and produced by the patients[5–7].

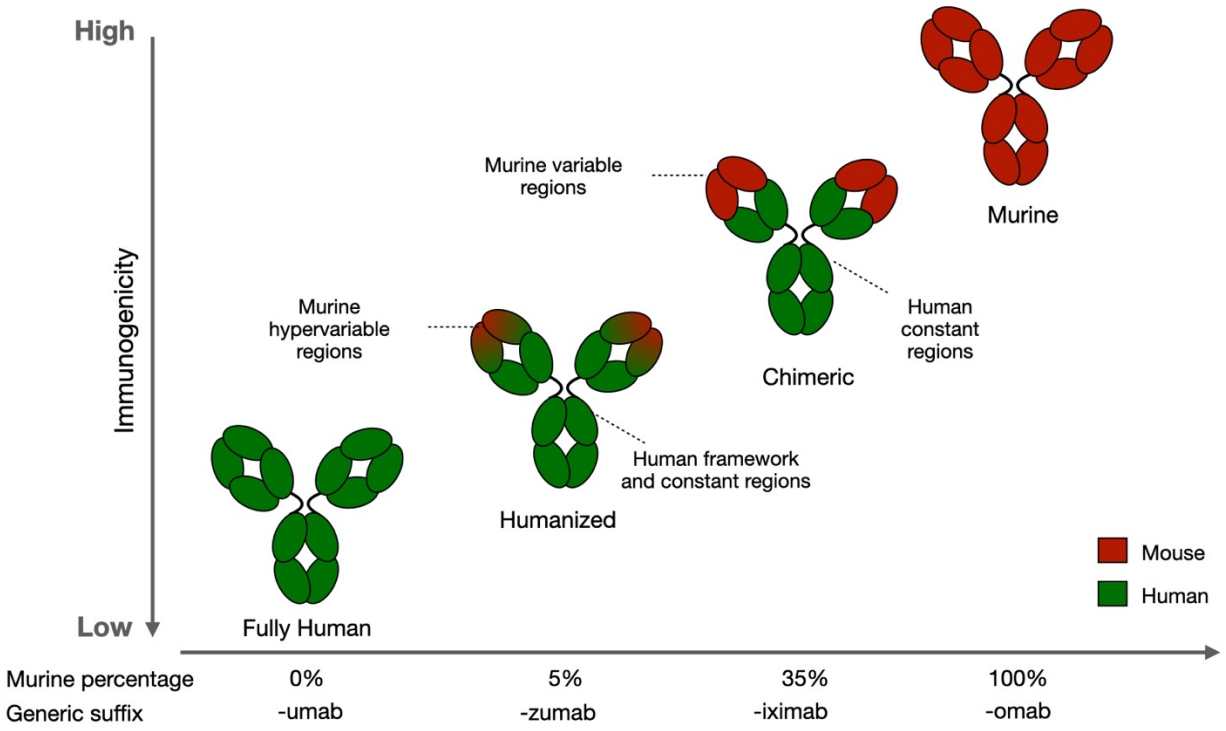

Figure 1: Monoclonal antibodies classification by origin organisms and immunogenicity potential. The mAbs nomenclature and classification are reported according to the origin organism and the relative murine genome percentage (x axis) vs the immunogenicity potential (y axis). Immunogenicity is very low for fully human antibodies and progressively increases for humanized, chimeric and murine mAbs. Figure adapted from Surjit and colleagues[8].

For what concerns their production, antibodies can be generated directly from immunized patients or animals and specifically by the isolation of antibody-producing B cells from these organisms. The antibody-encoding genes of isolated cells are then transfected into suitable producer cell lines to allow the large-scale production[9–11]. In this frame, since their high similarity with human post-translational modifications, mammalian cell lines are the primary choice for recombinant protein and mAb production and, among the most commonly used, Chinese hamster ovary (CHO) cells occupy the most relevant place, including over 60% of the total marketed products. The rest of commercial recombinant proteins is produced by baby hamster kidney cells (BHK), NS0 myeloma cells and Sp2/0 mouse myeloma line and human embryonic kidney 293 (HEK293)[12–16].

Based on structural and functional differences, antibodies or immunoglobulins (Ig) are classified in five subcategories: IgA, IgD, IgG, IgM and IgE. Among these, because they are the preferred choice in pharmaceutical development and also because they are of main interest in this thesis, next sections will be dedicated to a further description of IgG subtype.

1.2 Immunoglobulin G subclass

IgGs represent 60% of human serum antibodies and 10-20% of plasma proteins. As well as other Ig subclasses, IgGs are composed of a proteinaceous part, that accounts for 82-96% of the molecule, and for a minor fraction of glycans (4-18%)[17]. According to their relative serum abundance, IgGs can be further classified, from the most expressed to the least, in four subtypes: IgG1, IgG2, IgG3, IgG4[18]. Despite the huge sequence similarity (> 90%), each IgG subtype shows a unique profile in terms of antigen binding, secondary immune responses and activation of effector functions. On the other hand, concerning half-life and placental transport, that are regulated by the neonatal Fc receptor (FcRn), highly comparable profiles have been observed for all IgGs, excluding IgG3 that shows slight differences[17] (see Table 1).

In particular: IgG1 are mainly involved in responses to soluble protein antigens and membrane proteins[19]; IgG2-driven responses are restricted to bacterial capsular polysaccharide antigens[19–22]; IgG3 are particularly efficient in effector functions activation[23] and IgG4 trigger allergic responses[24]. However, many studies showed that each one of these subtypes, even if it results as the main responsible for the mentioned activities, does not drive stand-alone functions, but acts in a cooperative way with other immunoglobulins. For example, it has been demonstrated that: IgG1 response is accompanied by low levels of IgG3 and IgG4[19]; the IgG2 activation is associated also with IgG1 and IgG3 expression[25]; it is rare to have an immune response entirely dominated by IgG3, but it is more common a co-activation of IgG1[19,26–28] and finally, it is well known that allergic responses are mediated not only by IgG4, but also by IgG1 and IgE[29].

Table 1: Key features of IgG isotypes. The main physiological characteristics of IgG subtypes are reported here including both general molecular properties and Fc effector functions. The table was adapted from works by Vidarsson and Salfed and colleagues[17,30].

	IgG1	IgG2	IgG3	IgG4
General properties				
Molecular mass	146	146	170	146
Functional form in vivo	Monomeric bivalent	Dimeric tetravalent	Monomeric bivalent	Half-Ig monovalent
Biological role in host response	Protein antigens	Carbohydrate antigens	Protein antigens	Response to chronic stimulation, anti-inflammatory
Percentage of all IgG in humans	60%	25%	10%	5%
Allotypes	4	1	13	0
Half-life (days)	21	21	7/~21	21
Hinge length	15	12	62	12
Inter-heavy chain disulfide bonds in hinge region	2	4	11	2
Fc effector functions				
C1q binding	++	+	+++	-
FcγRI	+++	-	++++	++
$Fc\gamma RIIa_{H131}$	+++	++	++++	++
$Fc\gamma RIIa_{R131}$	+++	+	++++	++
FcγRIIb/c	+	-	++	+
FcγRIIIaF158	++	-	++++	-
FcγRIIIaV158	+++	+	++++	++
FcγRIIIb	+++	-	++++	-
FcRn	+++	+++	++/+++	+++

From a structural point of view, as well as other isotypes, IgG are composed of four polypeptidic chains: two identical γ heavy chains (HC) with a molecular weight of about 50 kDa, and two identical λ or κ light chains (LC) of about 25 kDa, with a total molecular mass of approximately 150 kDa. Each chain is organized in different domains:

- LC is composed of one variable (VL) and one constant (CL) domain
- HC presents one variable (VC) and three constant domains (CH1, CH2 and CH3)

The secondary structure of all these domains is mainly characterized by β-sheets linked by loops and stabilized by intrachain disulfide bridges. Looking at the tertiary structure, it may differ in some features among IgG subtypes[17]. Specifically, in IgG1 subtype, light and heavy chains are linked by a disulfide bridge between two conserved cysteines (Cys215 (LC) and Cys220 (HC), according to standard EU numbering[31]). Other four conserved cysteines (Cys226 and Cys229), two per HC, form two disulfide bonds with the respective counterpart in the other chain, allowing the formation of a Y-shaped molecule. These cysteines are located in a very flexible portion, called "hinge", that connects CH1 and CH2 domains.

The main structural differences with other IgG subtypes are summarized in figure 2 and table 1, highlighting that they essentially differ for the number and the position of interchain disulfide bonds and for the length of hinge region.

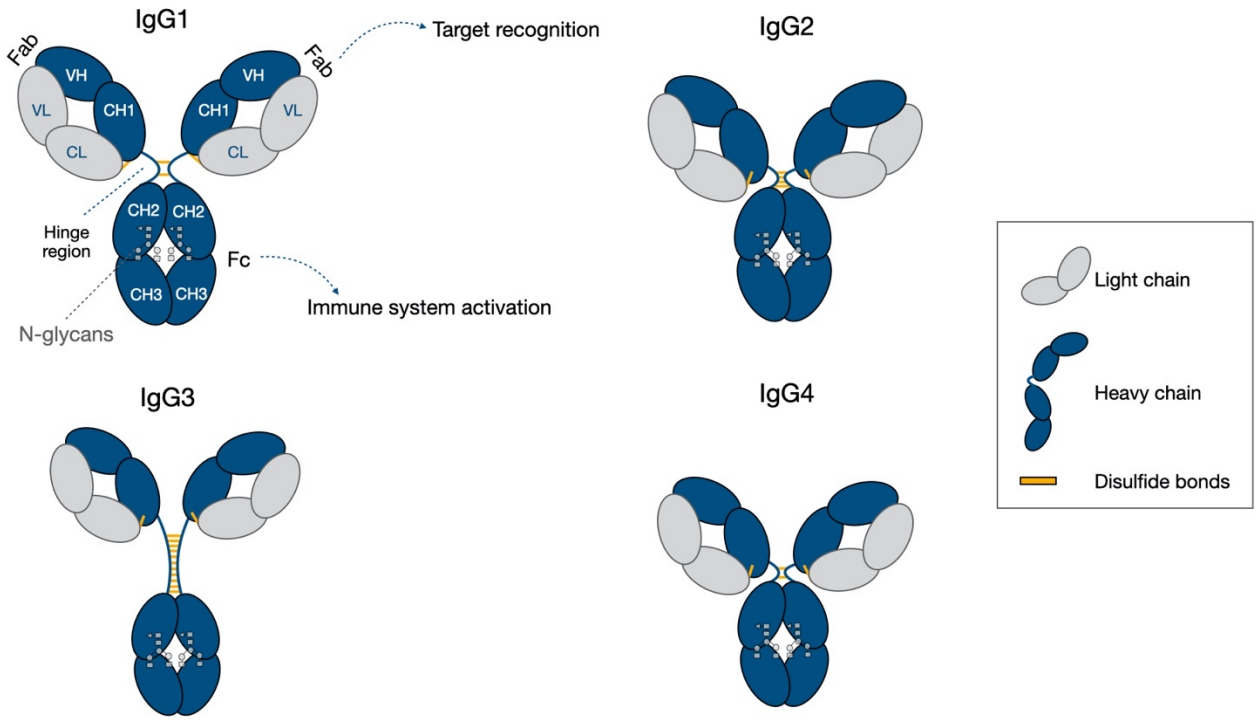

Figure 2: The schematic structural organization of four IgG subtypes. Light chains are represented in grey, heavy chains in blue, disulfide bonds as yellow sticks and N-glycans according to the symbol nomenclature for glycans (SNFG) system[32]. The major differences among subtypes are related to the length of hinge region and to the disulfide bridges assembly.

From a functional perspective, three domains can be distinguished in antibodies: two fragment antigen binding (Fab) domains, formed by the association of the light chain to VH and CH1 domains,

and one fragment crystallizable (Fc) formed by the lower hinge region and CH2-CH3 domains (Figure 2).

In Fab portions, variable domains contain "complementarity determining regions (CDRs)" that are responsible for antigen recognition and so for the high specificity of antibody-antigen interaction. In fact, these regions come out from the differential assembly of Variable, Diversity and Joining gene segments (VDJ) and from the insertion of somatic mutations in these genes, that make so specific the antigen binding and guarantee the great variety of specific antibodies in the serum[33–35]. On the other hand, Fc portion is generally N-glycosylated and it is involved in the activation of effector functions and the antibody recycling through the interaction with specific Fc receptors (see next sections)[36–38].

1.3 Fc effector functions

Fc domain is involved in many immune responses, such as antibody-dependent cell-mediated cytotoxicity (ADCC), antibody-dependent cell-mediated phagocytosis (ADCP) and complement-dependent cytotoxicity (CDC) by the interaction with specific Fc receptors and complement proteins, respectively[36–38]. All these functions represent a link between the innate and adaptive immune systems. In fact, the ability of innate immunity to destroy the target cell, is combined with the capacity of adaptive immunity to recognize in a selective way a wide range of antigens[39]. In this frame, Fc effector functions have been identified also as secondary mechanisms of action of mAbs and must be taken into account as an important biological aspect, especially in the development of new biological entities (NBEs). Considering for example a tumor cell, the treatment with antibodies that preserve their Fc effector functions can be useful in enhancing the therapeutic response. Specifically, many commercially available anti-cancer products, (*i.e.* rituximab, trastuzumab, avelumab)[40–42] show a positive therapeutic impact on the patients, since they attack the tumor not only through classical mechanisms, such as membrane antigen internalization, but also activating the innate immunity of the patient against it (Figure 3). Conversely, in the case of an autoimmune disease or in immunological tumors, it is important to downregulate the immune system of the patient, so the treatment with mAbs with abrogated Fc effector functions can be a strategy to selectively target an antigen without inducing secondary undesired responses. On this basis, it is very important for pharmaceutical companies and health authorities to constantly improve the knowledge in this field in order to improve the product development and define more accurate strategies.

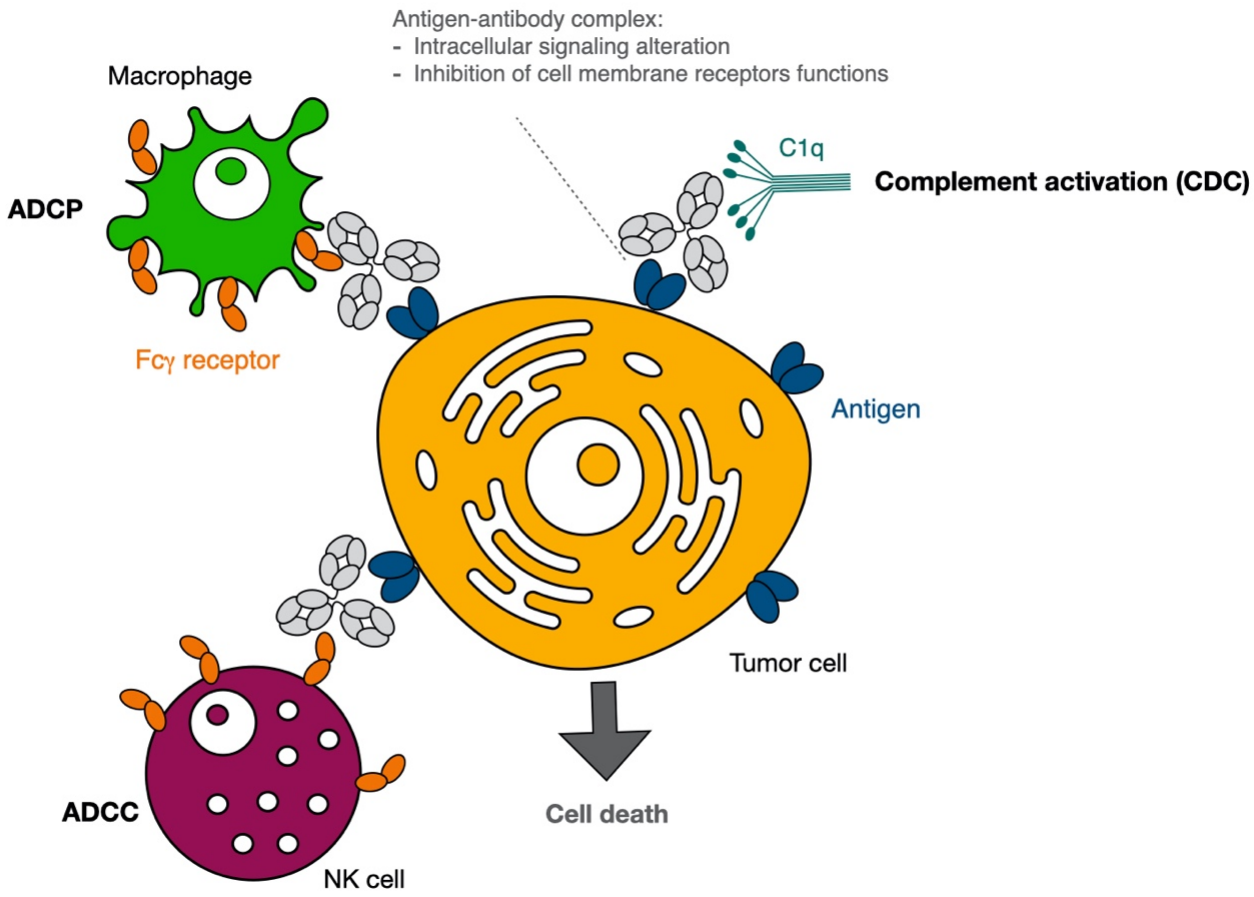

Figure 3: ADCC, ADCP and CDC mechanisms against a tumor cell. When the antibody (in grey) binds its target (in blue) on the tumor cell surface (in yellow), it can simultaneously trigger the activation of Fc effector functions, upon its binding to specific Fc receptors and complement proteins (C1q). Fc receptors are expressed on the surface of immune cells like natural killer (in bordeaux) and macrophages (in green) that are responsible for the activation of ADCC and ADCP mechanisms against the tumor and that, acting together with CDC, induce the target cell death and the enhancement of antibody pharmacological response.

ADCC, ADCP and CDC are key immune mechanisms naturally activated against pathogens or tumor cells after the antigen-antibody recognition. In ADCC, the secretion of cytokines (i.e. IFN-γ), perforins and granzymes by natural killer (NK) cells is activated upon the binding to Fc receptors expressed on the surface of effector cells. So, by the release of endogenous cytotoxic substances, target cell death is induced[43]. In ADCP, antibody-antigen complexes bind Fc receptors expressed on macrophages surface, inducing the phagocytosis of the target cell and its consequent elimination[44]. Finally, the complement cascade is activated by the interaction of antibody with C1q receptor. The deposition of complement components on the target cell surface promotes the cell cytolysis and simultaneously enhances other effector functions, acting in a synergic way with ADCC and ADCP[45–47]. Together to these, Fc drives the antibody recycling by the interaction with the FcRn. This receptor, that is involved

also in the IgGs maternal to fetal transfer, is expressed in a wide range of tissues, regulating the half-life of antibodies and becoming a key aspect to control in pharmaceutical development[48].

As well as any other aspect of the immune system, Fc activity is regulated on multiple levels. The main one concerns the ability of Fc to engage its cognate receptors, that is a very dynamic process mainly influenced by the structure and the intrinsic heterogeneity of this domain. In fact, even if it is classified as the constant part of the antibody, depending on IgG isotype, Fc can display considerable differences in amino acid sequence, thus resulting in a huge variety of Fc conformations potentially responsible for different effector functions. However, Fc receptors recognition is regulated also by the antibody N-glycosylation, that can directly impact the Fc conformation but can also play an active role in the engagement between the antibody and the receptors[49].

A further description of Fc receptors subfamilies and N-glycosylation mechanisms will be provided in next paragraphs.

1.4 Fc receptors classification and functions

Based on the conformation adopted by Fc, Fc receptors are classified in two subclasses, type I and type II receptors[50]. In particular, Fc fragment displays a horseshoe-like shape in which CH3 domains are highly associated while CH2 portions are more widely spaced forming a hydrophobic cavity generally occupied by N-glycans. However, despite the nomenclature that describes Fc as a constant domain, the structural orientation of this part can considerably vary especially in the CH2 region. In fact, the flexibility of the lower hinge and of the loops in CH2 domains together with N-glycans heterogeneity can lead to a huge variety of conformations that can be essentially grouped in “open” and “closed”. In the open conformation, CH2 domains are distant allowing the exposure of glycans that protect the hydrophobic cavity from the solvent. In the closed conformation, that is more common for example in aglycosylated species, CH2 domains are more associated inducing the closure of the cavity and the formation of a hydrophobic core[49].

Type I receptors interact only with open conformations of Fc with a binding stoichiometry of 1:1 (receptor/antibody) and in a binding site proximal to the hinge[51]. Among the others, type I subfamily includes the canonical Fcγ receptors (FcγRs) that preferentially bind IgGs. Fcγ receptors can be distinguished in the high affinity FcγRI and the low affinity FcγRIIa/c and FcγRIIIa/b, that are activating receptors, and FcγRIIb that has an inhibitory function (Table 1).

In contrast, type II receptors recognize only closed Fc conformations and include C-type lectin receptors, like FcRn and DC-SIGN (dendritic cell-specific intercellular adhesion molecule-3-grabbing non-integrin). Type II subclass binds antibodies in the interface between CH2-CH3 domains with a 2:1 (receptor/antibody) stoichiometry (Figure 4A)[49,52].

From a structural point of view, Fc receptors are all trans-membrane proteins, with an extracellular part involved in antibody molecular recognition mechanism, a transmembrane portion and a cytoplasmic domain responsible for the intracellular signaling. To date, several atomistic structures are available for the extracellular part of almost all the type I Fc receptors[53–57], revealing a structural architecture shared among subtypes. Excluding FcγRI, they are composed of two Ig-like extracellular domains, named D1 (amino-terminal, membrane distal) and D2 (carboxy-terminal, membrane proximal) with a conserved spatial orientation and a heart-shaped structure due to the 70° angle that they form[58]. For what concerns FcγRI, it is composed of three extracellular domains (D1, D2 and D3) and there is evidence that the presence of the third domain is responsible for the higher affinity of this receptor for IgGs with respect to the others[59]. Looking at the secondary structure of the extracellular part, all domains share a conserved immunoglobulin folding mainly characterized by β-sandwiches architecture and immunoglobulin-like topology stabilized through disulfide bonds (Figure 4B).

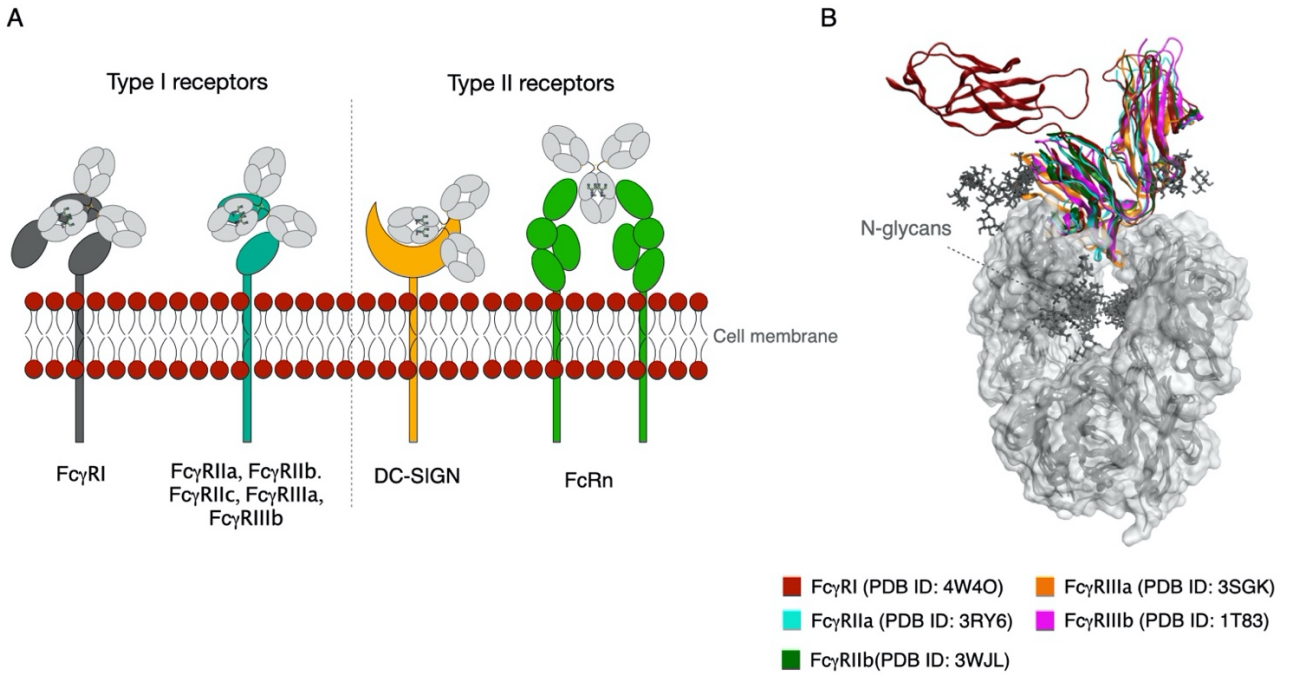

Figure 4: Schematic representation of FcγRs subclasses and structural superposition of X-ray structures available for Fc::FcγR complexes. (A) Schematic representation of FcγRs class I and II. Type I receptors bind antibodies in the proximal hinge with a binding stoichiometry of 1:1 (receptor/antibody); type II receptors bind mAbs at CH2-CH3 interface with a 2:1 stoichiometry. (B) Structural superposition of FcγRI, FcγRIIa, FcγRIIb, FcγRIIIa and FcγRIIIb X-ray structures in complex with IgG1 Fc portion. All the receptors show a conserved 3D orientation and position with respect to the Fc; FcγRI (in red) exhibits one extracellular domain more.

The engagement of FcγRs expressed on leukocytes by immune-complexes promotes several intracellular pro-inflammatory, anti-inflammatory and immune regulatory responses. Activator receptors carry out the intracellular signaling through the immunoreceptor tyrosine-based activation motif (ITAM) corresponding to the Yxx[L/I]$x_{(6-8)}$Yxx[L/I] sequence and located in the cytoplasmic tail. The intracellular signaling activation occurs upon the phosphorylation of conserved tyrosines in the ITAM motif by Src family kinases and the consequent activation of Syk tyrosine kinase[60]. This process activates several proteins, such as phospholipase C gamma 1 (PLCγ), Bruton's tyrosine kinase (Btk), guanine nucleotide exchange factor Vav and phosphoinositide 3-kinase (PI3K). Specifically, PLCγ promotes the hydrolysis of phosphatidylinositol 4,5-bisphosphate (PtdIns(4,5) P_2) in inositol 1,4,5-trisphosphate (IP_3) and diacylglycerol (DAG) inducing calcium mobilization and protein kinase C (PKC) activation, respectively. These pathways activate pro-inflammatory responses such as degranulation and cytokine production that are part of ADCC mechanisms. Vav factor is instead involved in ADCP processes by the cytoskeleton remodeling to control phagocytosis[50].

All these activating signals are regulated by tyrosine-based inhibition motif (ITIM)-bearing receptors, such as FcγRIIb that contains the single [I/V/L/S]xYxx[L/V] sequence. The inhibitory signal is activated upon the binding of immune complexes to FcγRIIb and the co-ligation of a heterologous activating receptor such as a B-cell receptor (BCR). This induces the recruitment of inositol phosphatases (SHIP-1 and SHIP-2) and blocks the activation of inflammatory cascades[61]. An ITAM-mediated inhibitory signal (ITAMi) has been proposed as another inhibitory pathway, promoted by ITAM motif itself. In particular, it has been observed that several low affinity receptors can act as dual receptors, inducing either activating or inhibitory responses and controlling in this way the immune homeostasis. The receptor binding by a single antibody induces the phosphorylation only of the last tyrosine in ITAM motif, thus promoting only a transient activation of Syk kinase. Syk transient activation is followed by the activation of SHP-1 that is responsible for an inhibitory signal and abrogates the immune activation[61–68]. All these mechanisms are summarized in figure 5.

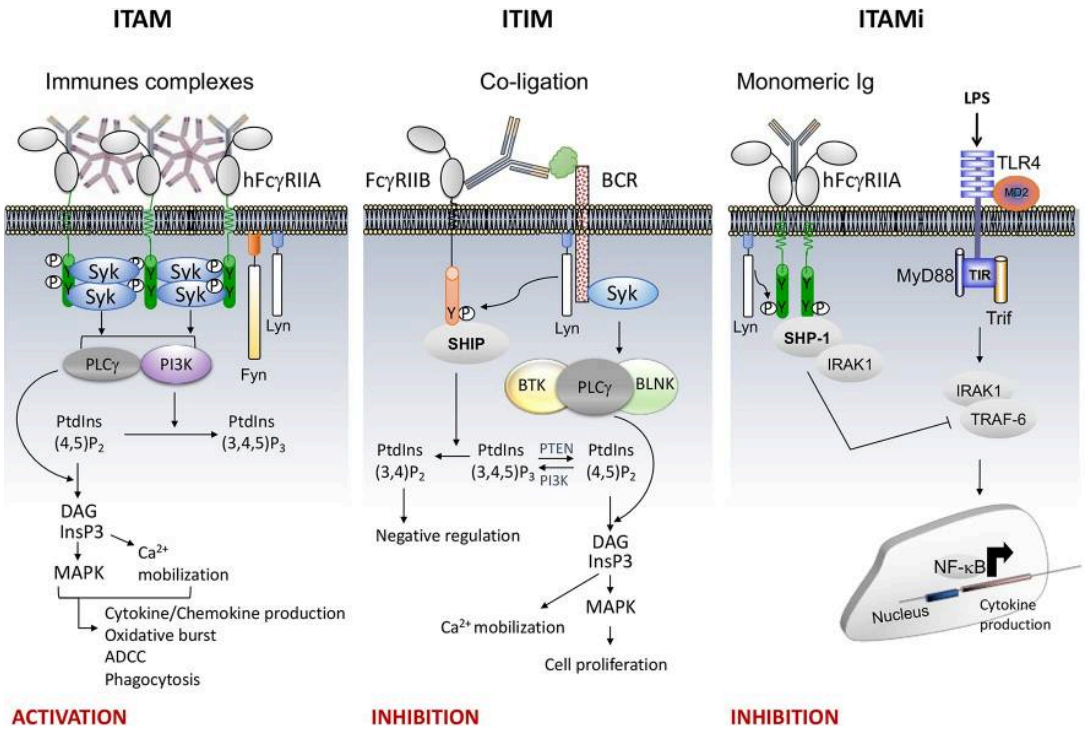

Figure 5: FcγRs intracellular signaling mechanisms. The ITAM, ITIM and ITAMi- mediated activatory and inhibitory intracellular pathways. Figure from Mkaddem *et al.*[50]

1.5 N-glycosylation

N-glycosylation is one of the most common post-translational modifications (PTMs) in antibodies that occurs in the endoplasmic reticulum (ER) and Golgi apparatus[69–71] on the conserved Asn297 (according to standard IgG EU numbering[31]) in the heavy chain. Asn297 is located in CH2 domain, in a specific sequence, the N-X-S/T motif (where X is not Pro)[72]. N-linked glycans type added to the asparagine may depend upon the expression system used to produce the mAb. As reported in figure 6A, three different glycan backbones can be found on IgGs: high mannose, complex and hybrid. The complex-biantennary type is the most common in humans and also in CHO cells[73,74]. In fact, because of their high similarity with human cellular machine and with respect to the glycan synthesis and expression, CHO cells are the preferred choice to produce therapeutic mAbs. On the contrary, the generation of glycans species not naturally expressed in humans, as those produced by murine cells, could lead to severe immunogenic responses in patients[73,75]. On this basis, a further description of N-glycans produced by CHO cells will be provided below.

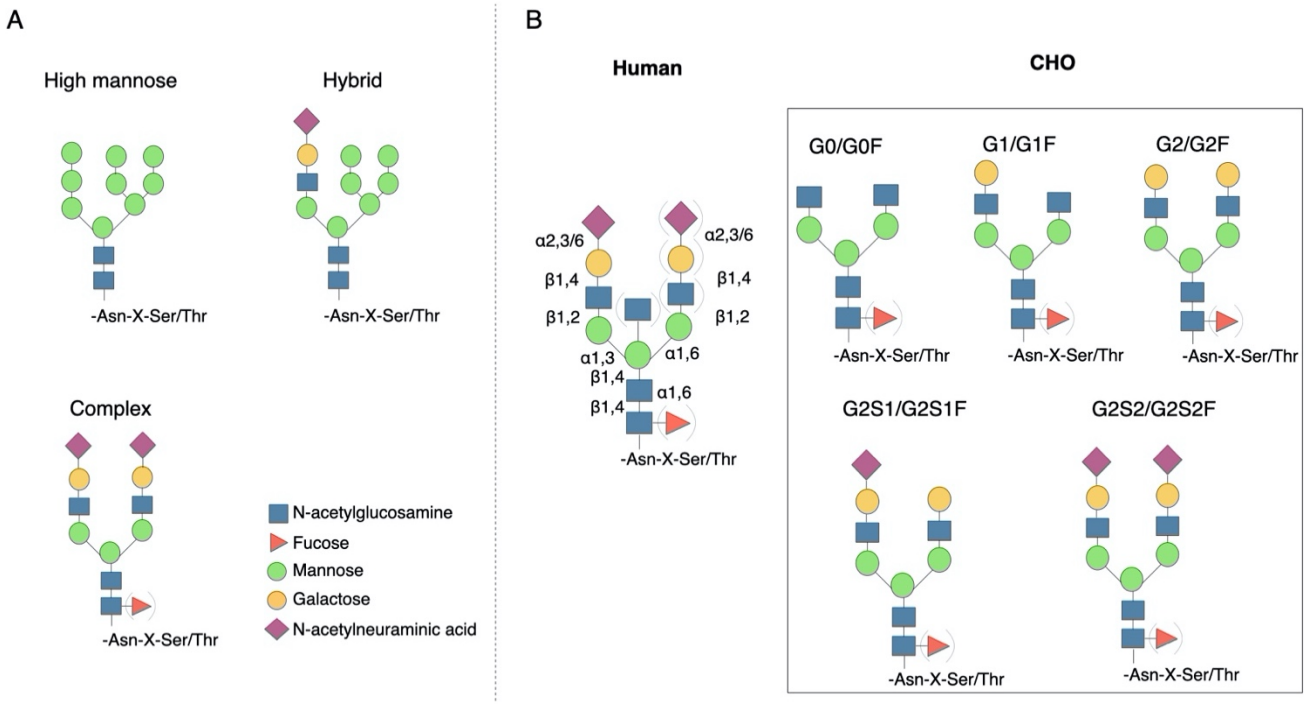

Figure 6: IgG N-glycosylation patterns. (A) The three glycan backbones found in IgGs: high mannose, complex and hybrid. (B) A comparison between the most common human and CHO cells complex-biantennary glycans. All glycans are represented according to the SNFG system[32].

As anticipated, the most common glycosylation pattern in this cell line is the complex-biantennary type, that consists of a conserved core structure, composed of four N-acetyl-glucosamine (GlcNac) and three mannose (Man) units. This backbone can be further modified by the addition of other sugars, as fucose (Fuc), galactose (Gal) and sialic acid (Neu) residues, generating more complex species with a huge heterogeneity, including several hundreds of glycoforms[76]. In figure 6B the most common glycosylation patterns expressed by CHO cells are summarized.

Concerning the N-glycosylation process in antibodies, it follows the same mechanism of other glycoproteins[77–79]. First, a pre-assembled oligosaccharide, Glc3Man9GlcNAc2 (from right to the left) is attached to Asn297 by an oligosaccharyltransferase complex in the ER. Then the removal of three glucose (Glc) residues and a Man unit is mediated by a glycosidase. The obtained species (Man8GlcNac2) translocates in the *cis*-Golgi where a mannosidase removes other two mannose residues. The resulting Man5GlcNac2 chain moves to the medial-Golgi to become a GlcNac2Man3GlcNac2 glycan, that is the conserved biantennary complex backbone. At the end, this chain moves to the *trans*-Golgi where it can be modified by the addition of other sugar units as previously described and shown in Figure 7[76,79].

In the context of mAbs, N-glycans play a key role not only in the stabilization of the antibody structure, but also in driving its effector functions. In fact, due to their position in the Fc domain and their accommodation in the interspace between two CH2 portions, N-glycans contribute to maintain the Fc conformation as well as its functionality. For this reason a change in N-glycan composition can alter the Fc conformation and its interaction with Fcγ receptors, with consequences in triggering the immune response[80]. According to literature, the loss of glycosylation can disrupt the Fc structural integrity, that is mandatory for the optimal binding to Fc receptors. In fact, it has been demonstrated that glycosylation thermally stabilizes mAbs and make them less prone to aggregation and unfolding[81,82]. In addition to this, it is well known that changes in the glycosylation pattern may modulate the effector functions of the IgGs, for example: Gal deficiency promotes complement activation[83], while a galactose abundance has been found in pregnant women, since Gal residues are involved in placental transport[84]. Another example is related to sialic acid that is involved in anti-inflammatory effects, so desialylation abrogates this function in knockout mice[85].

One of the most critical modifications, especially in the context of biopharmaceutical development, is the addition of a core fucose to the GlcNac residue linked to Asn297. It has been observed that the presence of the Fuc residue can strongly modulate the FcγRIIIa binding affinity for the antibody that

correlates with the ADCC activity. Since this aspect is of main interest in this thesis, it will be deeply analyzed in the next paragraph.

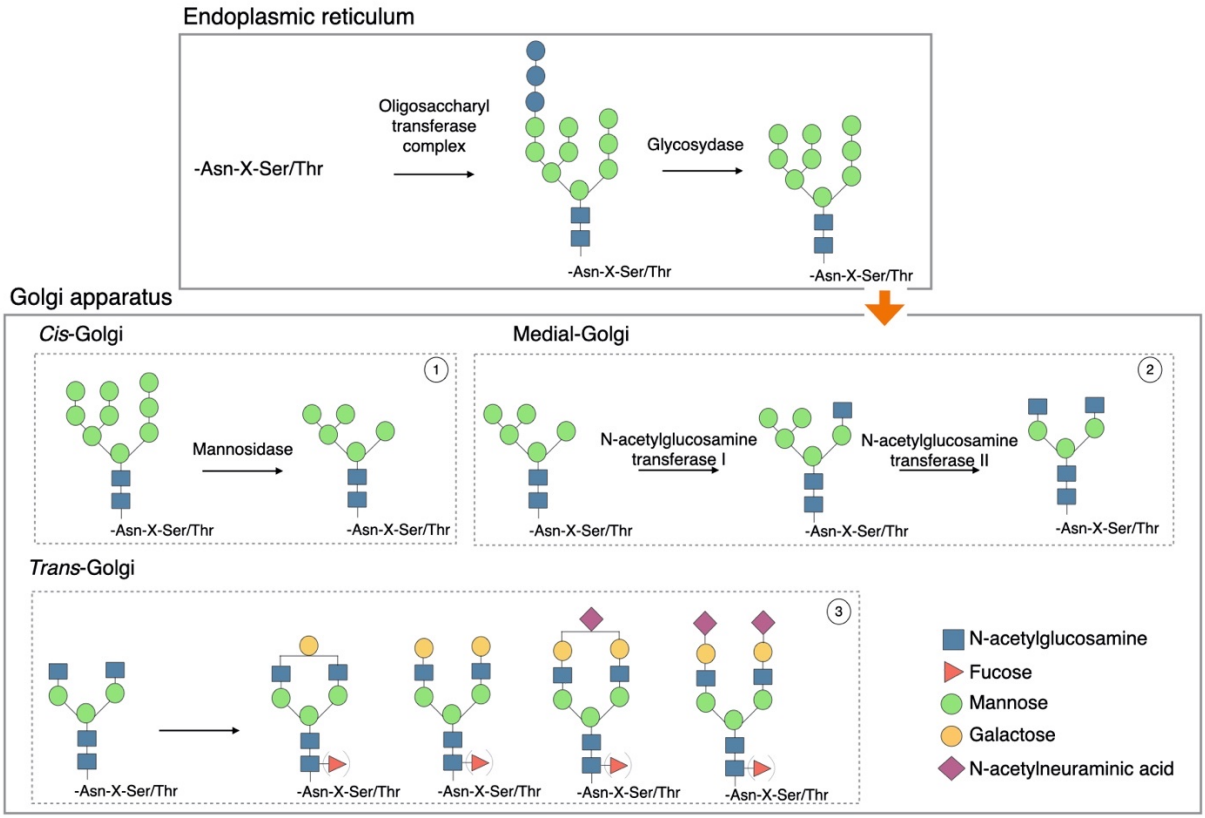

Figure 7: N-glycosylation process in IgGs. N-glycosylation in monoclonal antibodies starts in the endoplasmic reticulum where a pre-assembled oligosaccharide is attached to the conserved Asn297 and then modified to obtain a high mannose species. At this point the glycosylated protein moves to the Golgi apparatus where undergoes several modifications, first in the *cis*-, then in the medial and finally in the *trans*-Golgi. In this compartment the addition of sugars like fucose, galactose and sialic acid, can occur transforming the conserved G0 backbone in more complex species.

1.6 The role of fucosylation in regulating Fc effector functions

Rothman and colleagues gave the first evidence of the negative impact of fucosylation on ADCC activity. They investigated the effects of alterations in IgG glycosylation induced by the treatment with inhibitors of glycans biosynthesis, showing that it might be a correlation between glycosylation alterations and the Fc binding to FcγRIIIa[86]. In 2002, Shields *et al.*[87] confirmed that the antibody binding to FcγRIIIa is influenced by the presence of fucose. In fact, by expressing two different IgG1, namely Hu4D5 and HuE27, in Lec13 CHO cells, which are deficient in adding Fuc, they evaluated the binding affinity of the antibodies for the high affinity FcγRI and the low affinity FcγRII and FcγRIII. The

experiments showed that an equivalent binding affinity of FcγRI was detected for afucosylated and fucosylated antibodies and only a slight improvement was found in the affinity of FcγRII for afucosylated species, suggesting that, in both these cases, the presence of fucose may not have a significant effect.

On the other hand, the two FcγRIIIa polymorphic variants (Phe^{158} and Val^{158}), that are known to be the lower affinity and the higher affinity phenotypes, respectively[88,89], were tested against dimeric IgGs. As a result, in the case of Hu4D5-Lec13 mAb, FcγRIIIa (Phe^{158}) and FcγRIIIa (Val^{158}) showed a 42-fold and a 19-fold binding enhancement for the afucosylated species, respectively (Figure 8, panels A-B). Similarly, looking at HuE27-Lec13 dimers a 50-fold increment in binding affinity was detected for both FcγRIIIa allotypes. Authors also tested an IgG1 variant (S298A/E333A/K334A) that was demonstrated to have an improved binding to FcγRIIIa[90]. They produced the afucosylated species of this antibody that exhibited a 36- and a 12-fold improvement in binding to FcγRIIIa(Phe^{158}) and FcγRIIIa(Val^{158}), respectively, thus suggesting a synergistic effect of protein and carbohydrate alterations.

Experiments were also conducted to measure the effect of Hu4D5 fucosylation on ADCC response against human breast cancer cell line SK-BR-3. These cells were opsonized with different mAb concentrations and Peripheral Blood Mononuclear Cells (PBMCs) from three FcγRIIIa(Val^{158}/Phe^{158}) donors and three FcγRIIIa (Phe^{158}/Phe^{158}) donors. For all donors tested, the afucosylated IgG1 showed a significant increase in promoting ADCC with respect to fucosylated species (Figure 8, panels C-D). Moreover, as expected, the Phe^{158}/Phe^{158} donors showed a slightly lower cytotoxicity response than Val^{158}/Phe^{158} donors, since, as previously mentioned, the Phe^{158} polymorphic variant exerts a lower affinity for IgG1 than the Val^{158} one. Authors also confirmed the synergistic effect of antibody sequence variants and glycans alterations by a comparison between Hu4D5 antibody and its S298A/E333A/K334A variant with and without fucose through ADCC assays and immunofluorescence staining.

Many other *in vitro* and *ex vivo* studies confirmed what Shields and colleagues[87] had observed, leading to the assumption that the presence of fucose in IgG1 can have a detrimental effect on its FcγRIIIa recognition and consequently on the ADCC activity IgG1-mediated[91–96].

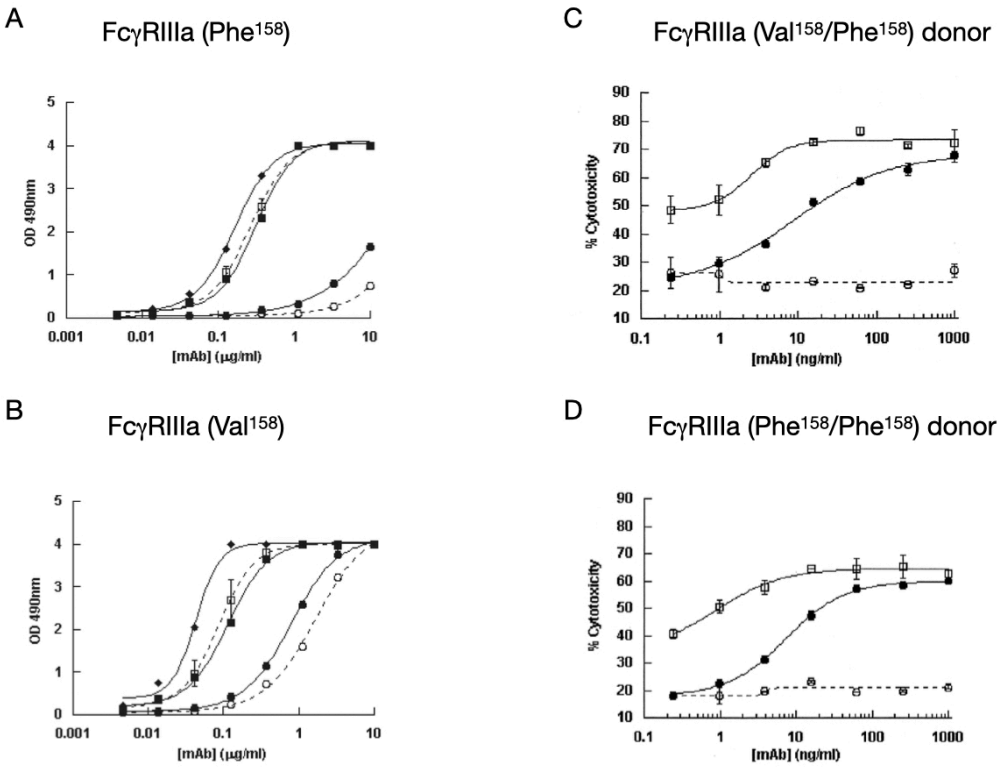

Figure 8: Binding of anti-HER2 Hu4D5 dimers to human FcγRIIIa in ELISA format assays and ADCC assays[87]. FcγRIIIa (Phe158) (A) and FcγRIIIa (Val158) (B) binding to anti-HER2 Hu4D5 dimers: *open circles*, fucosylated Hu4D5 expressed in CHO cells; *open squares*, afucosylated Hu4D5 expressed in Lec13 cells; *filled circles*, fucosylated Hu4D5 expressed in HEK293; *filled squares*, afucosylated Hu4D5 expressed in HEK293-AAA; *filled diamonds*, afucosylated Hu4D5 expressed in Lec13-AAA. (C-D) Representative plot of ADCC response using SK-BR-3 cells as target and PBMCs from one of three FcγRIIIa(Val^{158}/Phe^{158}) donors (C) and one of three FcγRIIIa(Phe^{158}/Phe^{158}) donors (D). *Open squares*, afucosylated Hu4D5 expressed in Lec13 cells; *filled circles*, fucosylated Hu4D5 expressed in CHO cells; *open circles*, spontaneous lysis. Each assay was performed in duplicate with *error bars* shown.

Structural studies tried to explain and better elucidate molecular mechanisms that drive the FcγRIIIa triggering and the role of sugars. Among others, Ferrara *et al.*[57] solved the atomistic structure of afucosylated (PDB ID: 3SGK) and fucosylated (PDB ID: 3SGJ) Fc in complex with FcγRIIIa, proposing that the reduced binding affinity of fucosylated antibody with respect to the afucosylated one is mainly due to a steric hindrance effect mediated by the fucose. More specifically, they crystalized the glycosylated FcγRIIIa-V158 variant comprising the extracellular part of the receptor (residues 1-191) glycosylated in only two of the five putative glycosylation sites (Asn45 and Asn162). Three mutations were introduced to abrogate glycosylation at Asn38, Asn74 and Asn169 that were replaced by Gln, since it has been demonstrated that glycosylation in these positions is not critical for the antibody recognition and for the protein expression, as for Asn162 and Asn45, respectively[97].

Moreover, the receptor variant was expressed in presence of a mannosidase I inhibitor in order to reduce the glycans complexity and block the sugar chain at high mannose stage. On the other hand, the IgG1 Fc fragments, both fucosylated and afucosylated, were instead obtained from the cleavage of a whole antibody expressed in CHO cells.

Looking deeply at the afucosylated X-ray structure, several hydrogen bonds can be found between the first two GlcNac residues linked to Asn162 in the receptor and the first GlcNac residue linked to the conserved Asn297 in the Fc. In addition, only a low number of interactions between the glycan chain at Asn162 and the protein part of Fc were detected as well as poor protein-protein interactions between the antibody and the receptor. In particular, according to crystallographic data only Gln295 and Tyr296 Fc residues are involved in an interaction network with the core mannose of the receptor glycan and the receptor residue Lys128, respectively. Thus, suggesting that the recognition is mainly driven by carbohydrate-carbohydrate interactions.

In the case of fucosylated Fc-receptor complex, the entire Asn162 oligosaccharide chain is displaced with respect to its position in the afucosylated Fc, due to the presence of fucose. As a result, there is an increased distance between the receptor GlcNac residues and the Fc GlcNac1 that is translated into a reduction of bond strength not only in the carbohydrate-carbohydrate interaction but also in the carbohydrate-protein and protein-protein bonding. In fact, an impairment of Gln295-Man5 contacts was observed together with the loss of Tyr296 (Fc) - Lys128 (FcγRIIIa) interaction. On this basis, authors proposed that the interaction network, described by the afucosylated complex, is responsible for an up to 100-fold increase in binding affinity of the receptor for the IgG. Inversely, this network becomes weak in the fucosylated complex, where the fucose operates a steric hindrance effect, inducing a reduction of Fc-receptor triggering (Figure 9).

Many other X-ray structures of differently glycosylated Fc in complex with FcγRIIIa are available, confirming the N-glycans assembly proposed by Ferrara and colleagues[57]. However, the lack of a complete crystallographic structure including the whole antibody in complex with the receptor makes it harder to fully understand the molecular mechanisms that drive the recognition and most of all which is the role of hinge and Fab domains in these.

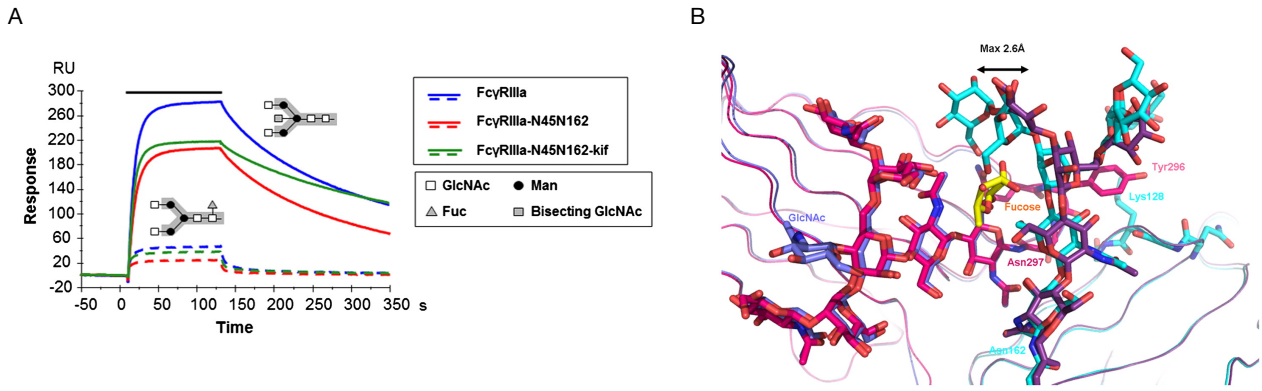

Figure 9: Surface plasmon resonance analysis of the interaction between FcγRIIIa and hIgG1 glycovariants and structural superposition of fucosylated and afucosylated Fc::FcγRIIIa complexes. (*A*) Overlay of sensorgrams for binding of 125 nM FcγRIIIa variants to fucosylated (dotted lines) and afucosylated (continuous lines) IgG1s. (B) Interaction interface between glycosylated FcγRIIIa and Fc fragment. In the afucosylated complex, glycan chain A of the Fc fragment is shown in blue, while the receptor in cyan. In fucosylated complex, glycan chain A of the Fc fragment is shown in magenta, with core fucose highlighted in yellow, and its complexed Fc receptor is in dark violet. The picture highlights the displacement of the oligosaccharide chain Asn162-linked in presence of fucose and the steric hindrance effect mediated by this sugar. Picture from Ferrara *et al.*[57]

1.7 Structural and computational studies on the N-glycosylation role: state of the art

Up to now, because of the high relevance of N-glycosylation in regulating antibodies' functionality, many experimental and computational studies have been published underlining how much controversial the current knowledge in this field is[98]. For what concerns, for example, the Fc portion orientation, as previously mentioned, it is known that this portion can assume both open and closed conformations depending on the glycan composition. In fact, some published studies based on crystallographic data strongly assert that the aglycosylated Fc domain shows a closed conformation that is not inadequate for receptor binding[99–102]. However, other more recent studies demonstrated that, even though not glycosylated, the Fc can assume both open and closed conformations and that the lower affinity for the receptor can be explained as a result of the low conformational stability of this species that is not stabilized by glycans[103]. This is confirmed also by X-ray structures[102] that show B-factor values higher for aglycosylated Fc portions than for glycosylated one, specifically for what concerns the loop in which the conserved Asn297 is located, and by solution NMR spectroscopy data[99].

Another example is the discrepancy between what is reported by Ferrara et al.[57] and Mizushima and colleagues[104], widely discussed in the previous section, and what has been observed by Falconer et

al.[105]. According to this one, that produced the X-ray structure of an afucosylated Fc in complex with FcγRIIIa, no interactions between receptor and Fc glycans were observed and this is in contrast with the specific carbohydrate-carbohydrate interaction network proposed by Ferrara et al[57]. Probably the contacts observed in previous studies were a result of crystallographic conditions and for this reason, an investigation of the dynamics of proteins and sugars is necessary to better elucidate the conformational behavior of the complex. Both Falconer[105] and Sakae *et al.*[106] reported molecular dynamics studies especially focused on the conformational behavior of Asn162-glycans, proposing also in this case controversial theories. Falconer and colleagues[105] observed that the fucose addition reduced the volume sampled by Asn162-glycans, suggesting a reduction of the conformational space explored by this region. On the other hand, Sakae et al.[106] observed that the fluctuation of this region is significantly higher in the fucosylated system than in the afucosylated one and supposed that this could be the cause of the carbohydrate-carbohydrate interactions disruption.

Among the published computational studies, only few works studied the mAbs conformational behavior *via* extensive MD simulations of full-length antibodies. Two studies carried out on trastuzumab, a marketed humanized mAb, have been reported. Brandt et al.[107] investigated the antibody exploration of conformational space during time by analyzing eight independent 40 ns long trajectories. A similar work, by Kortkhonjia et al.[108], was carried out for a longer simulation time (1 μs) and suggested a very high flexibility of the IgG1 showing that this is due to different types of contacts and interactions between domains.

However, more studies are related to specific portions of the antibody (*i.e.* Fab-antigen complexes, Fc-receptor complexes, etc.) or to isolated glycan chains[109] that, despite the significant scientific contribution, cannot give a complete picture of molecular mechanisms of IgG. Moreover, the lack of both full X-ray structures and computational studies focused on elucidating the glycans' contribution to the whole conformational behavior of the antibody, makes it really difficult to clarify the mechanisms that drive the biological activity of this class of biotherapeutics.

1.8 Quality by design

Quality by Design (QbD) is a novel strategy adopted from pharmaceutical companies to keep under control all the modifications potentially occurring in the product from the development stages to the launch on the market and also in the post-approval phase. Specifically, according to QbD concept the product quality must be designed as well as the product itself following a systematic development

approach that is focused on process understanding and control and is based on scientific knowledge and quality risk management[110].

As mentioned also by Lawrence et al.[111], the aims of pharmaceutical QbD may include the following:

- To achieve quality product specifications based on clinical performances
- To reduce product variability and enhance process capability by improving product and process design, understanding and control
- To enhance the product development and manufacturing efficiency
- To improve root-cause analysis and post-approval modifications management

In pharmaceutical development, QbD allows to identify specific product properties, namely critical quality attributes (CQAs), that may represent a concern for the patient, and to determine the relationship among these attributes and formulation/manufacturing variables. This approach should guarantee the delivery of a safe high-quality product.

QbD approach consists of five steps:

1. The drafting of a document, named quality target product profile (QTPP), that identifies and defines CQAs of the drug product (DP)
2. The product design and understanding by the definition of critical material attributes (CMAs)
3. The process design and understanding by defining critical process parameters (CPPs) and linking CMAs to CPPs and CQAs
4. A control strategy definition in which specifications for drug substance (DS), excipients and DP are defined
5. Process capability and continual improvement

Focusing on the first step of QbD, the QTPP consists of a summary of the DP characteristics that must be achieved to ensure the desired product quality, considering both safety and efficacy of the therapeutic molecule. Some examples of these properties include route of administration, dosage form, delivery system, dosage strength, container closure system, therapeutic moiety release and attributes affecting pharmacokinetics (PK). The QTPP and other product information, like the mechanism of action, are essential to identify a list of potential CQAs (pCQAs).

According to the International Conference on Harmonization guideline Q8 (R2) a CQA is defined as "a physical, chemical, biological, or microbiological property or characteristic that should be within an appropriate limit, range, or distribution to ensure the desired product quality"[110]. These attributes are considered critical or not critical based on the impact they have on biological activity,

pharmacokinetics/pharmacodynamics (PK/PD), immunogenicity and safety of the product. The criticality of each attribute is assigned using a specific risk ranking that is inferred by analytical and biological characterization data as well as structure-function studies and published literature. Of course, the preliminary identification of pCQAs can be helpful in focusing development efforts on attributes that need more control. The final list of CQAs is generally confirmed in the latest stage of commercial process, just before the finalization of commercial control strategy. Even if this approach requires a big analytical effort, it returns a deep understanding of the product itself and of the impact of its characteristics on efficacy and safety[112].

Considering mAbs, attributes may be divided in four categories:

- Product variants (see Table 2)
- Process-related impurities
- Obligatory CQAs
- Raw materials and leachable compounds

As reported in Table 2, glycosylation-related variants are considered as potential CQAs that must be monitored and characterized during mAb development. Among them, because of the role as modulator of the ADCC activity, as previously described, fucosylation may represent a concern for the bioactivity of the molecule. For this reason, a deep understanding of the role of fucose in the structural behavior of IgG1 is of fundamental interest, not only to support and increase the knowledgebase of these biotherapeutics, but also to help pharmaceutical companies in monitoring and controlling this attribute.

Table 2: List of molecular variant pCQAs for a monoclonal antibody[112].

Category	Critical quality attribute
Size-related variants	High Molecular Weight Species (HMWS) Low Molecular Weight Species (LMWS)
Charge-related variants (Acidic)	Deamidation in CDR Deamidation in Non-CDR Glycation in CDR Glycation in Non-CDR
Charge-related variants (Basic)	Aspartic Acid Isomerization in CDR Aspartic Acid Isomerization in Non-CDR N-Terminal Leader Sequence (may be molecule specific) N-Terminal Pyroglutamic Acid C-Terminal Lysine C-Terminal Proline (IgG1) or Leu (IgG4) Amidation
Oxidation-related variants	Oxidation in CDR (Met, Trp) Oxidation in Non-CDR (Met, homo-variant) Oxidation in Non-CDR (Met, hetero-variant)
Fc Glycosylation	Afucosylation Galactosylation High-Mannose Sialylation (NANA, NGNA) Non-Glycosylated Heavy Chain
Structural variants	Cysteine Forms Sequence Variants Protein Structure

Chapter 2

Aim of the study

Nowadays, monoclonal antibodies (mAbs) occupy a relevant position in the pharmaceutical market, since they are often the preferred choice in the treatment of several diseases. They are very selective and specific molecules for the targeted antigen, a feature that reduce the probability to exert side and off-target effects in patients. Among the different immunoglobulin (Ig) classes, IgG and in particular IgG1 are the most used, since their physical-chemical properties make them more manageable during development and production.

Both for mAbs and other biopharmaceutical products, a decisive step in their development is represented by the critical quality attribute (CQA) assessment. This process is part of a more complex and detailed procedure, namely the Quality by Design (QbD), that has been recently implemented by pharmaceutical companies to continuously control and guarantee the quality of a product, from the early development phases to the post-approval period. In the CQA assessment the criticality of several physical-chemical and biological properties, as well as process-related attributes of the product is evaluated and scored according to a defined risk ranking. The risk is calculated based on the impact that each quality attribute can have on the efficacy, safety, immunogenicity and pharmacokinetics of the product, by using literature data, prior knowledge and structural analysis, if an X-ray structure is available.

Recently, with the advent of novel computational resources and high-performance computers, many *in silico* approaches have been implemented by companies to speed up the identification of potential CQAs and to drive the product characterization. So, by merging *in silico* structural predictions, prior knowledge and experimental data, a significant contribution is given to the QbD process.

Within this context, among the most common attributes, N-glycosylation can be highly critical in terms of biological activity and immunogenicity of mAbs, because of its role in regulating Fc effector functions. In fact, it has been showed that the Fc conformation and functions can be strongly influenced by the N-glycans composition. In particular, several studies demonstrated that the presence of fucose can represent an issue for those antibodies that requires the activation of ADCC mechanisms to be effective. Specifically, it has been observed that afucosylated IgG1 can present an increase up to 100-fold in binding affinity for the FcγRIIIa with respect to fucosylated antibodies. This modification affects only the FcγRIIIa that is the main driver of ADCC process and consequently has an impact on the cytotoxic response. Many experimentally solved structures of Fc in complex with FcγRIIIa were published trying to elucidate the structural role of fucose in the interaction between antibody and receptor and many other controversial experimental and computational studies have been reported. However, the lack of an experimentally solved structure for a whole antibody in

complex with the receptor, together with the few MD simulation studies focused on explaining the glycans' structural role, make it really hard to understand if the glycosylation can have an impact also on hinge and Fab portions and if these domains contribute to the receptor recognition and to the ADCC triggering.

On this basis, the aim of this PhD thesis, that arises from a collaboration between the Laboratory of Computational Biochemistry and Biophysics at the Università degli Studi di Milano and Merck S.p.A., is to further characterize the structural role of N-glycosylation on IgG1, with particular attention to the role of core fucose. The final goal of the project, entirely performed using computational biochemistry approaches and considering adalimumab as a model IgG1, is to better understand at an atomistic level the role of glycans in modulating the structural and functional behavior of mAbs and to give a scientific contribution to the pharmaceutical development of these biotherapeutics.

Chapter 3

Materials and methods

3.1 Homology modeling

The three-dimensional (3D) structure of adalimumab was built by a chimeric homology modeling approach through the "Homology model" tool of the "Protein" module included in the Molecular Operating Environment 2019.01 (MOE, Chemical Computing Group, Montreal, QC, Canada)[113]. Fab domains were modeled according to the X-ray structure of adalimumab Fab in complex with TNF-alpha (PDB ID: 3WD5)[114], while hinge and Fc portions were built on the anti-HIV1 antibody (PDB ID: 1HZH)[115]. This template was selected from the MOE antibody templates library, that includes an optimized structure, refined *via* molecular dynamics by MOE experts. Both templates were further optimized and refined with the MOE "Structure preparation" tool[113], to correct any crystallographic issues, add missing hydrogens and adjust residues protonation states. Sequence alignment and structural superposition of 3WD5.pdb and 1HZH.pdb were performed to correctly orient the Fab domains with respect to hinge and Fc and to build each half of the antibody independently, adopting the "Override template" function of the MOE "Homology model" tool.

10 intermediate models were obtained by the homology modeling procedure and the final structure was selected basing on the best-scoring intermediate one. The score was computed according to the Generalized Born/Volume Integral (GB/VI) methodology that calculates the free energy of hydration as the sum of the electrostatic energy term and a cavitation energy based on a VI London dispersion energy, and not on a surface area (SA), as in the classical GB/SA function[116] . An energy minimization step was carried out until the root mean square (RMS) gradient reached a value of 0.5 kcal/mol/Å^2 by choosing the 'medium' option to operate only a moderate relaxation and relieve steric strain. For each heterodimer, free cysteines were manually bonded through the "Builder" tool in order to assembly the whole molecule. A further energy minimization (RMS gradient 0.01 kcal/mol/Å^2) was carried out to refine the final structure. Starting from the optimized aglycosylated antibody, two glycosylated structures of adalimumab were modeled. Since the topology of crystalized sugars included in 1HZH.pdb was partially incorrect and some units were missed, G0F and G0 glycan chains were manually added to obtain fucosylated and afucosylated species, respectively. Sugars were attached unit by unit to Asn302 (Asn297 according to the IgG1 standard numbering) on both heavy chains by the MOE "Carbohydrate builder". A final minimization step was carried out on entire glycosylated models until RMS gradient reached 0.01 kcal/mol/Å^2.

The 3D structure of both afucosylated and fucosylated adalimumab in complex with FcγRIIIa-V158 variant (hereinafter denominated FcγRIIIa) was built using a chimeric homology modeling approach,

too. The antibody molecule was modeled combining a centroid structure extracted from MD trajectories through a hierarchical cluster analysis performed by MDtraj[117] and the crystallographic structure of a fucosylated IgG1 Fc domain in complex with FcγRIIIa (PDB ID: 3SGJ[57]).

Specifically, Fab domains and hinge were built on the minimized centroid while the Fc portion was built for both complexes basing on 3SGJ.pdb[57] to allow the re-orientation of antibody side-chains with respect to the receptor. The same structure was available also for the afucosylated complex (PDB ID: 3SGK[57]), but 3SGJ.pdb was chosen for modeling both complexes since the higher Fc sequence coverage. This structure was optimized by "Structure preparation" module and protonation states were adjusted using "Protonate 3D" tool; the missing N-terminal Cys226 in one of the two Fc chains was rebuilt *ab initio* by the "Protein builder", the corresponding disulfide bridge was manually closed by the "Molecule builder" tool and a local minimization was run to correctly orient the bond. The receptor was only partially glycosylated, so G1F and G2F2 N-glycans were added on Asn45 and Asn162, respectively, through the "Carbohydrate builder" and an energy minimization (RMS gradient 0.1 kcal/mol/Å^2) of the whole system was performed to correctly orient the glycans with respect also to the Fc. Then, the prepared complex was superposed to the antibody centroid molecule to spatially orient the receptor with respect to the whole antibody. As well as for single antibody modeling, the final model was selected among 10 intermediates and an energy minimization step was carried out until the RMS gradient reached a value of 0.5 kcal/mol/Å^2. Once the final model was obtained, it was re-superposed to the Fc::FcγRIIIa complex, then the crystalized glycosylated Fc part was deleted and the antibody oligosaccharide chains were retained from the centroid structure. A further energy minimization of the complex was finally run to an RMS gradient of 0.01 kcal/mol/Å^2 to refine the glycosylated models and to fix the interaction network between the whole antibody and the receptor.

All the calculations in the modeling procedures were performed with the AMBER10:EHT force field[118] and the Reaction field (R-field) was applied to treat electrostatics contribution[119,120].

3.2 Molecular dynamics simulations

All the MD simulations reported in this work were performed by NAMD 2.13 package[121] handled by the MOE graphical user interface (GUI)[113]. All systems were solvated by the MOE "Solvate" tool that was used to add explicit water (TIP3P model) and NaCl (0.1 M). Then an energy minimization towards an RMS gradient of 0.001 kcal/mol/ Å^2 was performed. The simulations were carried out in NPT

ensemble (P=101.3 kPa; T=300 K) with periodic boundary conditions (PBC) enabled and by using AMBER10:EHT force field. The Langevin piston Nosé-Hoover method[122,123] was used to set constant pressure, the Langevin thermostat has been applied for temperature control, the sample time was set to 10 ps and the integration time step to 2 fs.

To simulate G0F glycan in water, the oligosaccharide chain was built by the MOE "Carbohydrate builder" and optimized through an energy minimization (RMS gradient 0.01 kcal/mol/Å^2). G0F chain was centered and oriented in a cubic water box with XYZ side of 44.0803 Å and the dynamics was carried out for 100 ns.

A 400 ns MD simulation was instead performed for each adalimumab model: aglycosylated, afucosylated and fucosylated. Each antibody was capped at N- and C-terminus of each chain with an acetyl (ACE) and an N-metyl amide (NME) group, respectively, and centered and oriented in a rectangular periodic box with the XYZ side dimensions of: 186.801 Å x 155.314 Å x 85.0184 Å (aglycosylated); 186.627 Å x 160.304 Å x 90.2284 Å (afucosylated); 185.041 Å x 161.404 Å x 90.1505 Å (fucosylated).

One MD simulation 1 μs long were run per each adalimumab:: FcγRIIIa complex (afucosylated and fucosylated). Firstly, all the N- and C-terminus of the proteins in the complex were capped with ACE and NME groups, respectively. After solvation, each complex was centered and oriented in a rectangular periodic water box with the following XYZ side dimensions: 185.4 Å x 162.9 Å x 92.4 Å (afucosylated); 170.5 Å x 146.2 Å x 95.8 Å (fucosylated), then both systems were minimized for 5000 steps.

An MD simulation 1 μs long of the X-ray structure of the human Fc in complex with FcγRIIIa-V158 variant previously used for antibody::receptor complexes modeling (PDB ID: 3SGJ[57]) was performed for both afucosylated and fucosylated Fc species. The structure was prepared and optimized as previously described (*see paragraph 3.1*): receptor N-glycans were added unit by unit *via* the "Carbohydrate builder" module, as well as in whole antibody::receptor complexes; concerning the Fc, G0F glycans were retained from the X-ray structure, while G0 sugars were obtained by manually removing fucose units. N- and C-terminus of both Fc and receptor were capped with ACE and NME groups and the complexes were solvated by TIP3P model in a rectangular periodic water box of the following XYZ side dimensions: 141.4 Å x 79.0 Å x 82.2 Å (afucosylated); 141.8 Å x 78.8 Å x 82.0 Å (fucosylated). Energy minimization of solvated systems was run for 5,000 steps.

3.3 Molecular dynamics analysis

The analysis of glycosydic bond distances over trajectory of G0F chain was performed by the GROMACS 2019.2 (GROningen MAchine for Chemical Simulations) package[124].

In MD of both antibodies alone and mAb::FcγRIIIa or Fc::FcγRIIIa complexes, geometric descriptors, such as Root Mean Square Deviation (RMSD), Root Mean Square Fluctuation (RMSF), radius of gyration and donor-acceptor distances, together with H-bonds and cluster analysis were computed by MDTraj[117]. The structural investigation on centroids and conformations sampled during the simulations and the ΔG binding free energy calculation of complexes were instead carried out by MOE software[113]. For ΔG binding free energy calculation, 21 conformations for each complex, each one saved every 50 ns, were considered. After an energy minimization run to an RMS gradient of 0.1 kcal/mol/Å^2, the interaction energy of the antibody::receptor complex was calculated by using the 'Potential Energy' tool, considering also glycans as part of the molecules and including their contribution to the interaction. By this function the interaction energy among a ligand and its receptor can be calculated as the sum of all the non-bonded interactions between the selected and the not selected atoms. In particular, antibody and receptor were distinguished as two different sets of atoms by the "Set create" tool, including the corresponding glycans. Then, by specifically selecting only one of the two, the interaction energy with the other protein was computed and evaluated for all the 21 conformations.

For each trajectory of isolated antibodies (aglycosylated, G0 and G0F adalimumab) an essential dynamics (ED) was computed by using the covariance analysis tool included in GROMACS 2019.2[124]. First of all, based on the fluctuation profiles of C-alpha atoms, the correlation matrix was computed per each antibody with respect to an average structure, to identify the correlation among the domains. Then, an eigenvalues decomposition of each correlation matrix was applied to generate a set of eigenvectors sorted in a descending eigenvalue index, in order to determine the principal components (PC) of each system. The trajectories were filtered along the eigenvectors associated with high eigenvalues allowing the identification of the two most prevalent protein motions, namely the PC1 and PC2. The two extreme projections of PC1 and PC2 on the average structure were computed per each system to visualize the type of motion described and to deeply analyze the conformational behavior of the molecules.

Chapter 4

Results and Discussion: part I

In this chapter, a detailed description of results obtained in the first part of the project is reported. In this phase, the study was focused on the 3D structure prediction of adalimumab, the IgG1 chosen as case study, and on molecular dynamics (MD) simulations analyses of three differently glycosylated forms.

In next sections, the following steps will be treated and described in detail:

- AMBER10:EHT parameters validation for glycans description in our study *via* MD simulation;
- Homology modeling of three differently glycosylated adalimumab species (aglycosylated, glycosylated fucosylated and glycosylated afucosylated) to rebuild the entire atomistic structure of the molecule;
- MD simulations of the three antibody models to investigate the conformational behavior of the antibody in presence of different glycosylation patterns and in absence of glycosylation.

4.1 Force field validation for glycans description

The main challenge in studying glycosylated proteins through MD simulations is the treatment of glycans, whose experimental parameters are fully characterized only in few force fields. Nowadays, GLYCAM[125] is the only force field entirely dedicated to the computational analysis of sugars, but it is not suitable to parametrize the proteins. For this reason, to carry out our simulations, we decided to use the generalist force field, AMBER10:EHT[118,126], which is suitable to both proteins and small molecules. AMBER10:EHT was validated for glycans parametrization by comparing *in silico* MD results with experimental data. Specifically, MD simulation of a complex fucosylated glycan chain, namely G0F, in explicit water was carried out for 100 ns (Figure 1A). G0F was chosen as case study for this validation since it is the most frequently sugar chain expressed in antibodies produced in CHO cells and because it is of main interest in this thesis. Glycosydic bond distances were computed over trajectory by GROMACS 2019.2[124] and compared to those reported in the experimental NMR analysis of a glycosylated protein selected as reference, namely the human chorionic gonadotropin (hCG; PDB ID: 1HD4; Figure 1B)[127] that is di-galactosylated (G2). Data analysis showed that bond distances are conserved over time with values spanning the same range of experimental NOE (Nuclear Overhauser effect) distances (Figure 1, panels C-D and Table 1). This suggests a suitable parametrization of the glycan chain and validates the use of AMBER10:EHT force field for the glycans studied in our research.

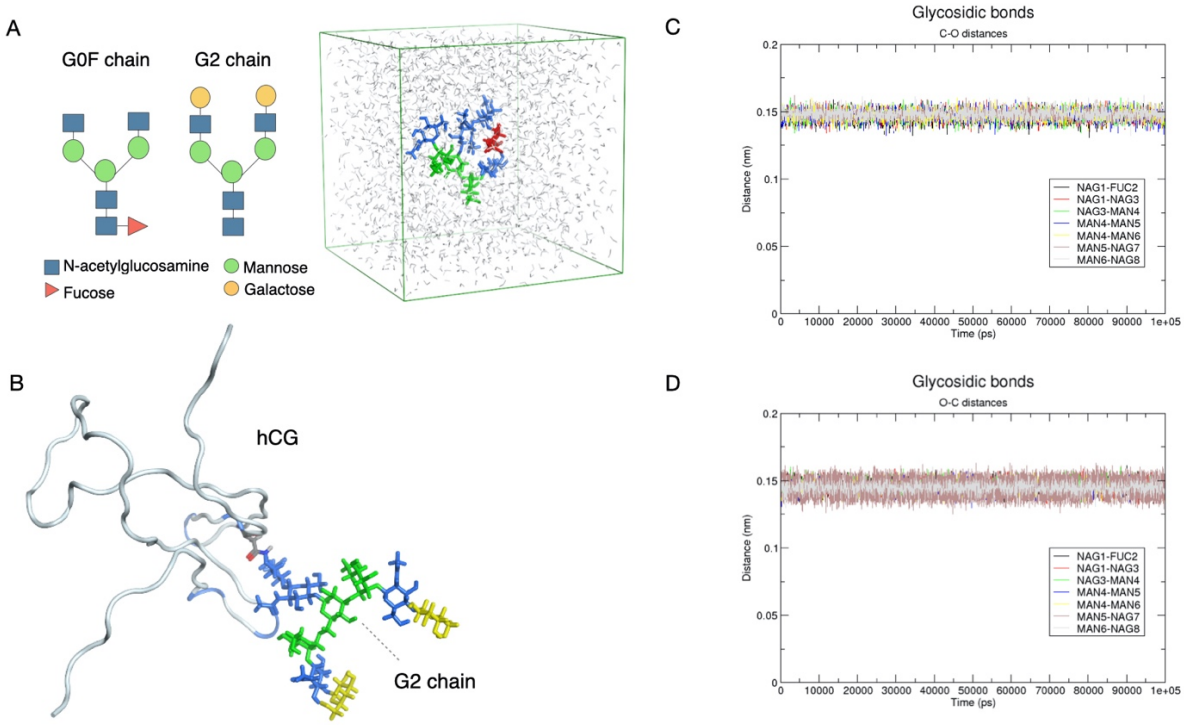

Figure 1: AMBER10:EHT parameters validation for glycans treatment in our study. (A) On the left, G0F and G2 glycans symbol representation; on the right, G0F chain in the cubic water box used for MD simulation. (B) NMR structure of glycosylated hCG used as reference and represented as a ribbon loop. In both A and B panels glycans are represented as sticks colored according to the SNFG system[32]. (C-D) Glycosydic bonds distances of G0F chain computed *via* MD simulation: (C) C-O distances and (D) O-C distances vs simulation time. The bond length range is conserved among all sugars couples.

Table 1: Experimentally calculated glycosydic bonds distances of a G0 chain. The table reports NOE distances calculated for the G0 portion of a G2 chain linked to human chorionic gonadotropin (hCG) for which the 3D structure was experimentally solved by NMR (1HD4.pdb). Sugars couples are numbered in a progressive way and the following abbreviations are used: N-acetylglucosamine (NAG), mannose (MAN).

Residue Couple	C-O distance (Å)	O-C distance (Å)
NAG1-NAG2	1.46	1.44
NAG2-MAN3	1.47	1.45
MAN3-MAN4	1.45	1.44
MAN3-MAN5	1.47	1.44
MAN5-NAG6	1.5	1.44
MAN4-NAG7	1.5	1.44

4.2 Homology modeling and MD simulations of aglycosylated, G0 and G0F adalimumab

The 3D model of aglycosylated adalimumab was obtained by a homology modeling approach, as described in previous sections (*see paragraph 3.1, Chapter 3*). Two templates were used to obtain the final structure: the only one human IgG1 currently available in PDB (PDB ID: 1HZH)[115] and the X-ray structure of adalimumab Fab domain in complex with the target antigen (PDB ID: 3WD5)[114]. However, a refined and equilibrated structure of 1HZH.pdb, included in MOE antibody templates library, was used in order to obtain a more accurate model. In figure 2 the sequence alignment among adalimumab primary sequence and templates is reported.

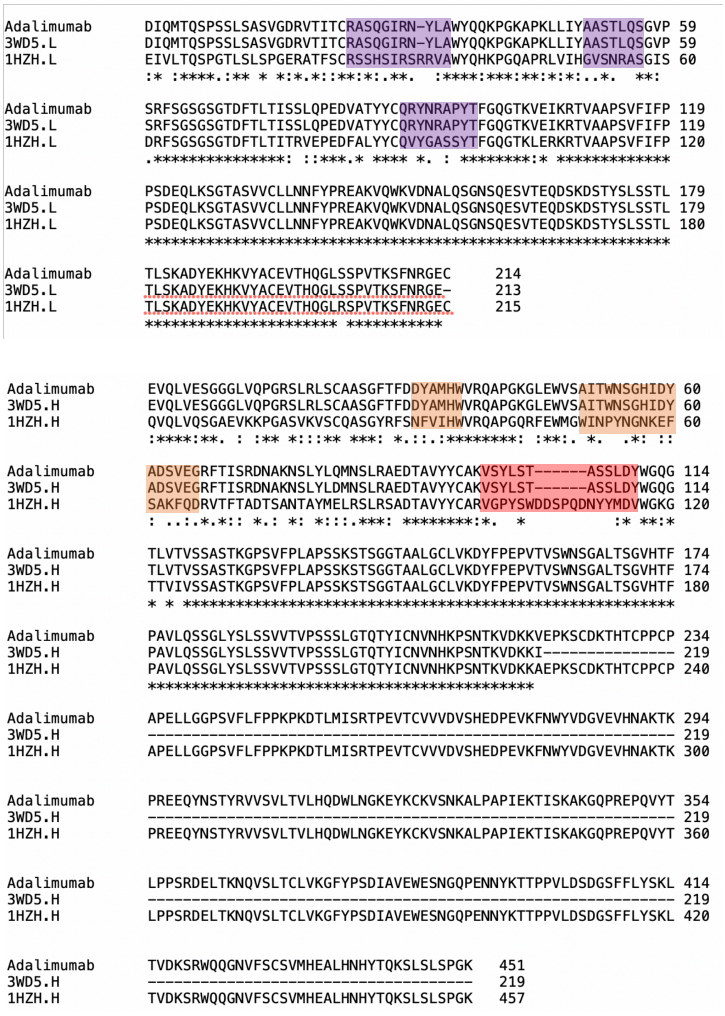

Figure 2: Sequence alignment between adalimumab, 1HZH.pdb and 3WD5.pdb. On the top LC alignment, on the bottom the HC one. CDR residues are colored according to Kabat convention: CDR1-2-3 (LC) in purple; CDR1-2 (HC) in orange and CDR3 (HC) in red. In the alignment: "*" corresponds to conserved residues; ":" to residues with strongly similar properties; "." to residues with weakly similar properties; "–" to a sequence gap.

According to the alignment, main differences among adalimumab and 1HZH.pdb are located in CDRs, that were modeled on the adalimumab Fab structure, while hinge and Fc domain are fully conserved. This suggests the good acceptability of the model, that as expected, show a conserved secondary structure with respect to crystallographic templates (Figure 3A). The Ramachandran plot of the final model showed 15 outliers, all located in loop regions (Figure 3B). The model was then modified by the addition of glycan chains leading to overall three different glycosylated species: aglycosylated, G0 and G0F adalimumab.

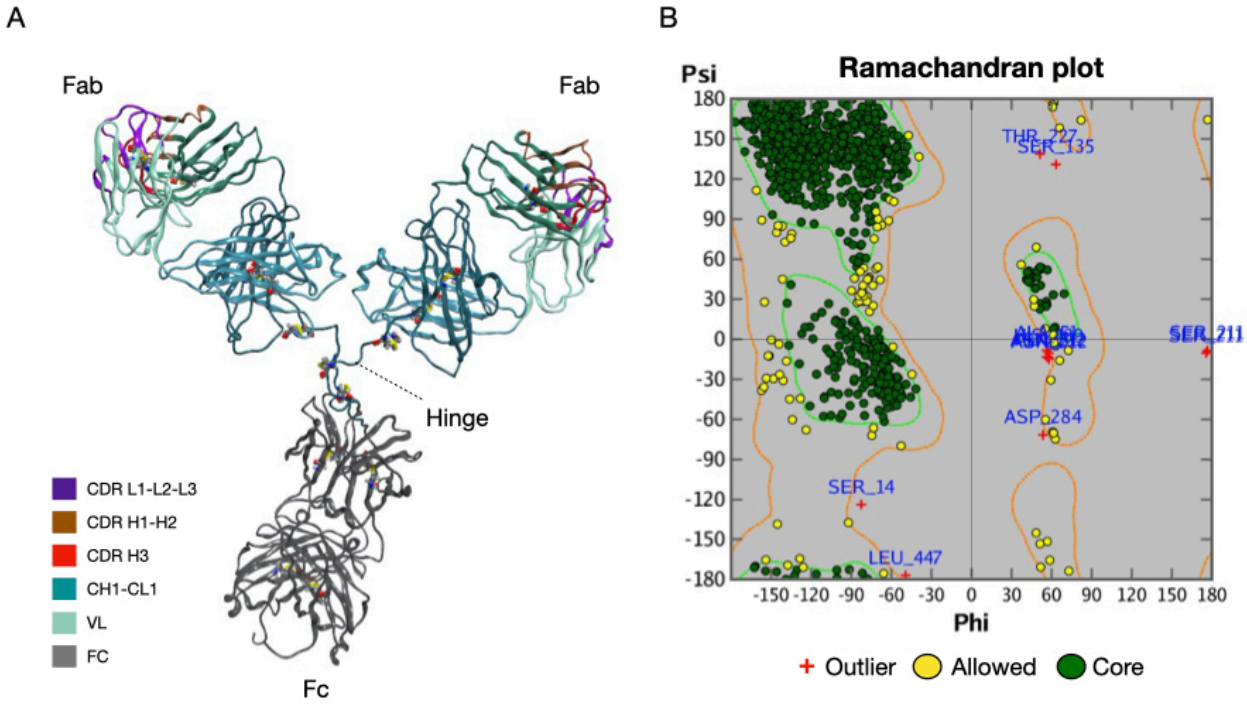

Figure 3: Homology model of aglycosylated adalimumab and corresponding Ramachandran plot. (A) The chimeric homology model of adalimumab rendered as ribbons colored according to Kabat convention[35]. (B) Ramachandran plot: 15 outliers are identified as red crosses, allowed and core angles are represented as yellow and green dots, respectively.

Three independent MD simulations, 400 ns long, were performed in parallel for the three mAbs to estimate the effects of different glycosylation patterns and the impact of glycosylation abrogation on the 3D structure of the protein. To estimate the convergence of simulations, both autocorrelation of potential energy and Root Mean Square Deviation (RMSD) analysis were computed. More specifically, the autocorrelation plots (Figure 4A) show that in all the systems the potential energy reaches a convergence within the first 5000 snapshots (corresponding to 50 ns of MD), suggesting the systems equilibration.

On the other hand, RMSD of atomic positions was computed for C-alpha atoms with respect to the homology model, showing that all the systems get out of the equilibration phase after the first 50 ns. Together to this, three different RMSD profiles were recognized, indicating a significant difference among the three mAbs in the explored conformational space within the simulated time-window (Figure 4B). In detail, the G0 mAb reaches an RMSD equilibrium in about 100ns with a maximum RMSD value of 1.25 nm; the G0F antibody shows an RMSD plateau only after 250ns, reaching a maximum deviation of 2.5 nm; finally, the RMSD of the aglycosylated adalimumab, as for the fucosylated antibody, oscillates during the simulation, with intermediate RMSD values with respect to the afucosylated and the fucosylated systems, spanning between 1-2 nm.

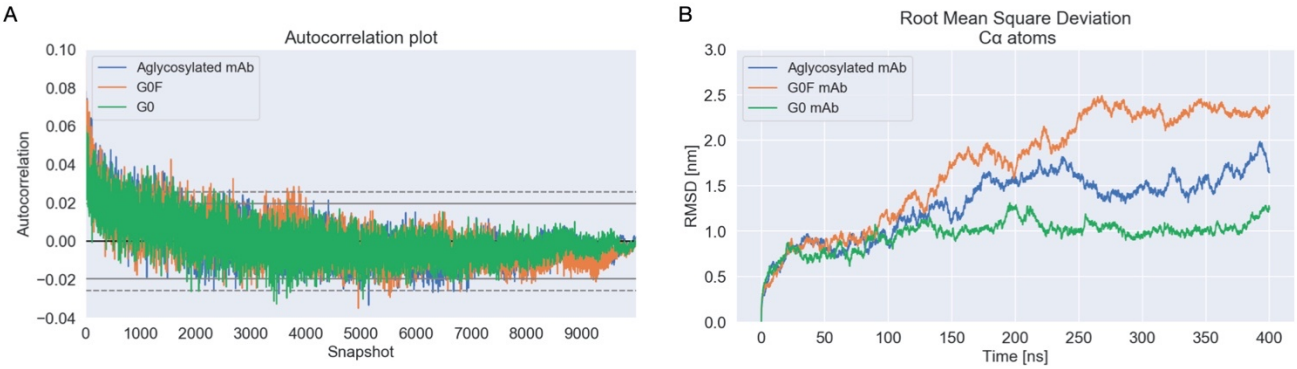

Figure 4: Autocorrelation plot of potential energy and Root Mean Square Deviation (RMSD) analysis. (A) Autocorrelation plot of potential energy computed for three systems. In all cases the autocorrelation value stabilizes under the confidence band within the first 5000 snapshots that corresponds to 50 ns of simulation. (B) RMSD of C-alpha positions computed over trajectory per all three adalimumab forms: aglycosylated (blue) shows an intermediate profile with respect to other antibodies, with some RMSD oscillation during the simulation; G0 (green) reaches a plateau state in 100 ns and G0F (orange) reaches an equilibrium only after 250 ns.

Starting from these preliminary observations, the species were analyzed excluding from calculations the first 50 ns of MD simulations.

The pairwise RMSD distribution was calculated for all systems, showing that the conformational space explored by the G0 antibody is lower than the other two molecules and suggesting that the G0F and the aglycosylated mAbs struggle to find a stable minimum of energy (Figure 5A). Starting from the distribution, a hierarchical divisive cluster analysis was performed for all the trajectories. This type of clustering allows to separate structures in groups basing on a specific cutoff distance. This is the reason why, despite the low exploration observed for the G0 antibody, three clusters were

identified for this trajectory, while two differently populated clusters were identified for the aglycosylated and the G0F antibodies.

The population percentage of computed clusters are the following:

- Aglycosylated mAb: cluster 1 = 33%, cluster 2= 67%
- G0 mAb: cluster 1 = 41%, cluster 2 = 32%, cluster 3 = 27%
- G0F mAb: cluster 1 = 47%, cluster 2 = 53%

This analysis was useful to identify a reference structure to use for visually comparing the conformations reached by antibodies and for illustrating subsequent analyses results. To this purpose, a centroid structure of the most populated cluster was selected per each mAb showing three completely different conformations that are reported in Figure 5B. In particular, the aglycosylated and the afucosylated antibodies show a comparable conformation, in which Fab portions are positioned far away from Fc and the hinge presents an extended orientation. Looking at the fucosylated form a more compact assembly can be recognized, where Fab domains, especially one of the two, are collapsed on the Fc and the hinge region is folded within itself.

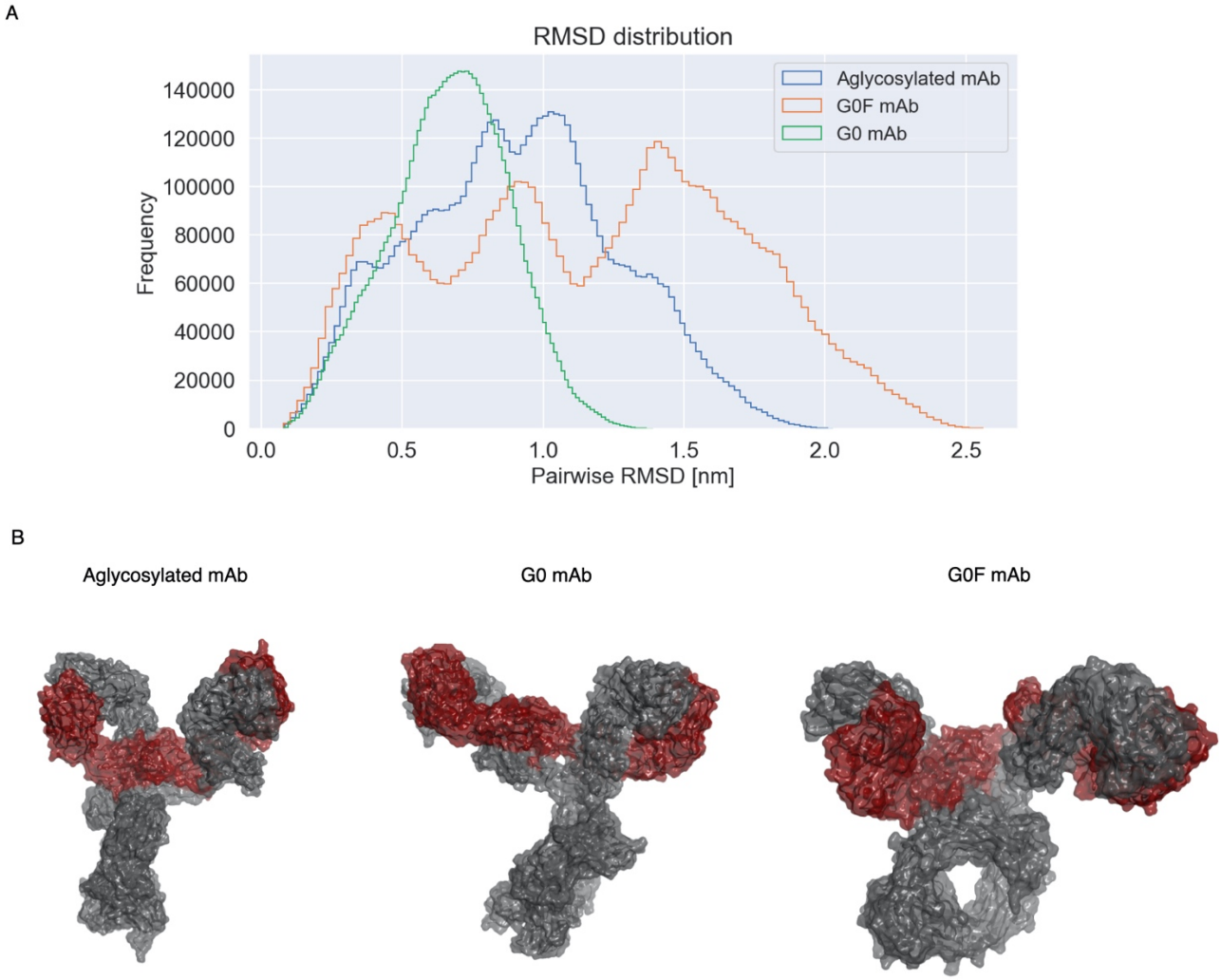

Figure 5: Pairwise RMSD distribution and centroid structures isolated by cluster analysis. In panel A, the pairwise RMSD distribution confirms G0 mAb (green) as the most stable, with less explored conformational space. In panel B, centroid structures identified by cluster analysis and rendered as red (LC) and grey (HC) molecular surface. Glycans are not displayed in this picture.

The radius of gyration (Rg) of the three molecules was calculated over trajectories to estimate the preferred conformation for the antibodies (Figure 6). In fact, Rg is defined as the mass weighted root mean square distance of a collection of atoms from their common center of mass. This analysis can provide an insight into the overall dimensions of the protein and an idea of how much the protein conformation is globular rather than extended.

According to this parameter, and as confirmed by the structural analysis of centroids, the aglycosylated and G0 adalimumab show a more extended and relaxed conformation than the G0F antibody, that, during the dynamics, tends to collapse in a more compact assembly. This is inferred from the higher values of Rg observed for aglycosylated and G0, approx. 4.7 nm and 5 nm, respectively, and the lower value showed by the G0F antibody (approx. 4.4 nm). Looking globally at

trends a displacement of about 1 nm from the start of the production phase to the end can be observed for the G0F adalimumab, suggesting that there is a significative conformational change in this molecule that does not occur in the others. In fact, in the case of aglycosylated mAb, a displacement of only 0.3 nm is recognized, while for G0 antibody the Rg value remains quite constant during the simulation with only some shifts located in specific time frames. This suggests that both aglycosylated and G0 mAbs do not move so far away from the starting Y-shaped conformation, unlike whatever happens for G0F species.

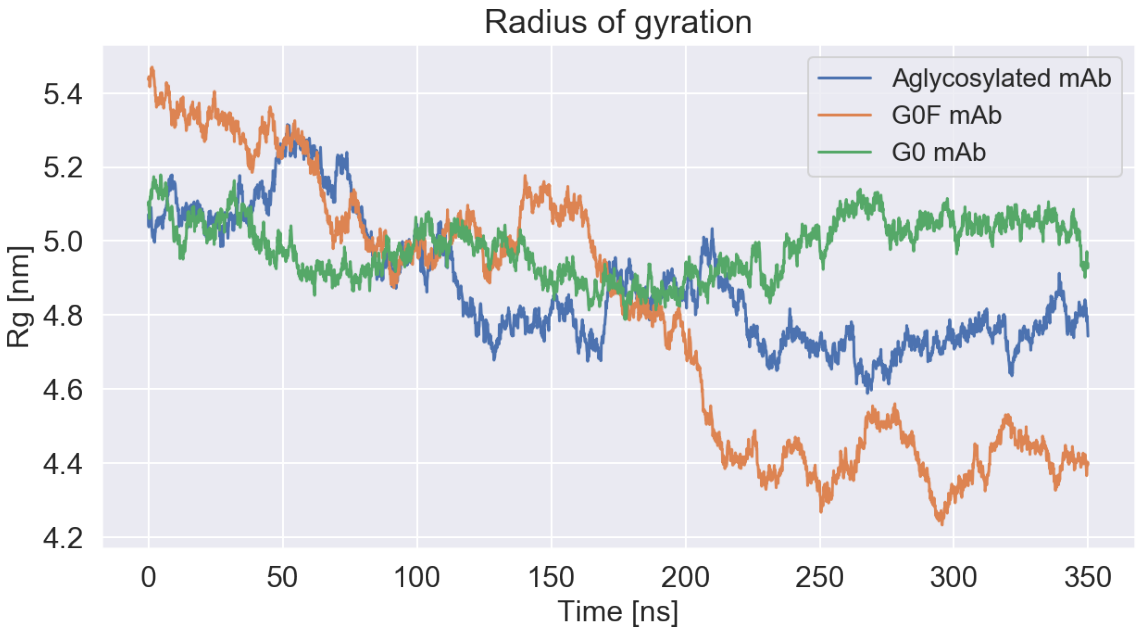

Figure 6: Radius of gyration computed for aglycosylated, G0 and G0F adalimumab. The radius of gyration was computed for the three simulated mAbs showing three different profiles describing three different conformations. The lowest Rg value (approx. 4.3 nm) has been detected for the fucosylated mAb (in orange) suggesting a compact conformation, while both the aglycosylated (in blue) and the afucosylated (in green) show higher values likely corresponding to extended conformations.

The Root Mean Square Fluctuation (RMSF) analysis was computed for C-alpha atoms with respect to the average structure calculated per each trajectory. Then, the pairwise differences among the RMSF values were calculated to identify a fluctuation ranking that can be summarized as follow: $RMSF_{G0F} > RMSF_{aglycosylated} > RMSF_{G0}$ (Figure 7). This ranking likely confirms what previously observed, hence that the fucosylated adalimumab is the most susceptible to conformational changes, followed by the aglycosylated and the afucosylated ones.

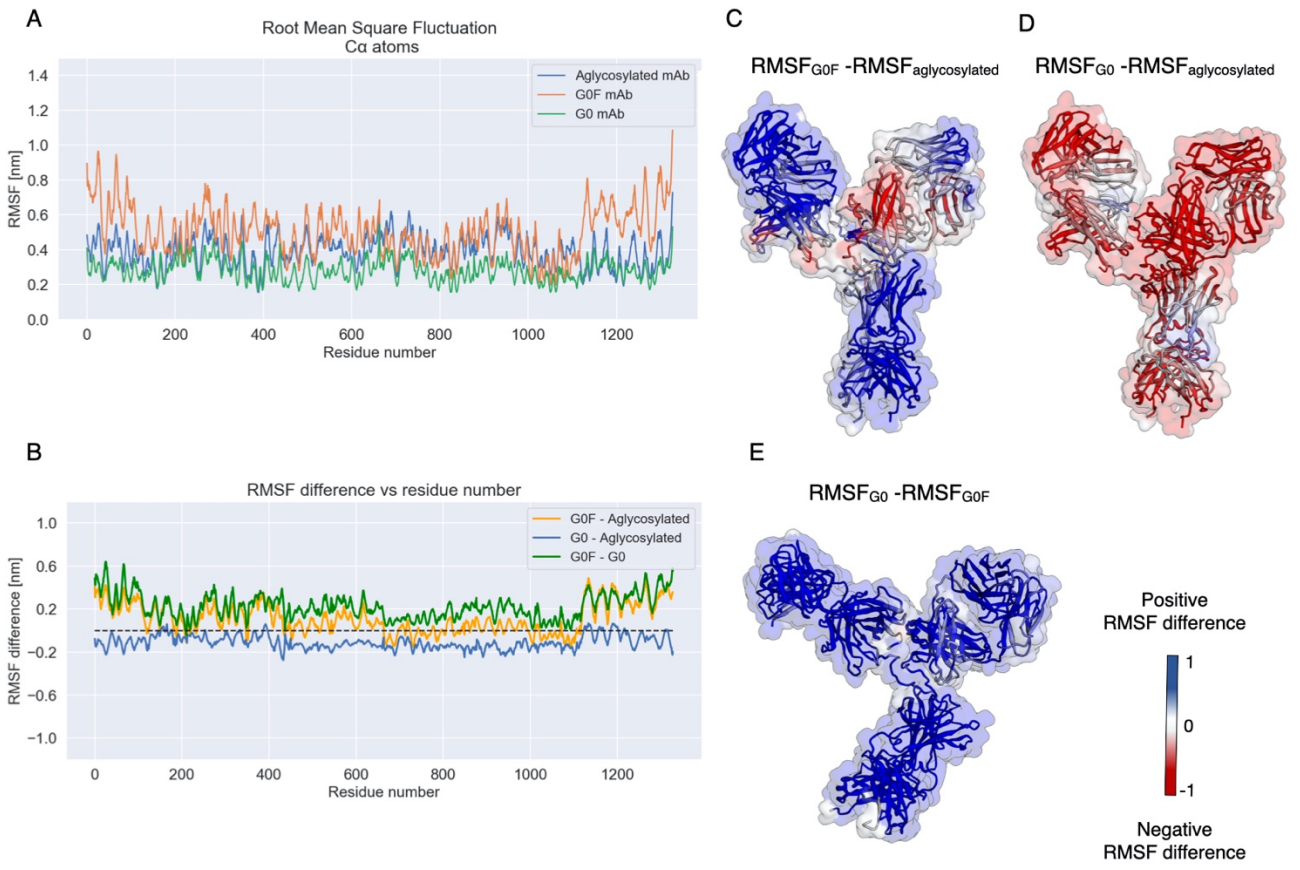

Figure 7: Root Mean Square Fluctuation (RMSF) and RMSF difference. (A) RMSF of C-alpha atoms computed over trajectory with respect to the average structures: aglycosylated (blue) shows an intermediate fluctuation profile, with some regions overlapping the fucosylated one (orange) which is the most fluctuating and other regions with a trend comparable to G0 mAb (green), which shows the lowest fluctuation. (B-E) A plot summarizing RMSF differences between systems and difference map reported in structures according to color gradient: (C) $RMSF_{G0F}$ - $RMSF_{aglycosylated}$; (D) $RMSF_{G0}$ - $RMSF_{aglycosylated}$; (E) $RMSF_{G0F}$ - $RMSF_{G0}$. Fluctuation ranking is the follow: $RMSF_{G0F}$ > $RMSF_{aglycosylated}$ > $RMSF_{G0}$. *In this picture, residues follow progressive numbering: Fab1 (res. 1-436), Hinge (res. 437-457 and res. 1113-1133), Fab2 (res. 677-1112) and Fc (res. 458-669 and res. 1134-1345).*

A structural analysis was computed specifically for the Fc portion, in order to highlight local differences among the three antibody forms. The RMSD contribution of this domain to the whole adalimumab dynamics was isolated, showing very similar trends among the three species (Figure 8A). RMSF calculation was also done, showing overlapped fluctuation trends and definitely confirming that, despite the different glycosylation pattern, the dynamical behavior of three Fc domains is almost conserved (Figure 8B). A structural superposition of Fc portions (Figure 8C) isolated from centroids was then performed showing that also the secondary structure is globally conserved and the main differences are recognized for the loops containing glycosylated Asn residues (Asn518 and Asn1194 in CH2 domains). In detail, as reported in Figure 8C, the loop goes from a closed

conformation (aglycosylated) to an intermediate (G0) and to an open one (G0F), suggesting that glycans induce such a conformational change in this portion, consequently influencing the CH2 domains orientation. This has been already observed in many published works[49] that proposed that an open conformation of Fc, mediated by the presence of sugars, is needed to allow the FcγRs recognition *(see paragraph 1.4, Chapter 1)*.

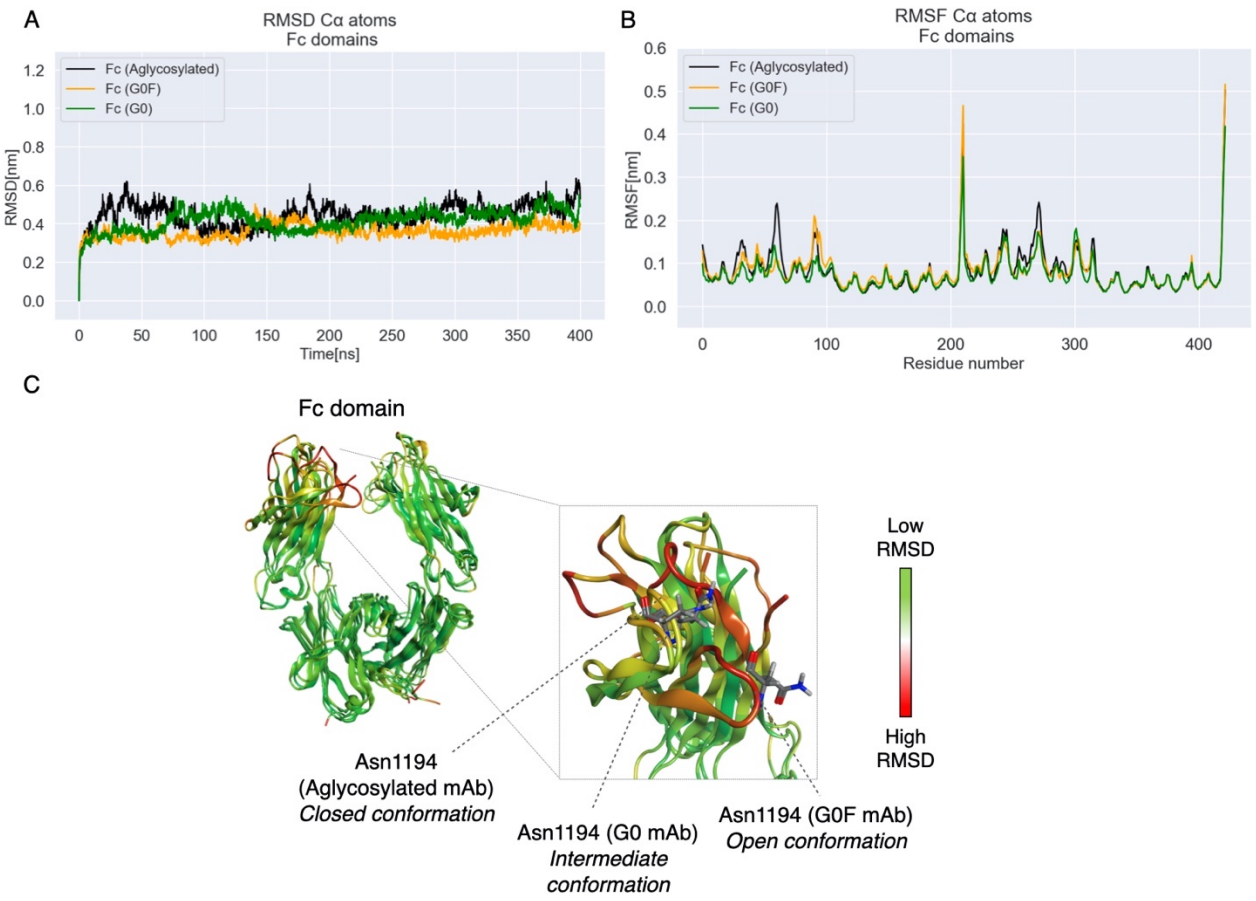

Figure 8: RMSD, RMSF and structural superposition of in aglycosylated, G0 and G0F adalimumab Fc domains. (A) The RMSD computed for C-alpha atoms of Fc portions and (B) the RMSF analysis performed with respect to the average structure shows quite overlapping trends among the three Fc. (C) Structural superposition of Fc domains rendered as ribbons and colored according to a RMSD gradient in which well superposed regions (low RMSD values) are colored in green and bad overlapping regions are colored in red (high RMSD values). The superposition points out a conserved secondary structure among the three domains with different orientations of the glycosylated loop.

Considering the high conformational similarity observed among Fc fragments, we decided to perform a structural superposition of one half of each antibody against the other half with respect to Fc in order to investigate the hinge and Fab domains dynamical behavior. Looking at the superposition

(Figure 9), the two specular Fc parts result well superposed in all antibodies, but Fab domains and hinge regions show different orientations. This suggests that a single antibody molecule can show a huge number of freedom degrees that allow the protein to explore different conformations. This mechanism is essentially due to the high flexibility of hinge portion that, since it is a not structured region, can assume many orientations driving the exploration of Fab domains. However, according to our data, the orientation assumed by the hinge and consequently by Fab arms can be influenced by the presence of glycans and in particular by the fucose. In fact, carefully looking at the three conformations, there is a huge difference in Fab position. This is highlighted both in cluster analysis and in the structural inspection. In particular, as a result of the superposition, in the aglycosylated mAb the two Fab are quite closer (Figure 9A), in the G0 one they are spaced (Figure 9B), with a more extended hinge conformation, and finally in the G0F adalimumab, Fab are located on opposite sides of the molecule, that loses its typical Y-shape (Figure 9C). Although this is a static representation of the molecules, because it represents the most frequent conformation taken by the proteins, it shows a different behavior of the three hinge portions. In fact, the Rg analysis, that is described above, shows a significative conformational change in G0F mAb that reaches a compact conformation during the dynamics, an intermediate dynamical behavior of the aglycosylated antibody and a stable conformational trend for the G0 one, confirming the different number of freedom degrees in the molecules. In conclusion, according to these data, the presence of fucose seems to be responsible for the loss of the typical antibody structural architecture and we hypothesize that this is the cause of the lower affinity to FcγRIIIa.

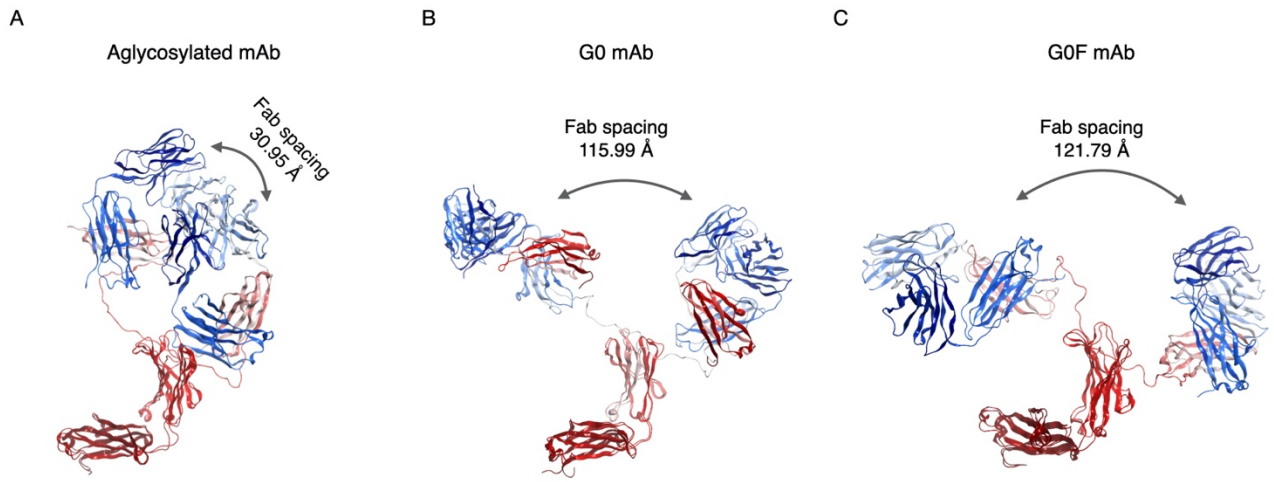

Figure 9: Structural superposition of the antibody's halves. The structural superposition of the two parts of antibodies computed for centroids highlights the huge freedom degrees of Fab domains. In the aglycosylated adalimumab (A) the distance computed among the N-terminal residues of LCs shows that the two Fab are quite close in this conformation; in the G0 form (B) they are more spaced with a distance of 115.99 Å and in the G0F one (C) the distance further increases. Antibodies secondary structure is rendered as ribbons colored according to a terminus color gradient, where N-terminus portions are represented in blue and C-terminus in red.

4.3 Principal component analysis (PCA)

An essential dynamics (ED) was carried out by GROMACS 2019.2[124] to identify principal motions of the protein in the three systems and to better explain the three observed conformations. Looking at the correlation matrices, as expected, a positive correlation of each domain with itself was found. Moreover, whereas a negative correlation between Fab and Fc domains was observed in aglycosylated and G0 mAbs, a positive interdomain correlation was identified between one Fab and Fc for G0F antibody. On the contrary, in all the three systems, Fab portions do not correlate each other suggesting an asymmetric behavior of these domains, that, as hypothesized before, is probably due to the high flexibility of hinge (Figure 10). However, this analysis suggests that more than the presence of glycans *per se*, the fucose can have a role in regulating the movement of single antibody domains, inducing one Fab to move together with the Fc.

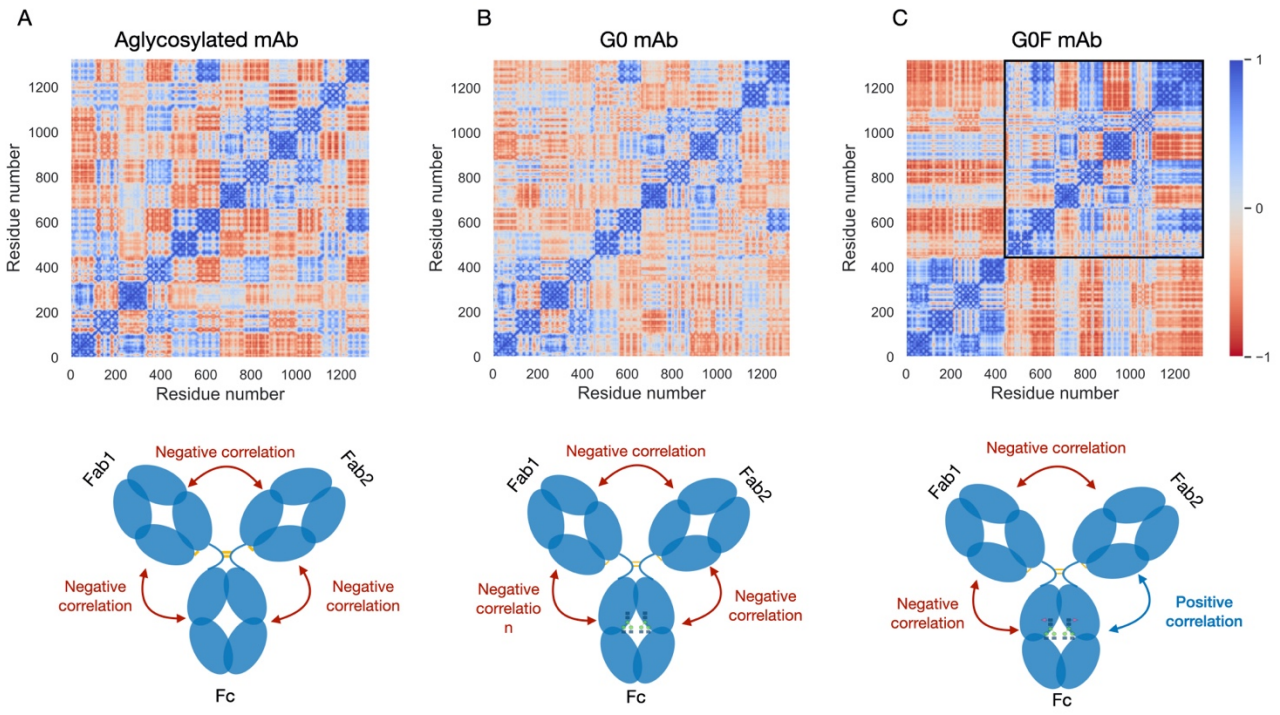

Figure 10: Correlation matrix computed per each trajectory and schematic view of inter domain correlations. Aglycosylated and G0 adalimumab (A-B) present a positive intra-domain correlation (in blue) and a negative inter-domain correlation (in red). Despite the others, fucosylated adalimumab (C) shows also a positive inter-domain correlation between Fab2 and Fc that is highlighted by the black square. *In this picture, residues follow progressive numbering: Fab1 (res. 1-436), Hinge (res. 437-457 and res. 1113-1133), Fab2 (res. 677-1112) and Fc (res. 458-669 and res. 1134-1345).*

Scatter plots representing the 3D subspace in which the first two principal components (PC) of each system exist resulted to be poor comparable, indicating that the three antibodies are characterized by different dynamical behaviors likely responsible of different biological functions (Figure 11 A-C). Moreover, extreme eigenvectors positions were projected to describe more deeply the type of motions. Concerning the aglycosylated mAb, the first component is related to a stretching of the hinge region that allows the molecule to compact and extend itself, while the second component is more related to an anti-correlative rotation of both Fab portions around the hinge. Looking at the G0 antibody, both principal motions are specifically related to one Fab domain that, in the first case makes a rotation around the hinge and in the second case moves far away from the Fc due to the hinge stretching. Regarding the G0F molecule, PC1 is a contraction of the entire structure that induces Fab domains to collapse on the Fc, while PC2 includes the correlated rotation of Fab2 and Fc. These evidences further confirm that the aglycosylated and G0 mAbs show comparable dynamics,

while the G0F one is characterized by a different conformational variability, suggesting the key role of fucose in modulating the structural behavior of IgG1.

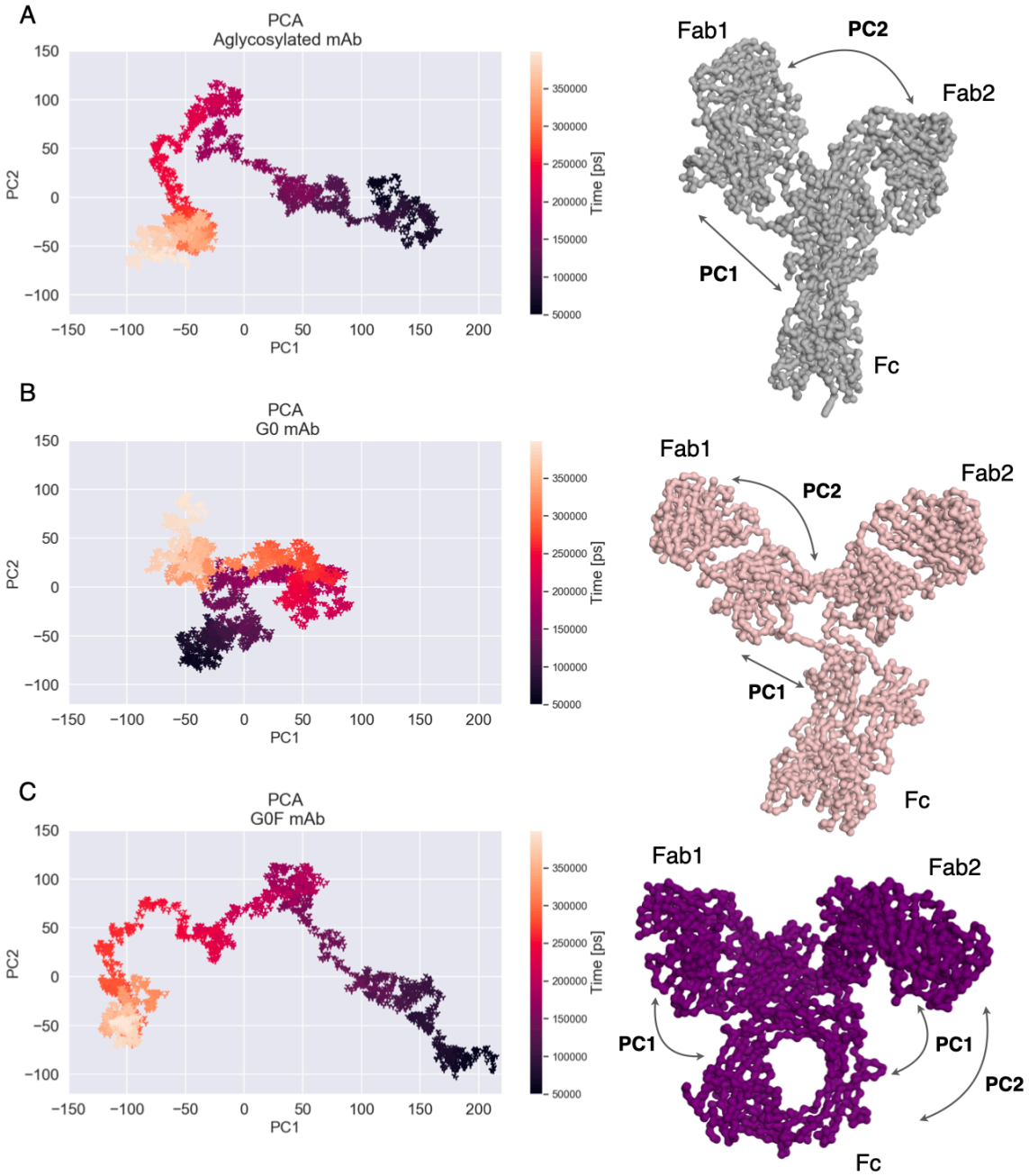

Figure 11: Principal component analysis. Bi-dimensional projection of first two principal components identified by ED and schematic representation of the isolated motions. Both aglycosylated (A) and G0F mAb (C) scatter plots show two well defined motions summarized in structure rendered as C-alpha surface. In the aglycosylated antibody PC1 is a hinge stretching, while PC2 is a rotation of Fab1 around hinge; in the fucosylated mAb PC1 corresponds to a collapse of both Fab domains on the Fc and PC2 to a correlated rotation of Fab2 and Fc. Analyzing G0 mAb components (B), a homogeneity is recognized in the scatter plot between two components resulting into two motions mainly related to Fab1 portion. PC1 corresponds to a rotation of Fab1 around the hinge and PC2 represents a distension of the hinge with a displacement of Fab1.

4.4 Sugars analysis

An analysis of dihedral angles that define the glycosydic bonds among glycan residues was performed in order to estimate the conformational space explored by glycans and to assess their contribution to the variability of dynamic behavior in the two glycosylated molecules (Figure 12). To facilitate data discussion, sugars were numbered progressively and the two chains attached to each half of Fc were named chain A and chain B. First of all, a different behavior of glycan chains connected to the same antibody was observed. In particular, in the chain A of the afucosylated mAb (Figure 12A), the dihedral angles between NAG1-NAG2, MAN4-NAG6 and MAN5-NAG7 resulted to explore a major rotational space with respect to the corresponding couples in chain B (Figure 12B). In fact, concerning chain B, low frequency exploration motions were reported only for MAN3-MAN4 couple, suggesting that, globally, the explored conformational space is higher in chain A than in chain B. Looking at fucosylated mAb (Figure 12C and 12D), the major differences were recognized for MAN4-MAN5 dihedral angle in chain B, which assumes two different orientations, and for MAN6-NAG8 which shows a slight exploration. The other glycan residues of G0F chains (both in chain A and B) seem to be locked in a single state. Moreover, according to the data shown above and by comparing overall G0 and G0F, different rotational freedoms were observed for G0 and G0F sugars and, more specifically, G0 appears more flexible than G0F (Figure 12E and 12F).

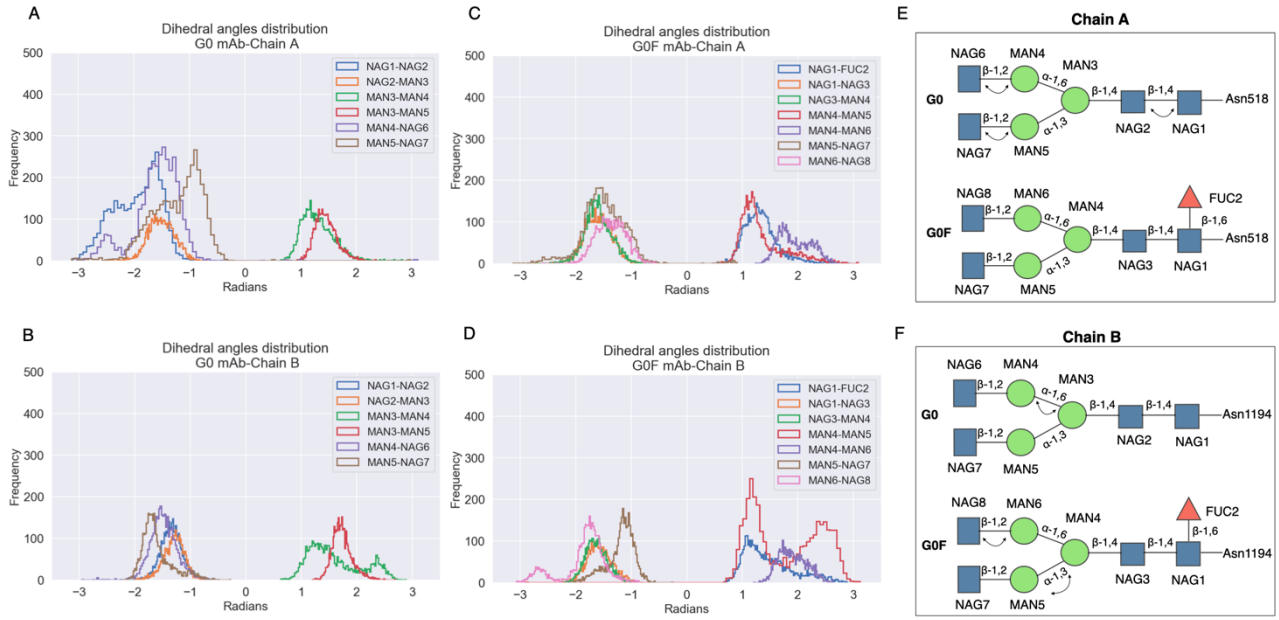

Figure 12: Distribution of dihedral angles in sugars. (A-B) Distribution of dihedrals amplitude in G0 glycan chains A and B. In chain A dihedrals explore a higher conformational space than in chain B, mainly located in terminal sugars (NAG1-NAG2; MAN4-NAG6; MAN5-NAG7) for chain A and in MAN3-MAN4 couple for chain B. (C-D) Distribution of dihedrals amplitude in G0F glycan chains A and B. A very low exploration is recognized for both chains: only the angle formed by MAN4 and MAN5 residues in chain B explores two states, while a slight exploration is observed for MAN6-NAG8. On the right (E-F) a schematic representation of glycan chains according to the SNFG system[32] is reported together with the most flexible angles indicated by arrows.

An analysis of the hydrogen-bonds (H-bonds) network between sugars and antibodies was performed to further assess the role of carbohydrates in stabilizing or destabilizing the antibody 3D structure. A list of H-bonds computed according to the Baker-Hubbard criterion and occurring with a frequency up to 10% is reported in Tables 2 and 3.

Table 2: H-bonds list between G0 glycan and adalimumab. H-bonds were computed according to Baker-Hubbard criterion and with a frequency threshold equal or up to 10%.

G0 glycan (Chain A) - antibody		G0 glycan (Chain B) - antibody	
Antibody residue	Glycan unit	Antibody residue	Glycan unit
Lys1217.NZ	NAG1.O5	Gly457.N	MAN4.O6
Lys1217.NZ	NAG1.O6	Val461.N	NAG6.O3
Lys1231.NZ	MAN5.O4	Glu554.N	NAG6.O6
Thr1232.N	MAN5.O3	Lys555.NZ	NAG6.O4
Thr1232.OG1	MAN5.O3	Gly1134.N	MAN4.O2
Ser1234.OG	NAG7.O7	Tyr1193.OH	NAG1.O5
		Tyr1193.OH	NAG1.O6

Table 3: H-bonds list between G0F glycan and adalimumab. H-bonds were computed according to Baker-Hubbard criterion and with a frequency threshold equal or up to 10%.

G0F glycan (Chain A) - antibody		G0F glycan (Chain B) - antibody	
Antibody residue	Glycan unit	Antibody residue	Glycan unit
Tyr517.OH	NAG3.O7	Ser460.OG	MAN5.O6
Arg522.NH2	NAG1.07	Val544.N	NAG7.O3
Thr1233.N	FUC2.O2	Ser1137.OG	NAG3.O3
Thr1233.OG1	FUC2.O3	Val1138.N	NAG8.O4
Ser1235.OG	MAN5.O5	Gln1193.NE2	NAG1.O5
Ala1237.N	NAG8.O7	Gln1193.NE2	NAG1.O6
Lys1238.N	MAN5.O6	Arg1199.NH1	FUC2.O2
LYS1238.N	NAG7.O7	Lys1232.NZ	MAN5.O2
Ser1273.N	MAN6.O6	Lys1232.NZ	MAN5.O3
		Lys1232.NZ	NAG8.O6
		Lys1232.NZ	MAN5.O2
		Lys1232.NZ	MAN5.O3
		Ser1137.OG	NAG3.O3
		Val1138.N	NAG8.O4

The total number of H-bonds computed over time per each glycan chain is also reported in Figure 13 panels A-B, showing that G0F chain is involved in a higher number of interactions than G0 (a total of 23 vs 13 H-bonds, respectively, see Tables 2 and 3). Specifically, concerning G0 glycans only NAG1, MAN5 and NAG7 in chain A and NAG1, MAN4 and NAG6 in chain B are involved in multiple interactions with the antibody, while looking at G0F, almost all glycan residues make H-bonds interactions with the protein. These data suggest, once again, the higher flexibility of G0 with respect to G0F.

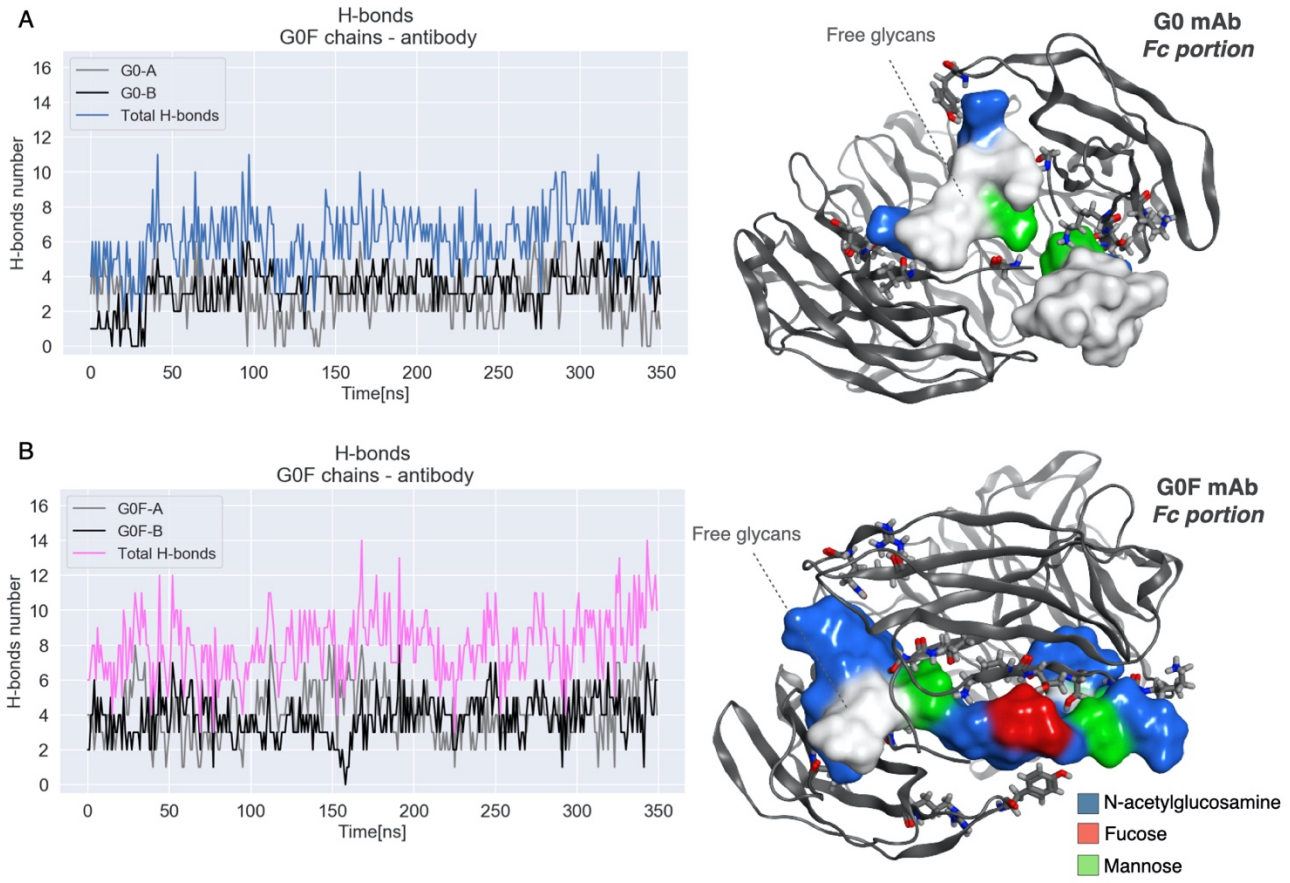

Figure 13: H-bonds number between glycans and respective mAb vs simulation time. (A) The H-bonds number between single G0 chains (A and B, in grey and black) and the antibody and the total number of interactions (in blue). (B) The H-bonds number between single G0F chains (A and B, in grey and black) and the antibody and the total number of interactions (in magenta). On the right a zoom of afucosylated and fucosylated Fc portions rendered as grey ribbons and the graphical representation of identified H-bonds. Glycans involved in H-bonds are represented as sticks colored according to the SNFG system[32], free glycans are colored in grey.

4.5 Discussion

One of the main peculiarity of antibodies is their high flexibility that is mainly due to the hinge region. This portion is completely not structured and can adopt a great number of orientations influencing the antibody tertiary structure. Because of this feature, strong efforts are required to experimentally investigate the conformational behavior of mAbs. In fact, to determine the whole atomistic structure of these molecules *via* crystallography or other experimental techniques is a big challenge, thus up to now only one structure of a whole IgG1 is available in PDB[115]. Moreover, investigating the entire conformational space explored by proteins, especially antibodies, is really hard by using experimental methods *(i.e.*, X-ray), since by crystallography only a snapshot of the molecule in specific experimental conditions can be observed. For this reason, MD studies can be a very useful tool to elucidate the dynamics of antibodies and to isolate the huge variety of possible conformations explored by the molecule.

On this basis, the first part of this PhD thesis has been focused on the prediction of the 3D structure of the whole adalimumab molecule, for which the crystal structure of Fab portion is published, and on MD simulations of the aglycosylated and two differently glycosylated adalimumab forms, G0 and G0F.

According to reported data, a wide range of conformations is explored by antibodies in all the simulated systems, both in the aglycosylated one, where the impact of glycans is not considered, and in the two glycosylated forms. However, three different dynamics were observed for the three species, suggesting that antibodies are very flexible molecules able to adopt a huge number of reasonable conformations and that Fc N-glycosylation, particularly the fucosylation, extensively affects their whole conformational behavior and not only the Fc structure.

This was confirmed by the geometric parameters, like RMSD, RMSF and radius of gyration and by the PCA. In fact, according to our data, three different RMSD profiles were detected, suggesting that a different conformational space is explored by the three antibody forms. In particular, the afucosylated mAb resulted to be the most stable one, reaching an RMSD equilibrium within the first 100 ns of simulation, likely corresponding to a stable conformation. On the other hand, the fucosylated antibody reaches an RMSD plateau only after 250 ns, showing also the highest fluctuation profile among the three mAbs. For what concern the aglycosylated form, it shows an intermediate behavior in all the computed parameters, by which we cannot say that the system does not reach a real equilibrium or that it does. This suggests that the absence of glycans negatively contributes to

the stability of the molecule, but probably is not so critical for maintaining the tertiary structure as the presence of fucose. In fact, by comparing antibodies, the absence of sugars likely induces conformations not so different from the starting one, similarly to what happens for the afucosylated antibody, while the presence of fucose is responsible for a huge conformational exploration of the molecule. The structural analysis of centroid structures obtained *via* cluster analysis better showed that the different trends recognized by geometric analysis correspond to three different conformations of simulated antibodies. This observation was confirmed by the Rg calculation, that supports the structural analysis and better defines the compact conformation reached by G0F antibody and the extended orientation observed for G0 and aglycosylated mAbs.

Focusing on the dynamics of Fc fragment, that according to literature should be the domain mostly influenced by glycosylation, comparable geometric parameters among the three investigated mAbs were obtained, suggesting that this portion does not undergo to significative conformational changes. However, the structural superposition highlighted a difference in the loop linked to sugars, that can adopt different orientations depending on the glycosylation. This is perfectly aligned to what is reported in published studies, that demonstrate a role of glycans in modulating the Fc orientation, particularly the glycosylated loops and CH2 domains. So, the structural superposition of the two halves of each antibody with respect to the Fc, deeply clarified that most of conformational rearrangements occur in Fab domains. These portions, driven by the high hinge flexibility, can assume a wide range of orientations and in these are influenced by the presence of glycans, particularly the fucose that determines the freedom degrees of the molecule. This finding was further confirmed by PCA, demonstrating that each antibody is characterized by different principal motions, influenced by the glycosylation pattern and translated in different antibody conformations, likely responsible for different biological functions. Moreover, by PCA a negative correlation between all domains can be detected in aglycosylated and G0 adalimumab, suggesting that they do not show essential concerted motions. Considering G0F mAb, a positive inter-domain correlation between one Fab and Fc was instead revealed, indicating that these two domains move in a synergistic way, but also that even in this case Fab arms move independently. So, the hypothesis is that the presence of fucose induces some conformational constraints that force two domains (one Fab and Fc) to move in a coordinated fashion, but generally in all the investigated forms Fab domains are not affected by the same dynamics.

Moreover, the modulatory role of fucose has been further confirmed by the analyses performed on sugars that show a higher mobility of G0 chains with respect to G0F, which is completely involved in

H-bonds interactions with the protein. Therefore, sugars and protein influence each other and, whereas more flexibility is observed for glycan chains, less fluctuations are recognized for the corresponding antibody. According to these evidences, the conclusion of the first part of this thesis is that the G0F antibody needs to more extensively explore its conformational space to find stable conformations since the fucose introduces some structural constraints that can change both the sugar conformational freedom and protein dynamics. Moreover, there is an intrinsic flexibility in antibodies that allows a huge conformational exploration of Fab arms, but the type of explored space is strongly influenced by glycans composition. According to the data shown above, in fact sugars act as structural and dynamic modulators of IgG1 and specifically the presence of fucose has an impact on the overall antibody conformation.

Taken together, all these data can give a structural explanation of why fucosylated antibodies, despite the open Fc conformation, are less prone to interact with FcγRIIIa, as reported by published experimental data. Hence, we propose that the G0F antibody is blocked in a conformation which could not be properly compatible with accommodating the receptor and that the fucose, modulating both glycans and antibody behaviors, is the main responsible of this. Differently, in the G0 mAb, the lack of fucose confers to the molecule more freedom degrees, allowing it to adopt a conformation suitable for FcγRIIIa binding. Thus, the changes observed in Fc conformation, that are mainly related to CH2 domains, are probably a necessary but not sufficient condition to stabilize the receptor binding and there is a mechanism of interaction regulated by the dynamics of the whole antibody, likely influenced by glycans.

The conformational change as mechanism of interaction between the mAb and the receptor has been already proposed by Kiyoshi and colleagues[56] who, starting from an X-ray structure of Fc::FcγRI complex, suggested that Fab portions may adopt a specific conformation to allow the antibody-receptor interaction, highly supporting our findings. In fact, even if the study by Kiyoshi *et al.* was performed for the high affinity receptor, a mechanism based on conformational changes could be more critical for the recognition of low affinity receptors, like FcγRIIIa, and for this reason the impact of fucose on the whole antibody conformation may be more detectable for the binding to this receptor.

Since the scope of this thesis is to elucidate the role of fucose in modulating Fc effector functions, particularly ADCC activity, the next chapter will be focused on the study of antibody::FcγRIIIa complexes that was carried out to further clarify this preliminary hypothesis.

Chapter 5

Results and Discussion: part II

In this chapter, the dynamical behavior of afucosylated and fucosylated adalimumab in complex with FcγRIIIa-V158 variant (hereinafter denominated FcγRIIIa) is investigated and compared with the behavior observed for a crystalized Fc::FcγRIIIa complex *via* molecular dynamics simulations.
In next paragraphs, the following steps, that were performed to this scope, will be better described:

- Homology modeling, starting from conformations obtained from previous simulations, of fucosylated and afucosylated adalimumab in complex with FcγRIIIa;
- MD simulations of modeled complexes to analyze structural differences together with the structural stability of differently glycosylated species;
- MD simulations of X-ray structures of both fucosylated and afucosylated Fc::FcγRIIIa complexes to compare the behavior of the complexes in absence of Fab domains.

5.1 Homology modeling and MD simulations of G0 and G0F adalimumab in complex with FcγRIIIa

The 3D model of fucosylated and afucosylated adalimumab in complex with FcγRIIIa-V158 variant (hereinafter denominated FcγRIIIa) was obtained by a chimeric homology modeling approach (*see section 3.1, Chapter 3*), merging two different templates: a centroid structure extracted from previously analyzed MD trajectories was used to model the antibody molecule, while the X-ray structure of a Fc::FcγRIIIa-V158 complex (PDB ID: 3SGJ[57]) was chosen to orient the receptor with respect to the antibody. Ramachandran plots of two complexes show 10 outliers in the G0 model and 12 in the G0F complex, all located in loop regions. Looking at secondary structure, both in antibodies and in the receptor a typical Ig-like assembly is observed, characterized by β-sheets connected by loops and stabilized by disulfide bonds. For what concern the receptor glycosylation patterns, only two out of five N-glycosylation sites were considered. In particular, G1F and G2F2 glycan chains (Figure 1) were added to Asn45 and Asn162 (X-ray numbering[57]), respectively, because, as reported by literature, the glycosylation at these two sites is necessary for the cellular expression and the biological activity of FcγRIIIa[57,128]. Moreover, the other three potentially glycosylated sites were mutated both in the X-ray structure (N38Q, N74Q, N169Q mutations) and in the model and finally, since for crystallographic studies the receptor was expressed in HEK293 cells, glycosylation patterns were chosen basing on glycans species abundance in this cell line, as reported by Zeck *et al*[129].

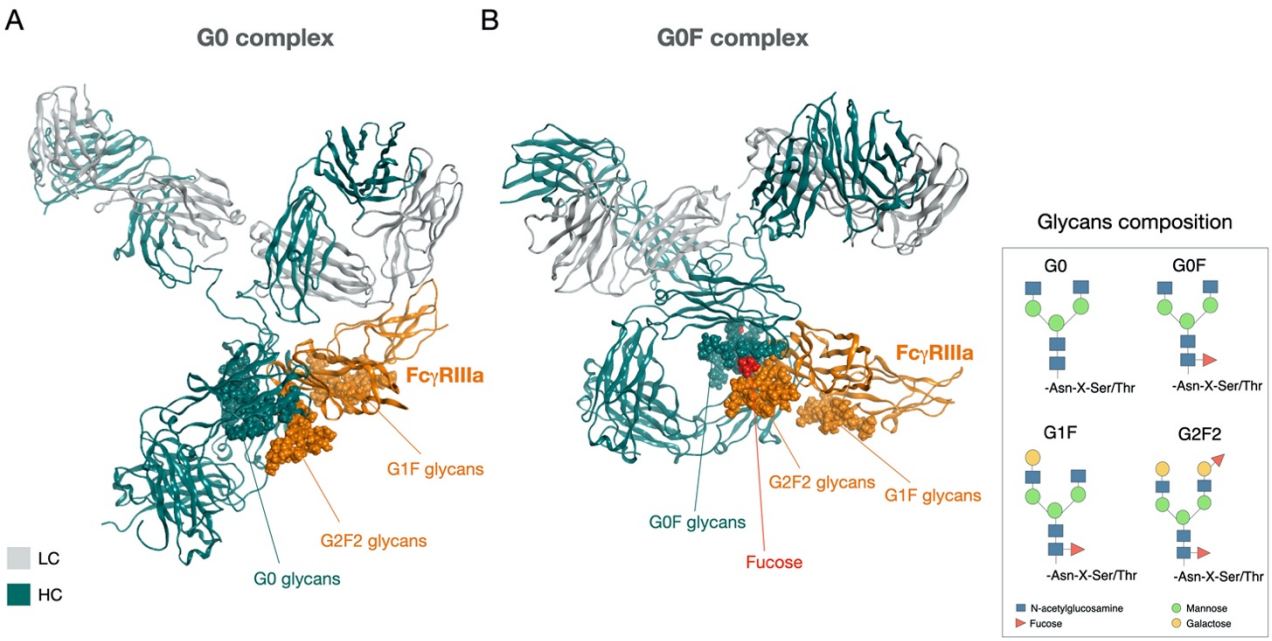

Figure 1: Homology modeling of G0 and G0F adalimumab in complex with FcγRIIIa. (A) G0 and (B) G0F adalimumab in complex with FcγRIIIa. The structures are represented as ribbons: antibody LC in grey, antibody HC in green and the receptor in orange. Glycans are represented as spheres and colored according to the same color code. On the right a scheme of glycans present in the complexes is reported according to the SNFG[32].

An MD simulation 1μs long was carried out for each complex (G0/G0F adalimumab::FcγRIIIa) by NAMD 2.13 package[121] handled by MOE GUI[113] (*see section 3.6, Chapter 3*).

The autocorrelation plot of potential energy (Figure 2A) was computed to evaluate the systems convergence and basing on this, the first 50ns of trajectory were excluded from the analyses and considered as equilibration step. In fact, in both G0 and G0F systems, the autocorrelation value is stabilized in the confidence band within the 0-50 ns time-window.

RMSD profiles were computed for C-alpha atoms positions, splitting the antibody and the receptor contributions (Figure 2B). In particular, for both complexes FcγRIIIa immediately reaches an equilibrium with a maximum RMSD value of 0.27 nm for the G0 system and 0.23 nm for the G0F one. As for the antibodies, two different conformational behaviors were observed. In the G0 an RMSD plateau is reached within the first 300 ns with a maximum RMSD value of 0.9 nm, on the other hand, the G0F adalimumab seems to find a stable conformation after 650 ns of simulation. However, this equilibrium seems to be lost in the last 50 ns, where the RMSD reaches a value of 1.66 nm.

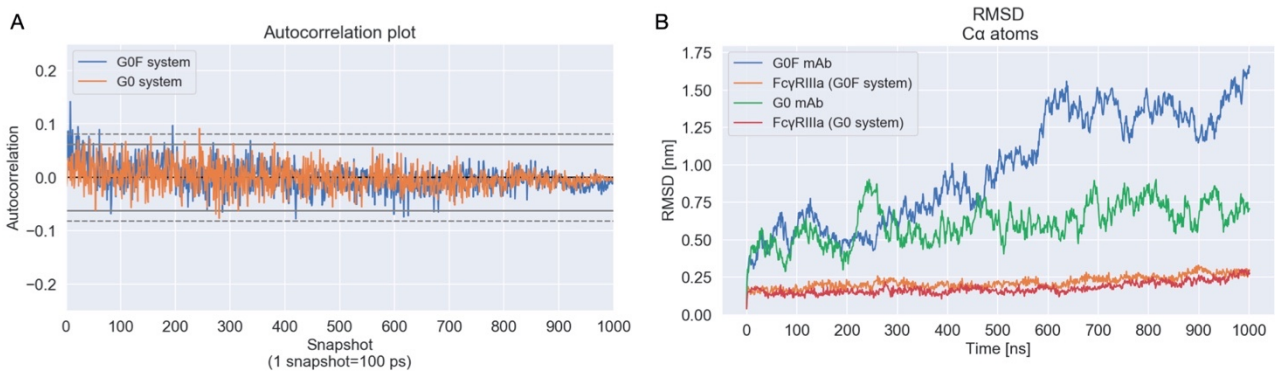

Figure 2: Autocorrelation plot of potential energy and RMSD profiles of systems. (A) Autocorrelation plot of potential energy computed for G0 and G0F systems. In both cases the autocorrelation value stabilizes under the confidence band within the first 500 snapshots that corresponds to 50 ns of simulation. (B) RMSD calculation computed for C-alpha atoms of both antibodies and receptors. The RMSD plot shows overlapping trends for the receptors and different profiles for the antibodies, suggesting the great impact of adalimumab conformational changes on the stability of the whole complex. G0 adalimumab (in green) seems to reach a stable conformation after 300 ns, while G0F (in blue) only after 600 ns, with an increase in RMSD value in the last 50 ns of simulation.

Since the main contribution to system stability is given by the antibodies, RMSD calculation was also performed for each antibody domains to evaluate the impact of each portion on the conformational behavior of the whole molecule (Figure 3). In order to facilitate data discussion, the following nomenclature was chosen as a convention to distinguish Fab parts and corresponding hinge regions: Fab1 refers to the Fab positioned in proximity of the receptor, Fab2 is the domain located oppositely to the receptor and the two hinge parts are named Hinge 1 and Hinge 2, respectively.

Whereas in G0 adalimumab, a general conformational stability was detected for all domains, which is aligned with the RMSD profile of the whole antibody (Figure 3A), in G0F mAb Fab domains and Fc do not seem contributing to the higher exploration of the molecule and unexpectedly, also the hinge portion seems not so relevant toward the overall movement of the protein (Figure 3B). To deeply elucidate why G0F mAb struggles to find a stable conformation, 10 residues upstream and 10 residues downstream to the hinge regions were considered for RMSD calculation. Specifically, a huge instability was detected for Hinge 1 $\pm$ 10 residues, suggesting that this portion is responsible for most of conformational changes in the G0F molecule and that probably it can drive the movement of the corresponding Fab domain, namely Fab1. The same analysis was performed for G0 antibody, where this RMSD oscillation is not detected and there is a major stability even in this portion. Figure 3C contains a graphical representation of domains considered for this analysis.

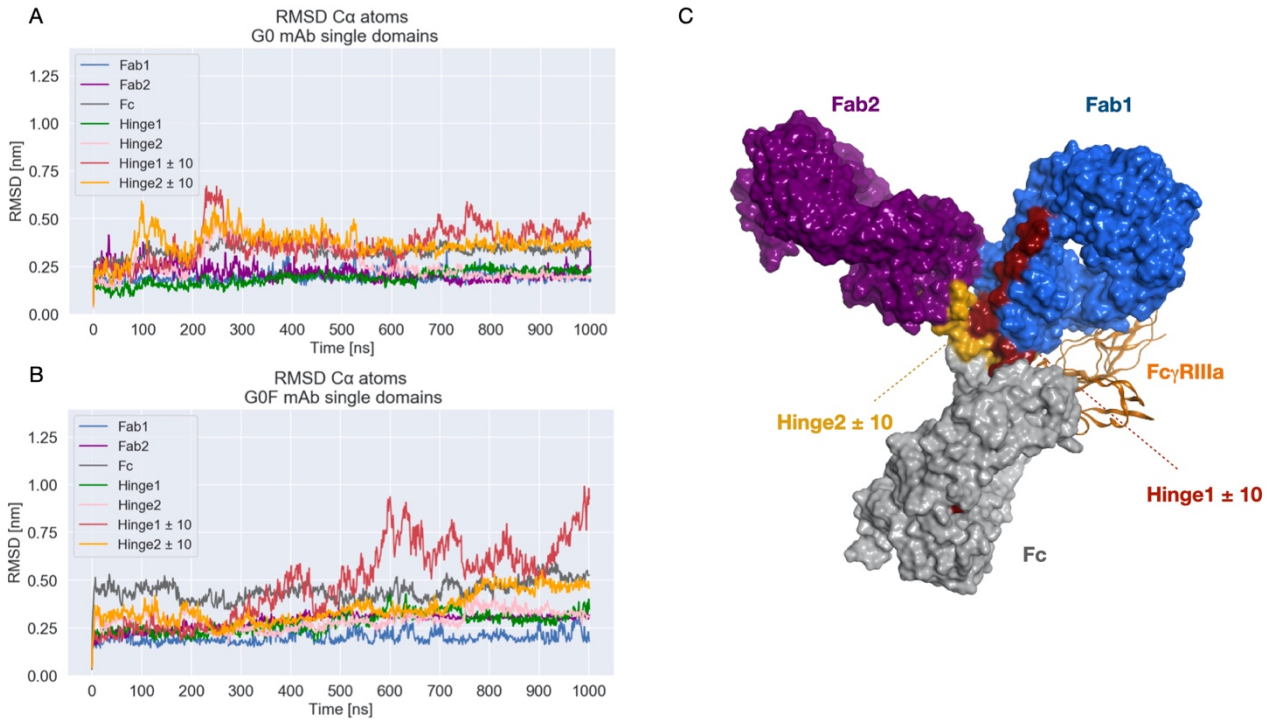

Figure 3: RMSD of C-alpha atoms computed for single antibody portions. (A) RMSD of G0 domains; (B) RMSD of G0F domains; (C) Schematic representation of antibody domains organization: Fab1 (in blue), Fab2 (in purple), Fc (in grey). For what concern the hinge region, Hinge1 and Hinge2 $\pm$ 10 residues are indicated in red and orange, respectively. Afucosylated adalimumab model was used for the illustration.

RMSF analysis was carried out for the complexes and also in this case the antibody and the receptor fluctuation profiles were separated (Figure 4). Globally, a higher fluctuation trend was recognized for G0F antibody than for G0 one, while overlapping trends were observed for receptors. Specifically, whereas FcγRIIIa reaches very similar RMSF values in the two systems (with a maximum of 0.23 nm and 0.27 nm in G0 and G0F system, respectively), the antibodies RMSF profiles are quite different as confirmed by the maximum values reached (0.57 nm in G0 mAb and 0.8 nm in G0F one).

The highest fluctuation observed for G0F mAb is mainly related to Fab1, Hinge1 and the corresponding CH2-CH3 domains in Fc, suggesting that one half of the mAb is more susceptible to conformational changes with respect to the other one and confirming what observed in the RMSD analysis, that shows that this movement is driven by Hinge1. So, basing on this analysis, the antibody half located in proximity of the receptor, shows a different structural behavior in the two glycosylated species. However, we cannot exclude that this movement can interest also the other part of the antibody, since we must consider that the structures used for these simulations were obtained from the previous ones and an extensive set of simulations would be required to further investigate this aspect.

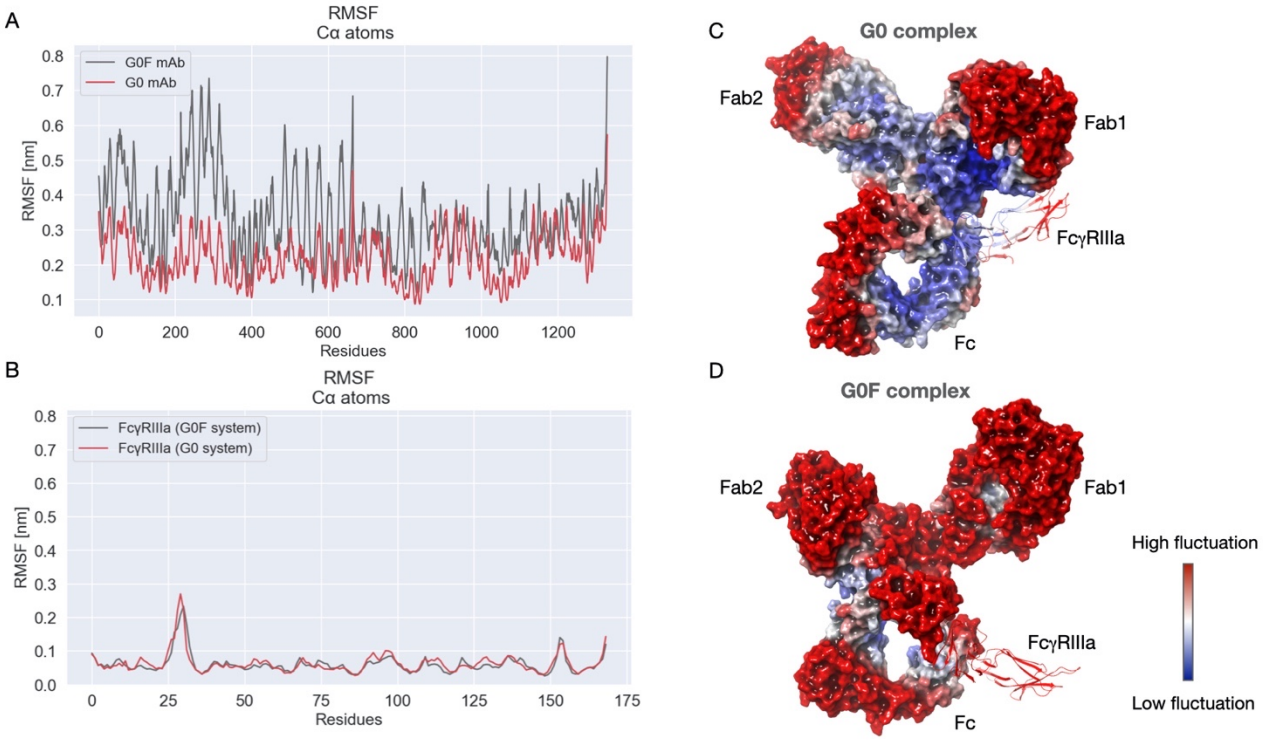

Figure 4: RMSF analysis computed for C-alpha atoms of G0 and G0F systems. (A) RMSF profiles of G0 and G0F antibodies and (B) of FcγRIIIa in the two systems. Panels C-D show a graphical representation of RMSF values as B-factor in the 3D structure of complexes. Antibodies molecular surface and receptors secondary structure are colored according to a red-white-blue gradient scale that corresponds to high-no-low fluctuation. G0F adalimumab shows a higher fluctuation profile than G0 one and by structural representation the difference between Hinge1 and Hinge2 fluctuation is also highlighted. *In this picture, residues are numbered as follow: Fab1 (G0: res. 876-1310; G0F: res. 209-643), Fab2 (G0: 207-642; G0F: res. 878-1312), Hinge1 (G0: res. 1311-1330; G0F: res. 644-664), Hinge2 (G0: res. 642-661; G0F: res. 1313-1333) and Fc (G0: res.663-873 and res. 1332-1542; G0F: res. 665- 875 and res. 1334-1544); FcγRIIIa (res. 1-171).*

5.2 Structural analysis of complexes

A hierarchical cluster analysis was carried out for both trajectories to isolate the most frequent conformations. First, the RMSD distribution was computed, highlighting the higher exploration performed by G0F system (data not shown). Then, two clusters were isolated from each trajectory with the following population percentage:

- G0 system: cluster1= 72%, cluster2= 28%
- G0F system: cluster1= 35%, cluster2= 65%

A structural superposition of centroid structures computed per each cluster was performed in order to identify structural differences among the two pools of conformations highly explored by complexes (Figure 5). Since, as observed by previous geometric analysis, the FcγRIIIa was stable in

both cases, the structural superposition of centroids was performed with respect to the receptor, in order to better highlight the differences in antibodies orientation.

Carefully looking at G0 clusters, the main differences can be recognized in the orientation of Fab domains that result to be slightly displaced after the superposition, thus suggesting that in this case most of exploration occurs in these portions. Analyzing G0F centroids, the difference is more specifically related to the Fab positioned near to the receptor (Fab1) that can assume two different conformations, one close to the Fc and the other one far away from it. This is likely due to the higher fluctuation of Hinge 1 and near residues, as previously observed in RMSD and RMSF analysis. The dynamics of Hinge1 can be explained as a compensatory effect due to the blocking of Hinge2 and corresponding Fab and Fc domains that is mediated by fucose, as demonstrated by sugars network analysis and PCA conducted for previous simulations (*see paragraphs 4.2 and 4.3, Chapter 4*).

However, since among centroids there are not significative differences in Fc orientation and in the region involved in binding with receptor, structures obtained from the most populated clusters have been used for further evaluations.

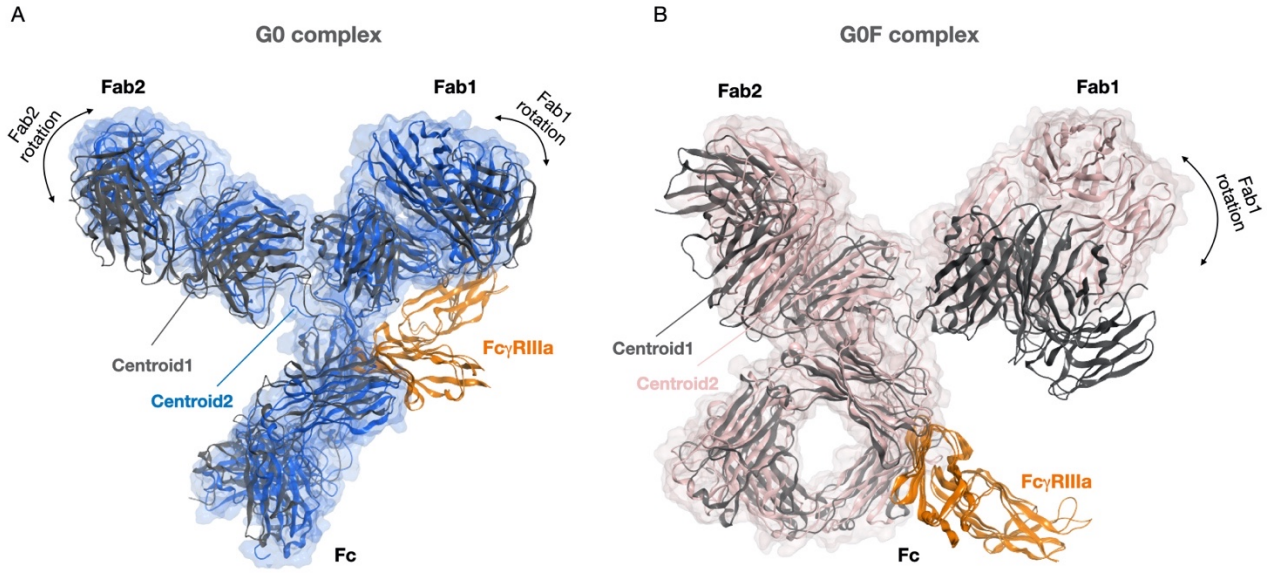

Figure 5: Structural superposition of centroids identified by cluster analysis. (A) The superpose of G0 centroids highlighted a conformational exploration essentially driven by Fab domains. (B) In the case of G0F structures, the main difference among two centroids is due to the exploration done by Fab1 domain.

In order to deeply describe the conformational behavior of antibodies, a more detailed structural analysis was carried out on specific conformations reached by complexes during the dynamics. In detail, 21 structures, each one saved every 50 ns of simulation, were isolated and superposed per each complex after a minimization step towards an RMS gradient of 0.1 kcal/mol/Å^2 (Figure 6). In

both systems, only low conformational exploration can be detected for Fc and receptor, while more mobility is recognized for Fab domains. Considering the molecular assembly, the comparison between Fab domains was done basing on the receptor position, showing that the Fab domains located in proximity of the receptor exert a different behavior in two systems. In particular, whereas in G0 complex this Fab seems to be involved in some interactions with the FcγRIIIa, that probably stabilize its dynamics, in G0F complex the same domain shows a huge flexibility, exploring a wide variety of conformations and never interacting with the receptor.

So, as previously observed, there is a clear conformational asymmetry in the antibody molecule, that is mainly related to the Fab domains and in the frame of the interaction with FcγRIIIa, the asymmetric behavior of the mAb, that is regulated by sugars, can affect the receptor recruiting. In fact, the FcγRIIIa recognition may depend on the whole conformation of the mAb, since when the antibody reaches an orientation similar to that observed in G0F system, probably the access to some residues essential for the complex formation is blocked and the Fab domain located near to the receptor cannot be stabilized. On the other hand, when the antibody conformation is similar to that identified for G0 adalimumab, the antibody is more prone to accommodate the receptor and the fluctuation of Fab domains is moderate. This asymmetry is surely influenced both by glycosylation and intrinsic molecular properties, but in-depht studies would be required to further confirm this finding.

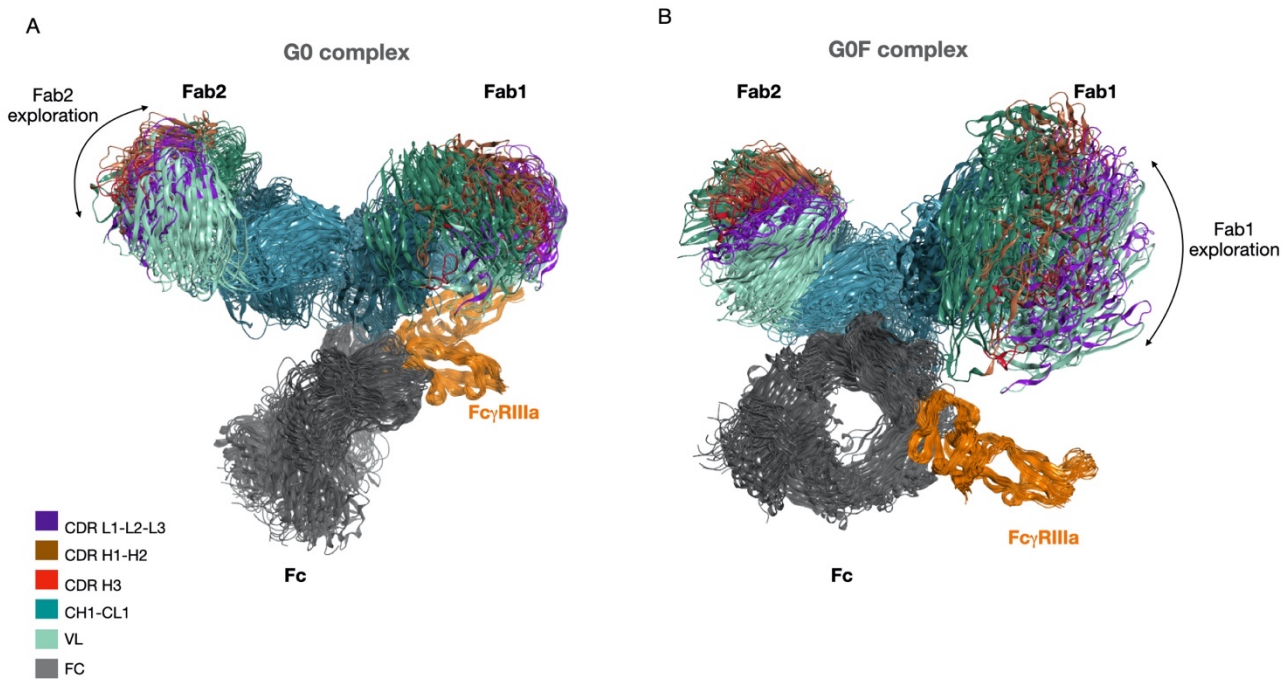

Figure 6: Structural superposition of 21 snapshots identified by MD of G0 and G0F systems. (A) Structural superposition of G0 complex conformations showed the high stability of Fab1, that is located in proximity of the receptor, and the flexibility of Fab2. (B) On the contrary, in G0F complex, Fab1 seems not to be stabilized by the receptor, showing a huge conformational variability. On the other hand, Fab2 is more stable, since the compact conformation reached together with Fc. The complexes are rendered as ribbons colored according to Kabat convention[35].

Focusing on hinge regions, there is a different behavior in G0 and G0F adalimumab, as already shown by RMSD analysis. Specifically, the G0 hinge explores less conformational space than the G0F one, for which a huge instability is detected (Figure 7). In fact, by structural superposition, G0 hinge tends to conserve its orientation, exploring conformations near the starting one. On the other hand, G0F hinge, particularly Hinge1, can adopt a wide range of orientations, suggesting its higher mobility.

Analyzing the structural behavior of FcγRIIIa, the highest variability can be detected in both systems for residues 27-35, localized in a loop that connects the first two β-sheets in the first Ig-like domain. Only slight differences in terms of fluctuation can be observed for this portion among the two systems, but in general it represents in both cases the receptor region with the highest fluctuation profile.

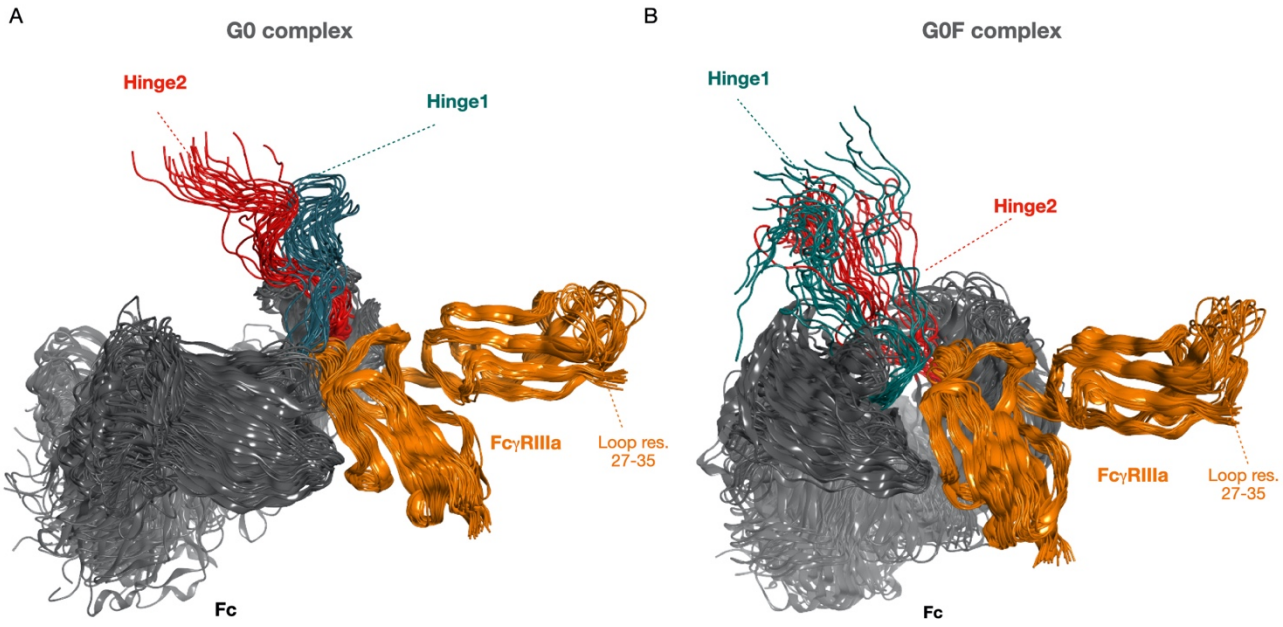

Figure 7: Structural superposition of hinge region and receptor in G0 and G0F complexes. (A) In G0 complex, both Hinge1 and Hinge2 regions show conserved orientations; (B) in G0F complex, the two hinge regions, especially Hinge1, explore more, suggesting that they drive also the Fab domains exploration. Complexes are rendered as ribbons colored as follows: Hinge1 in dark green, Hinge2 in red, the Fc in grey and the FcγRIIIa in orange.

To better define their structural role in regulating antibody conformational behavior, an analysis of dihedral angles of sugars chains was performed (Figure 8). For this analysis, sugars were numbered progressively and, as reported also in chapter 4, the two antibody N-linked chains were named chain A (connected to Asn1392 in G0 and Asn725 in G0F) and chain B (connected to Asn723 in G0 and Asn1394 in G0F). The following abbreviations have been used for sugars in this chapter: NAG (N-acetylglucosamine), MAN (mannose), FUC (fucose), GAL (galactose).

Results showed that, oppositely to what previously observed (*see Chapter 4, paragraph 4.3*), G0F glycans show more mobility with respect to G0 chains. In fact, looking at the angles distribution, in the case of G0 glycans, only the couple MAN5-NAG7 in chain A show a marked conformational exploration; while analyzing G0F behavior, NAG1-FUC3 couple in chain A and NAG2-MAN4 and MAN5-NAG7 couples in chain B, explores different conformational spaces. This could suggest that G0F chain is in some way less involved in interactions, both with the antibody residues and with the receptor (see next paragraph for further description).

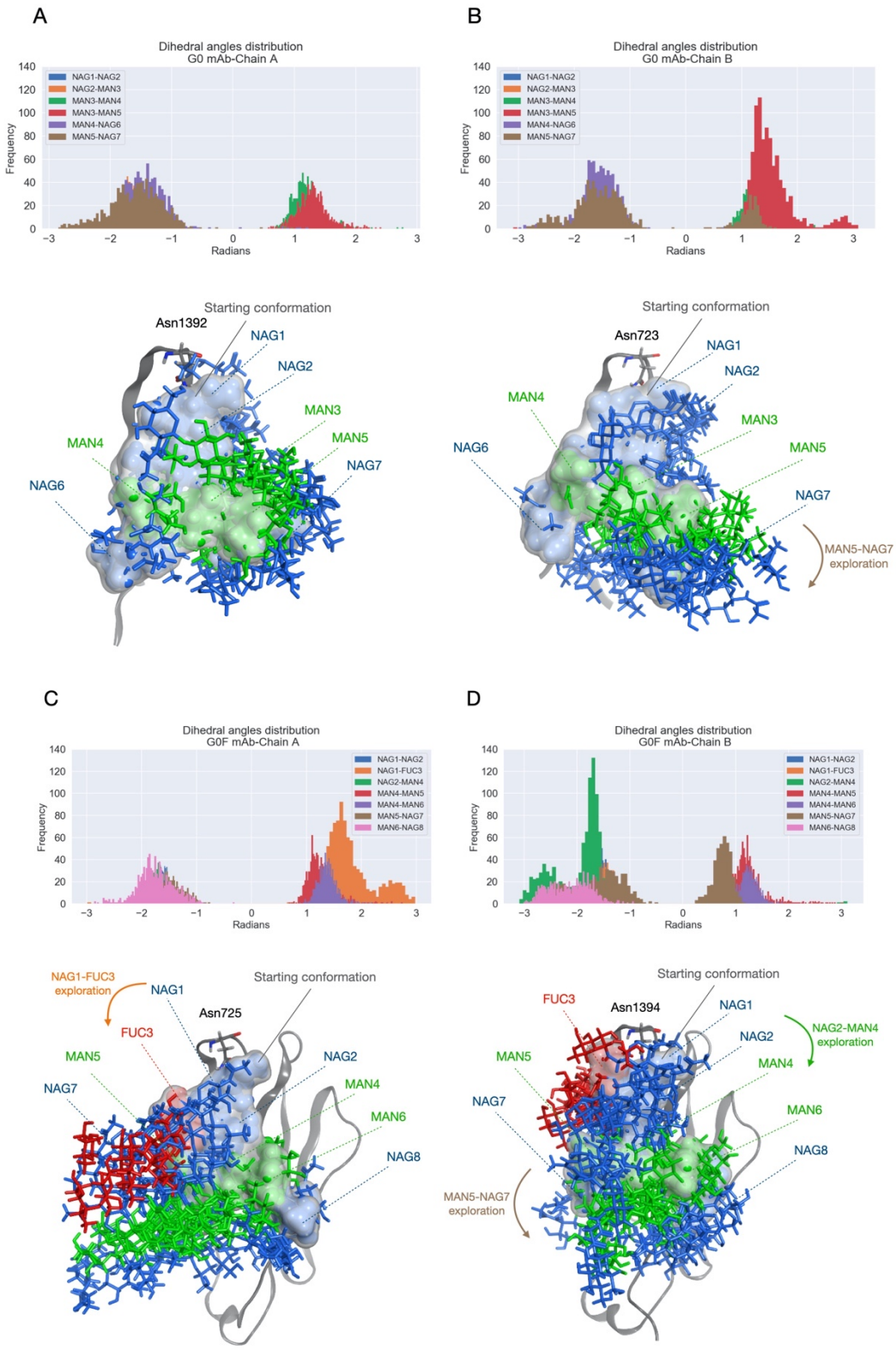

Figure 8: Dihedral angles analysis and conformational exploration of glycans. (A-B) G0 and (C-D) G0F dihedral angles exploration and corresponding structures isolated from trajectories. In both panels a conformational analysis of sugars is reported to describe their movement during the dynamics. One structure every 100 ns was considered for this analysis. Sugars are represented as sticks colored according to SNFG system[32] while the molecular surface of starting conformation is colored in grey.

5.3 Hydrogen bonds analysis

Hydrogen bonds (H-bonds) analysis was computed to identify the interactions among the antibody and the FcγRIIIa and to evaluate differences between G0 and G0F systems. The H-bonds calculation was performed according to the Baker-Hubbard criterion, considering significative all the interactions occurring for more than 10% of the simulated time. Tables 1 and 2 report the list of all single protein-protein interactions specifying donor and acceptor atoms for each couple and, to facilitate data discussion, the antibody residues listed according to Kabat numbering[35]. In figure 9 a structural representation of identified residues in centroids of G0 and G0F complexes is reported.

Looking at tables, first of all, a quantitative observation related to the number of interactions was done. Specifically, in G0 system 20 H-bonds among antibody and receptor were identified by this analysis, oppositely to what happen in G0F one, where only 7 interactions were detected. From a qualitative point of view, only 3 antibody residues involved in H-bonds with the receptor are in common between G0 and G0F adalimumab, namely Gly241, Asp269 and Tyr300 (according to Kabat numbering[35]).

Table 1: H-bonds interactions in G0 system. The list of H-bonds occurring among FcγRIIIa and G0 adalimumab with a frequency equal or up to 10%. For each residue involved in the interaction, the donor/acceptor atom is reported. A column reporting the residue numbering by Kabat is also present. Residues located in Fab domain are highlighted in yellow, otherwise hinge and Fc residues are colored in light blue.

FcγRIIIa residues	G0 Antibody residues	Antibody residues according to Kabat numbering[35]
Glu8.OE1/OE2	Arg983.NH1/NH2	Arg108
Glu31.OE1/OE2	Ser887.OG	Ser12
Ser49.OG	Val985.N	Val110
Ser50.OG	Thr984.OG1 Val985.O	Thr109, Val110
Asn110.ND2	Gly1233.O	Gly142
Ala112.N	Ser1286.OG	Ser195
His114.NE2	Gly1331.N Gly1332.N	Gly240, Gly241
Lys115.NZ	Asp1360.OD1/OD2	Asp269
Gly124.N	Tyr1391.O	Tyr300
Gly124.O	Ser1393.OG	Ser302
Lys126.NZ	Glu1364.OE1/OE2	Glu273
His130.NE2	Leu1329.O	Leu238
Ser155.N	Leu661.O	Leu239
Lys156.NZ	Leu661.O, Gly662.O, Gly663.O, Pro664.O, Asp691.OD2	Leu239, Gly240, Gly241, Pro242, Asp269

Table 2: H-bonds interactions in G0F system. In this table, all the H-bonds occurring among FcγRIIIa and G0F adalimumab with a frequency up to 10% are listed. A column reporting the residue numbering by Kabat is also present. In this case, no residues located in Fab portions are involved in the interaction and as for table 1, hinge and Fc residues are colored in light blue.

FcγRIIIa residues	G0F Antibody residues	Antibody residues according to Kabat numbering[35]
Lys115.NZ	Gly665.O Ser667.OG Asp693.OD2	Gly241, Ser243, Asp269
Gly124.N	Tyr724.O	Tyr300
His130.NE2	Ser695.OG	Ser271
His130.ND1	Gly665.N	Gly241
Lys156.NZ	Asp1362.O	Asp269

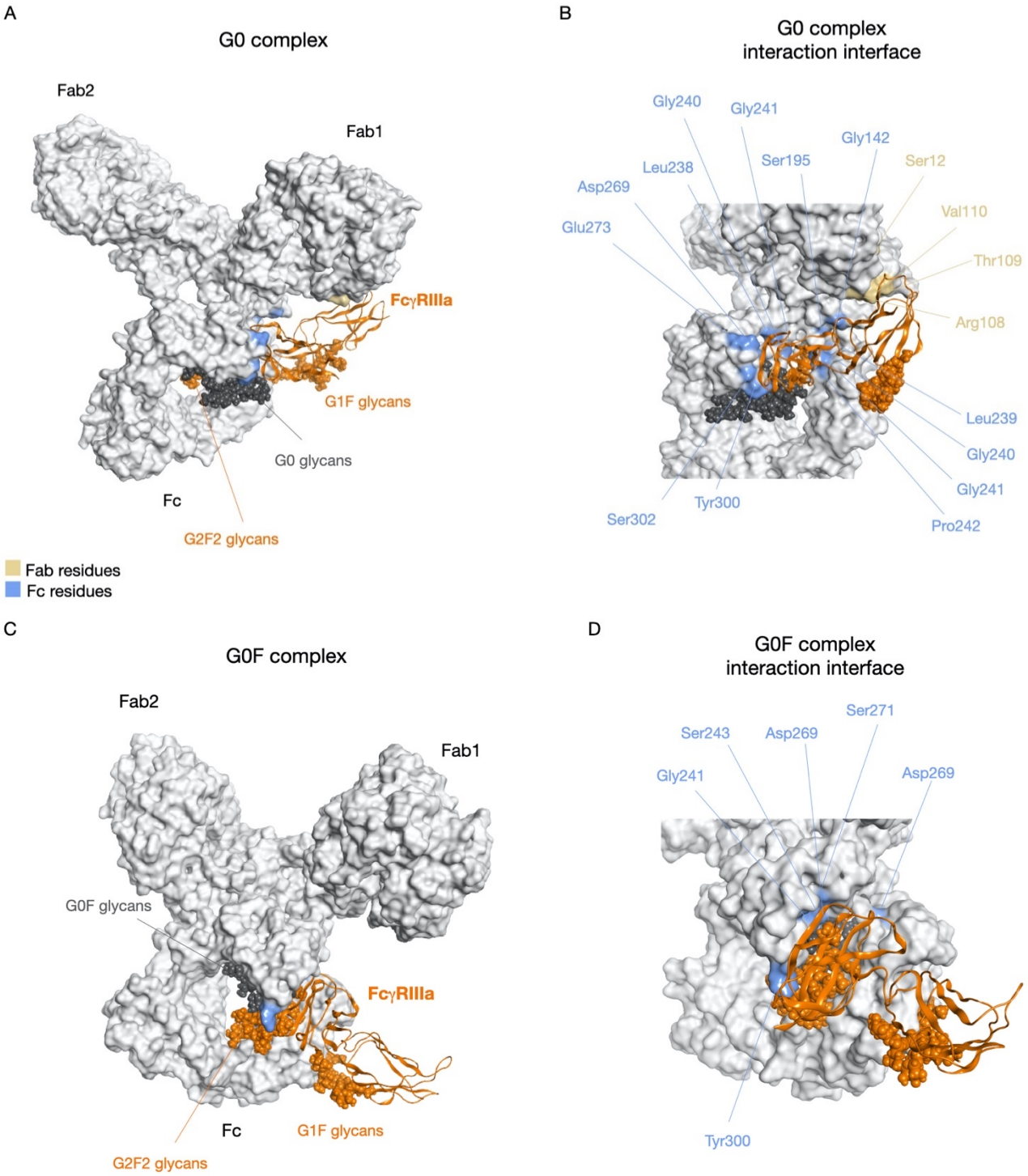

Figure 9: Structural representation of G0 and G0F adalimumab binding sites. Molecular surface and mapping of antibody residues involved in the interaction with FcγRIIIa in G0 (A-B) and G0F (C-D) complexes. Residues located in Fc are colored in light blue, residues located in the Fab are represented in yellow.

The adalimumab residues involved in interactions with FcγRIIIa and identified by MD were compared to those IgG1 residues reported in literature as key amino acids for the complex formation (Table 3). These residues were identified by mutagenesis analysis performed by Shields and colleagues[130]. In this work, authors defined for each Fc receptor type a pool of IgG1 residues critical for the antibody::receptor complex formation.

According to this analysis, 7 residues in G0 adalimumab (Leu238, Leu239, Gly240, Pro242, Asp269, Glu273, Tyr300) are conserved with respect to those reported by Shields *et al.*[130], while in G0F only 2 out of the 21 mentioned amino acids (Asp269, Tyr300) result to be involved in the interaction with the receptor. In G0 system, the involvement of many residues considered critical by experimental data for the interaction with all Fcγ receptors, namely Leu238, Leu239, Gly240, Pro242 and Asp269, suggests that the conformation reached by the afucosylated adalimumab may be potentially more prone to interact with all the receptors than the G0F one, and not only with the FcγRIIIa.

Moreover, even if in G0 system only 7 out of 21 residues have been identified by MD analysis, many other amino acids potentially critical for the complex formation were recognized. In particular, some of these (Ser12, Arg108, Thr109, Val110) are located in the Fab1 domain and particularly in the LC, both in variable and in the constant regions, suggesting a putative involvement of this domain in triggering the receptor binding and, of note, new perspectives in studying the recognition mechanism. In fact, these residues are not involved in the interaction between the fucosylated antibody and FcγRIIIa, indeed the Fab domain is positioned far away from the receptor and shows a high fluctuation during the MD, as highlighted by structural analysis.

Table 3: A comparison among experimentally identified key residues and those involved in H-bonds interactions by MD analysis of both G0 and G0F systems. In this table, a comparison among all the residues considered critical for the formation of the IgG1::FcγRIIIa complex and the residues identified as involved in the interaction *via* MD simulation. To facilitate data analysis, the critical residues are reported according to standard EU numbering in the first column and to Kabat convention in the other three. In green residues considered essential for the interaction with all the FcγR are highlighted.

Key residues by Shields *et al.*[130] according to standard EU numbering[31]	Key residues by Shields *et al.*[130] according to Kabat numbering[35]	G0 Adalimumab conserved residues by MD analysis	G0F Adalimumab conserved residues by MD analysis
Glu233	Glu246		
Leu234	Leu247	Leu238	
Leu235	Leu248	Leu239	
Gly236	Gly249	Gly240	
Pro238	Pro251	Pro242	
Ser239	Ser252		
Asp265	Asp278	Asp269	Asp269
His268	His281		
Glu269	Glu282	Glu273	
Asp270	Asp283		
Glu293	Glu310		
Gln295	Gln312		
Tyr296	Tyr313	Tyr300	Tyr300
Asn297*	Asn314		
Arg301	Arg320		
Val303	Val322		
Lys322	Lys341		
Ala327	Ala346		
Pro329	Pro348		
Lys338	Lys358		
Asp376	Asp399		

**Asn297 is considered critical since a mutation in this site abrogates N-glycosylation and consequently Fc effector functions*

An analysis of distances between acceptor and donor atoms of residues participating to the interaction was performed (Figure 10). A threshold of 0.5 nm has been considered to discriminate stable interactions from unstable ones. Globally, the analysis highlighted that residues experimentally determined as critical for the binding, in G0 system interact in a constant manner with the receptor, while they are not part of fucosylated antibody interaction network.

In figure 10A and 10B the distances computed for the most critical interactions in G0 and for all the couples in G0F are respectively represented.

Looking carefully at G0 system (Figure 10A), Leu239, Gly240, Pro242 and Asp269 are involved in many interactions with different amino acids of the receptor, *i.e.* Lys156, that forms interactions for most of the time of simulation, Ser155, Hi114 and Lys115, that alternatively form a network with the mAb over the trajectory. Together to this, the interaction between Gly124 (FcγRIIIa) and Tyr300 (antibody) results to be stable for the first 600 ns of the dynamics and then is lost in the last part of simulation. Moreover, the Lys126 (FcγRIIIa)-Glu273 (antibody) interaction is always present during the dynamics. Overall, for G0 system, even though the H-bonds between the mAb and receptor show a dynamic behavior, a high stability of the complex is almost guaranteed over the trajectory by the presence of other interactions in most of the explored conformational states.

On the contrary, looking at G0F system (Figure 10B), the network of Lys156 of receptor is not present and this residue interacts with Asp269 of adalimumab only for a limited time (200-550 ns). Furthermore, the interaction network observed in the G0 complex is replaced by another network that involves Lys115 and His130 of the receptor in stable interactions with Gly241, Ser243 and Ser271. Differently from G0 system, among the G0F antibody amino acids involved in the interactions, only Gly241 and Asp269 are critical for the receptor recognition by the site-direct mutagenesis experiments[130].

Globally, data shown above suggests that the presence of many interactions observed for G0, including those located in Fab region, is mandatory for receptor recruiting and activation. These observations can support the hypothesis that the conformation adopted by the fucosylated antibody is not suitable for FcγRIIIa triggering, since both key residues and the Fab cannot bind the receptor.

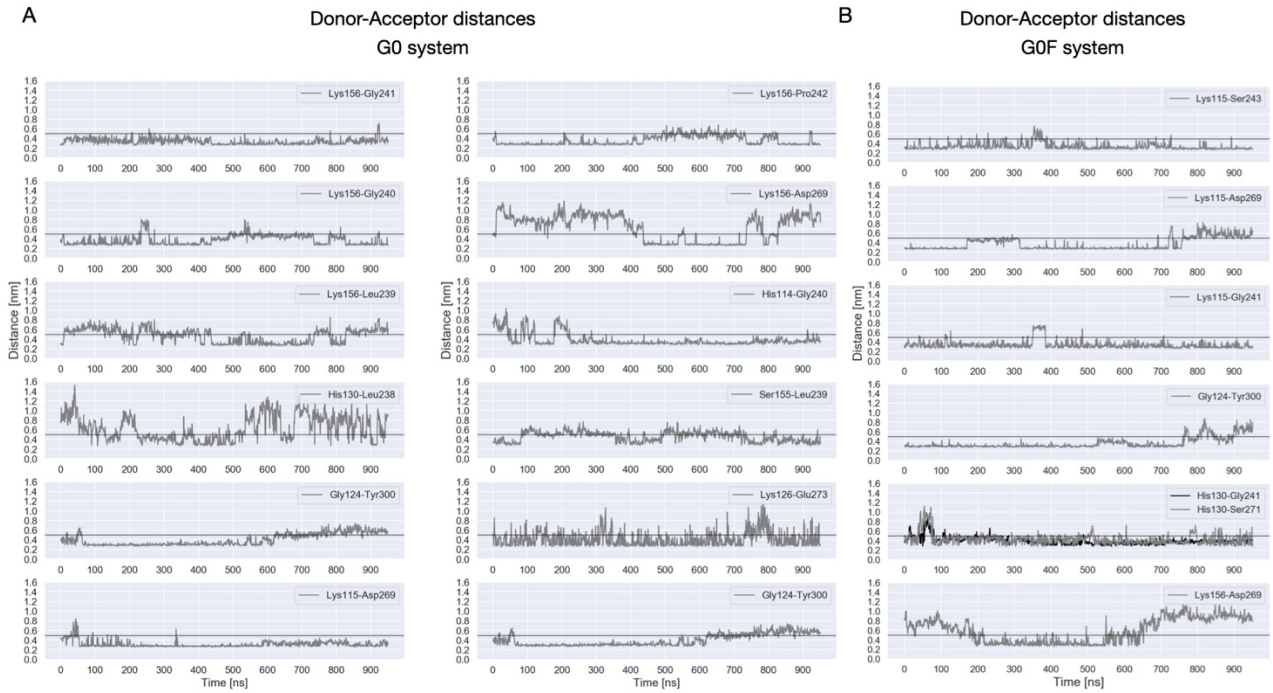

Figure 10: Acceptor-donor distances computed for G0 and G0F key couples. Acceptor-donor distances computed for G0 (A) and G0F (B) residues involved in H-bonds with the receptor. For G0 system, since the high number of interactions, only those experimentally considered critical are reported. The black line reported in all graphics corresponds to the 0.5 nm threshold used to discriminate stable and unstable bonds.

The H-bonds analysis was performed also for investigating glycans interaction network, both for the receptor and for antibodies. In table 4 the list of all the detected interactions is reported. The table shows that G0F glycans chains make a higher number of interactions with the own antibody amino acids than G0 ones. This confirms, as previously observed, that the role of G0F sugars is to maintain a compact conformation of the antibody by blocking the Fc in a specific state. However, comparing these data with those previously reported (*see section 4.3, Chapter 4*), G0F chains have lost some interactions with the antibody and this is probably the reason why we observed a higher mobility in these glycans. Moreover, since G0F chain B makes H-bonds with residues considered critical for complex formation by experimental data, probably G0F glycans can make also a steric hindrance effect on these residues, not allowing receptor recognition.

For what concerns the network made by receptor glycans, only terminal sugars interact with antibody residues and the number and the type of interactions are highly comparable among the two systems, suggesting that they are not so relevant in discriminating between the two types of antibodies.

Table 4: Glycans interaction network. In this table all the glycans interactions with both antibody and FcγRIIIa are reported. In yellow, interactions made with residues critical for the complex formation.

G0.A - antibody	G0.B - antibody	G0F.A - antibody	G0F.B - antibody
NAG2.O7-Arg305.NE/NH2	NAG2.O7-Arg305.NE/NH1	NAG2.O7-Arg305.NE/NH1	NAG1.O3-Gly241.N
NAG7.O6-Leu246	MAN6.O4/O6-Ser243.N	MAN4.O3-Arg305.NH1	NAG2.O6-Ser243.OG
	NAG5.O6-Arg305.NH1	NAG7.O7-Lys338.NZ	FUC3.O2/O3-Tyr300.N
			FUC3.O2-Asn301.N
			MAN6.O5/O6-Lys338.NZ
			MAN6.O6-Val244.N
			NAG7.O3-Arg305.NH1
			NAG8.O7-Lys338.NZ
G0.A - FcγRIIIa	**G0.B - FcγRIIIa**	**G0F.A - FcγRIIIa**	**G0F.B - FcγRIIIa**
NAG7.O3/O7-Asn157.N	NAG1.O3-Lys115.NZ	NAG1.O7-Arg150.NH2	-
G1F – G0 antibody	**G2F2 – G0 antibody**	**G1F – G0F antibody**	**G2F2 – G0F antibody**
GAL9.O3-Asn329.N	FUC2.O2-Tyr300.OH	NAG7.O3-Lys278.NZ	GAL9.O3-Ser341.N
	MAN6.O6-Tyr300.OH	GAL9.O4-Lys278.NZ	GAL10.O3-Thr339.N
	GAL10.O- Tyr300.OH	GAL9.O3-Thr293.OG1	
		GAL9.O4-Phe279.N	

Furthermore, no H-bonds among antibodies and receptor sugars were detected and this may be due to the presence of water in the pocket. In fact, there is a high probability that water molecules are located in the interface between different sugars chains, coordinating the interaction. In this case, it may be hard to identify specific carbohydrate-carbohydrate interactions. To validate this hypothesis, since all the trajectories analyses was performed excluding water, a solvent analysis was performed by MOE[113] using the 3D reference interaction site model (3D-RISM) method[131–133] that analyzes the role of solvent in macromolecular systems. Specifically, this tool combines the time-averaged distribution of water (H and O atoms) densities together with the free-energy maps in order to compute the solvent contribution to binding free energy. As a result, a map of water molecules located in the binding site is obtained allowing the estimation of water placement in the receptor-ligand interface. In the case of G0 and G0F systems, the 3D-RISM calculation was carried out on carbohydrate-carbohydrate interface, in order to evaluate the solvent contribution in coordinating the interaction. In both systems, as reported in Figure 11, a huge quantity of water molecules was predicted to be positioned among glycans, suggesting that direct interactions among sugars do not occur because they are coordinated by water molecules.

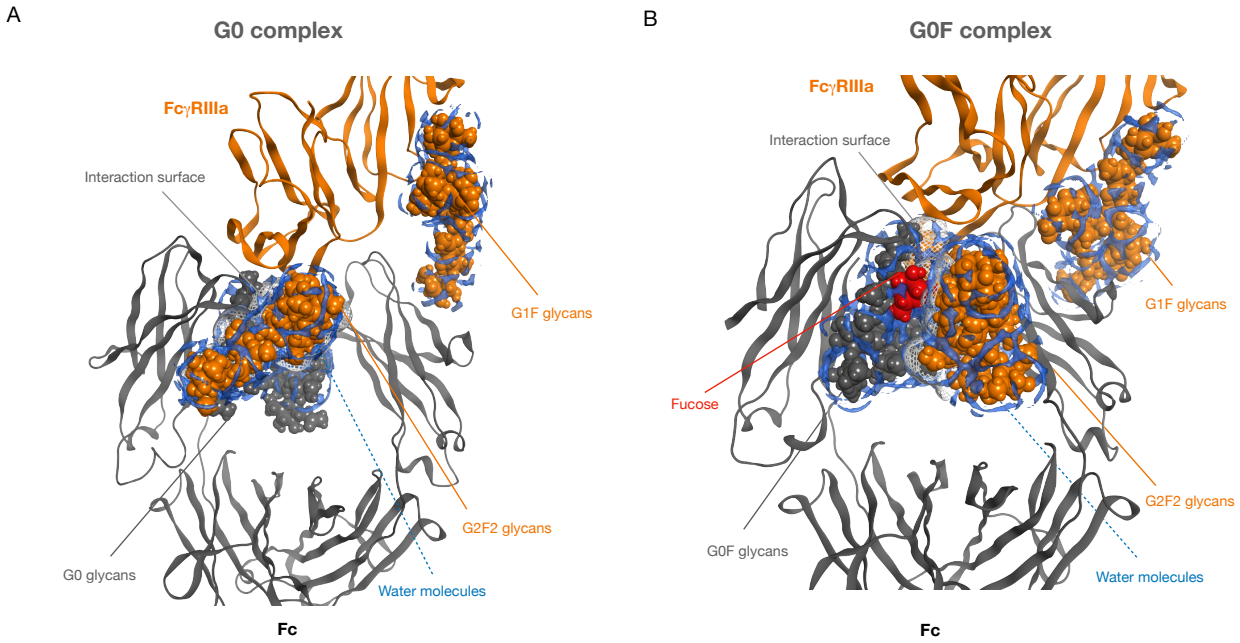

Figure 11: 3D-RISM calculation in the carbohydrate-carbohydrate interface of G0 and G0F systems. Carbohydrate-carbohydrate interface of G0 (A) and G0F complex (B). In grey ribbons the Fc portion of antibodies, in orange ribbons the FcγRIIIa. Glycans are represented as orange (receptor) and dark grey (antibody) spheres, the fucose is colored in red. Estimated water molecules positions at glycans-glycans interface are represented in light blue. In both systems, G1F glycans do not interact with antibody sugars. An interaction interface is instead detected between G2F2 and antibody glycans with a huge density of water molecules within.

5.4 MD simulations of Fc:: FcγRIIIa complexes

Considering all the reported data, we hypothesized that the fucose behaves as an allosteric modulator able to regulate both the exposure of residues critical for the interaction with FcγRIIIa and the Fab arms orientation and flexibility. We supposed also that a specific orientation of Fab domains is essential to trigger the FcγRIIIa recognition so, to further demonstrate this hypothesis, MD simulations 1 μs long was carried out by NAMD 2.13 package[121] for the crystalized Fc::FcγRIIIa (PDB ID: 3SGJ[57]) complex used to model the previous structures. The structures of one fucosylated and one afucosylated complex were prepared using MOE GUI[113]. Glycan chains were manually added to the Fc, since in the PDB structure some units were missed, and the same glycosylation patterns chosen for the whole complexes were used for the receptor (*for further details see section 5.1*). Figure 12 contains a representation of the 3D structures of simulated complexes.

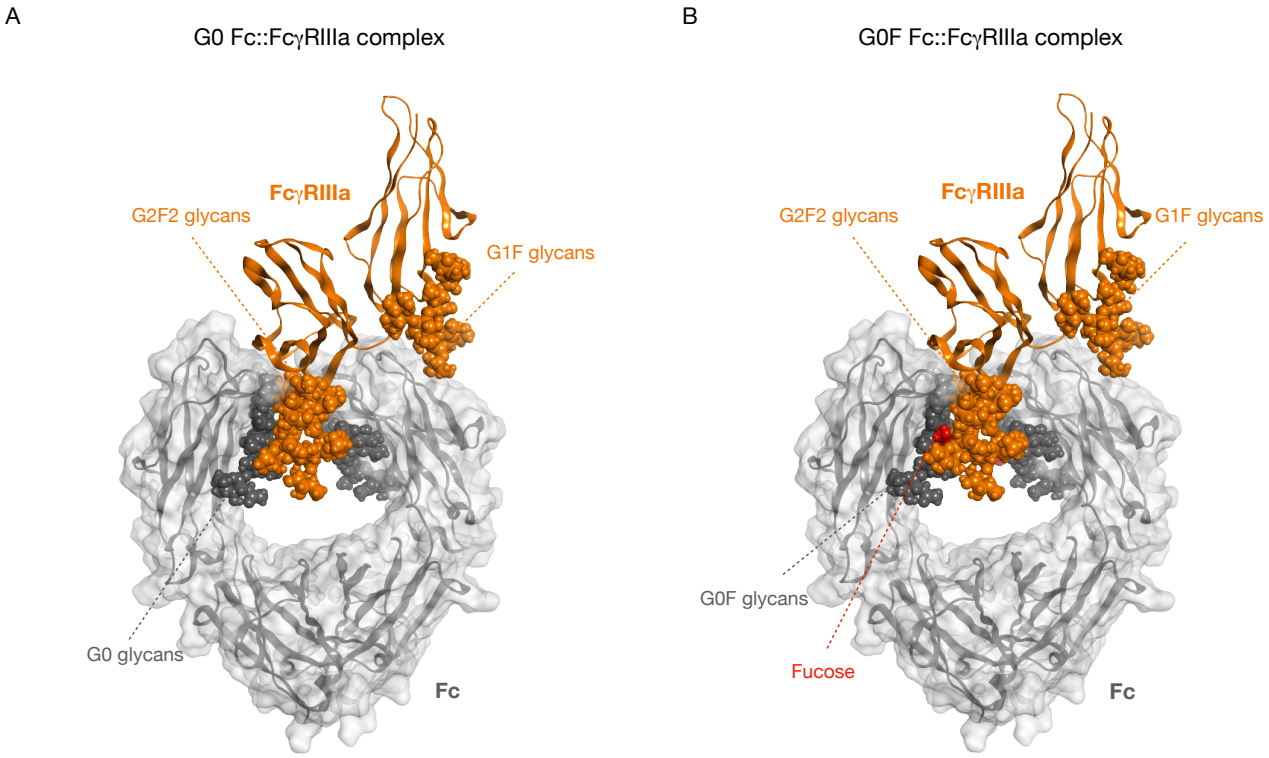

Figure 12: 3D representation of crystalized Fc::FcγRIIIa (PDB ID: 3SGJ). The 3D structure of the crystalized Fc::FcγRIIIa complex in its afucosylated (A) and fucosylated (B) forms. The molecular surface of Fc portion is colored in grey, as well as the secondary structure that is represented as ribbons; the receptor is represented as orange ribbons. Grey (Fc) and orange (receptor) spheres correspond to glycans, while the fucose is highlighted in red.

The autocorrelation of potential energy was computed to estimate systems convergence and equilibration (Figure 13A). Globally, the plot suggests that both systems reach an equilibrium in the dynamics. Moreover, as for other systems, the first 50 ns of trajectory were considered as an equilibration step and excluded from further analysis. For both systems, RMSD was computed for C-alpha atoms of Fc portion and receptor, splitting the contribution of single parts (Figure 13B). From this analysis, it is clear that, oppositely to what observed for complexes including the whole antibody, both G0 and G0F show highly comparable RMSD profiles and, in particular, the maximum standard deviations that they reached are very close. In detail, the afucosylated Fc reaches a maximum RMSD value of 0.45 nm and the corresponding FcγRIIIa a value of 0.25 nm. On the other hand, the maximum RMSD value reached by the fucosylated Fc is 0.35 nm and by FcγRIIIa in G0F system is 0.32 nm. These values, together with the RMSD plateau state shown for all the simulated time, suggest that the conformations explored by fucosylated and afucosylated systems could be very similar.

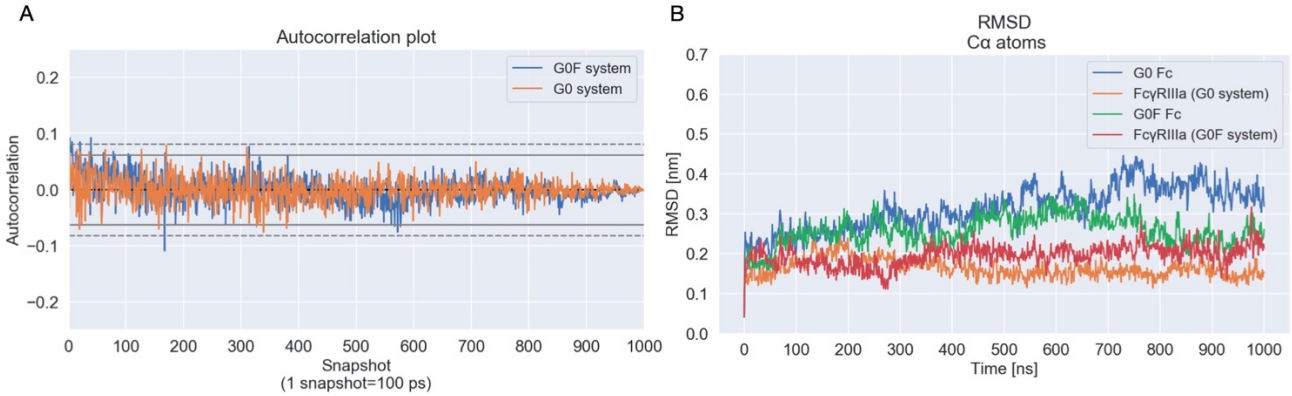

Figure 13: Autocorrelation plot of potential energy and RMSD analysis. (A) Autocorrelation plot of potential energy computed for G0 and G0F systems. In both cases the autocorrelation value stabilizes under the confidence band within the first 500 snapshots that corresponds to 50 ns of simulation. (B) RMSD of C-alpha atoms of Fc portions and FcγRIIIa shows very similar profiles among the fucosylated and afucosylated systems, with highly comparable RMSD maximum values and an RMSD equilibrium present for all the dynamics.

RMSF analysis confirmed what observed by RMSD: fluctuation profiles are highly overlapped and comparable, suggesting a similar dynamical behavior of the two complexes (Figure 14). Moreover, the observed maximum fluctuations are the following: in G0 system, 0.25 nm for the Fc portion and 0.17 nm for FcγRIIIa; in G0F system, 0.20 nm for Fc domain and 0.26 nm for FcγRIIIa.

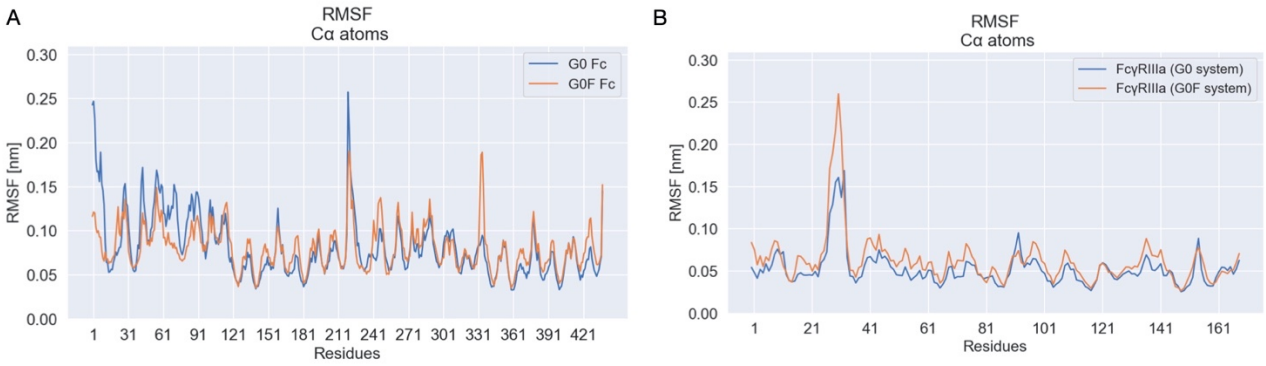

Figure 14: RMSF analysis of C-alpha atoms computed for G0 and G0F systems. RMSF profiles of both G0 and G0F Fc portions (A) and those of FcγRIIIa (B) are quite overlapped, suggesting that fluctuation profiles are mostly the same, as observed also by RMSD analysis.

A hierarchical cluster analysis was then performed to isolate specific conformations and to deeply analyze the structural behavior of complexes. The RMSD distribution (Figure 15A) showed that the conformational space explored by two system is mostly limited, in fact we can observe only one peak per each distribution. However, the clustering identified two clusters for the afucosylated complex (Cluster1=56% and Cluster2=44%) and three clusters for the fucosylated one (Cluster1=35%, Cluster2=24% and Cluster3=41%). The centroid structure of the most populated group was considered for structural evaluation. The structural superposition of G0 and G0F complexes centroids pointed out the high similarity of two conformations. In fact, as reported in figure 15B, the structures are perfectly overlapped and the RMSD among the two complexes is only of 2.1 Å, thus suggesting that in absence of Fab domains and upper hinge region the fucose induces only small changes in conformation.

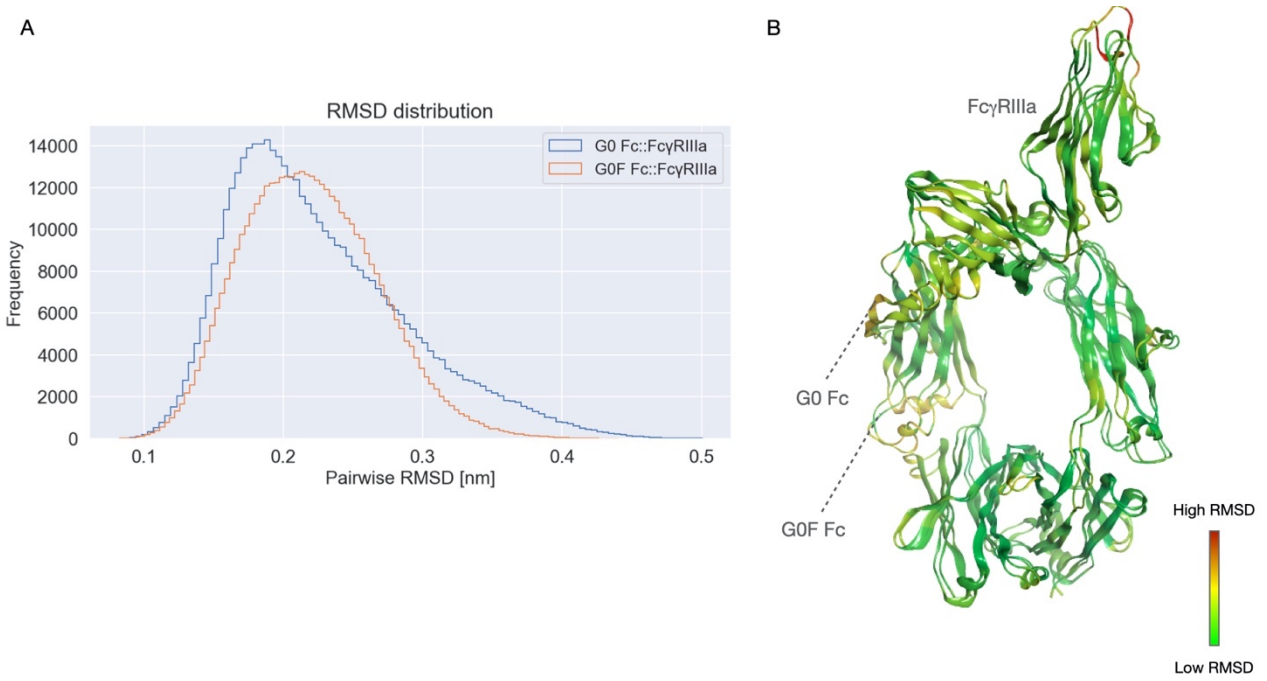

Figure 15: RMSD distribution and structural superposition of centroid structures. (A) The RMSD distribution shows the low exploration of conformational space both for G0 and G0F systems. (B) The structural superposition of centroid structures is reported according to a red-yellow-green RMSD gradient corresponding to bad, medium and good superposition, respectively.

Glycans exploration was evaluated considering dihedral angles distribution. Carefully looking at dihedral's profile, not so relevant differences can be observed, suggesting that the conformational behavior of sugars is quite similar among two systems and that in this case, the presence of fucose does not have a detectable impact on glycans dynamics (Figure 16).

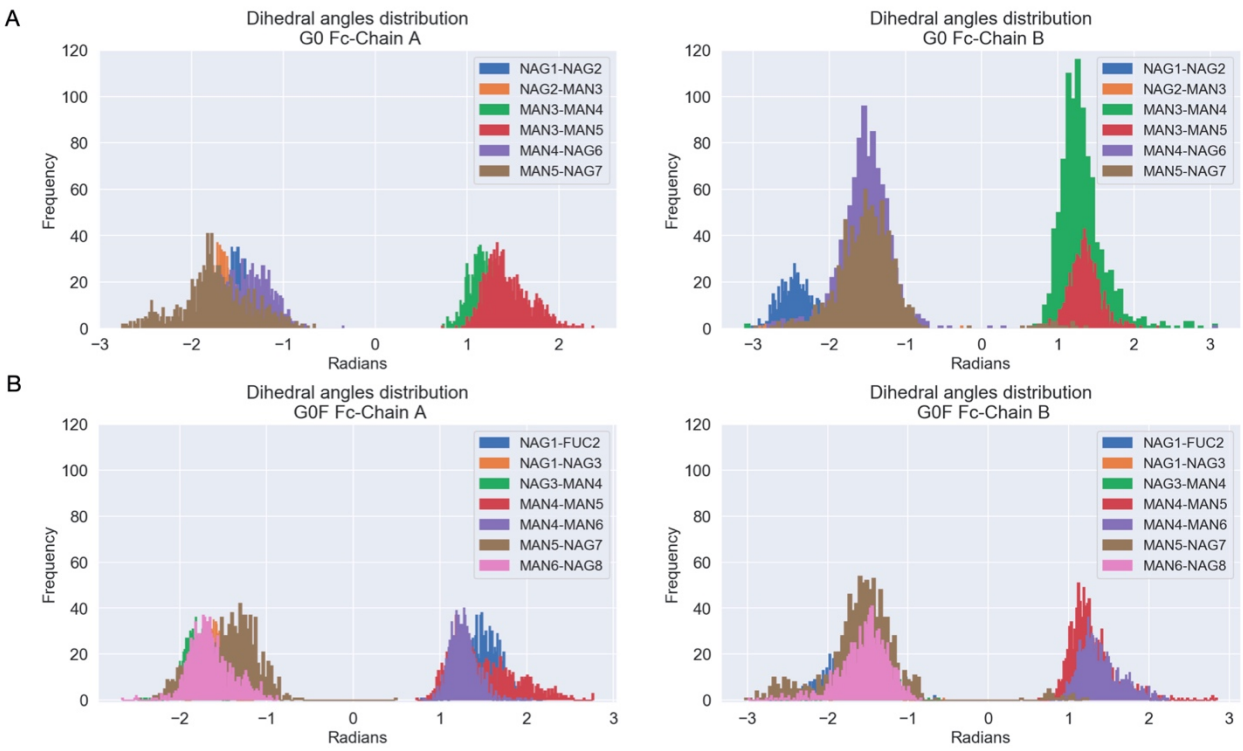

Figure 16: Dihedral angles distribution of G0 and G0F glycans. The dihedral angles distribution of G0 (A) and G0F (B) chains A and B show that all the glycans are locked in a single state, suggesting that they do not explore different conformations.

5.5 Mapping of Fc::FcγRIIIa complexes interaction network

H-bonds analysis was computed allowing the identification of specific interactions between the Fc portion and the receptor. In detail, a number of 6 (G0) vs 11 (G0F) couples of residues interacting each other was detected, by using the Baker-Hubbard criterion and considering all the bonds occurring with a frequency equal or up to 10% of the simulated time. The residues couples involved in H-bonds are reported in tables 5 and 6.

Table 5: H-bonds interactions in G0 system. A list of all the H-bonds occurring among FcγRIIIa and G0 Fc computed by Baker-Hubbard criterion and occurring with a frequency equal or up to 10%.

FcγRIIIa residues	G0 Fc residues according to Kabat numbering[35]
Lys115.NZ	Gly240.O Asp269.OD1/OD2
His130.NE2	Ala331.O
Ser155.N	Glu237.O
Lys156.NZ	Gly240.O Pro242.O

Table 6: H-bonds interactions in G0F system. A list of all the H-bonds occurring among FcγRIIIa and G0F Fc computed by Baker-Hubbard criterion and occurring with a frequency equal or up to 10%.

FcγRIIIa residues	G0F Fc residues according to Kabat numbering[35]
Lys17.NZ	Pro333.O
Lys115.NZ	Gly240.O Asp269.OD1
Thr117.OG1	Asn301.O
Gly124.N	Tyr300.O
Lys126.NZ	Glu273.OE1/OE2
Tyr127.OH	Asp269.O
Lys156.NZ	Gly240.O Pro242.O
Ser155.N	Glu237.O
Ser155.OG	Gly241.O

The structural localization of identified residues is reported in figure 17 (panels A and B) together with the comparison of the total H-bonds numbers computed per each system vs simulation time (panel C). Essentially, a very similar number of protein-protein H-bonds was detected in both afucosylated and fucosylated systems. Moreover, the analysis pointed out that, comparing the two complexes, residues involved in interactions are mostly the same. This suggests that, if we consider only the Fc portion for investigating the recognition mechanism of IgG1::FcγRIIIa complex, not so relevant differences can be observed.

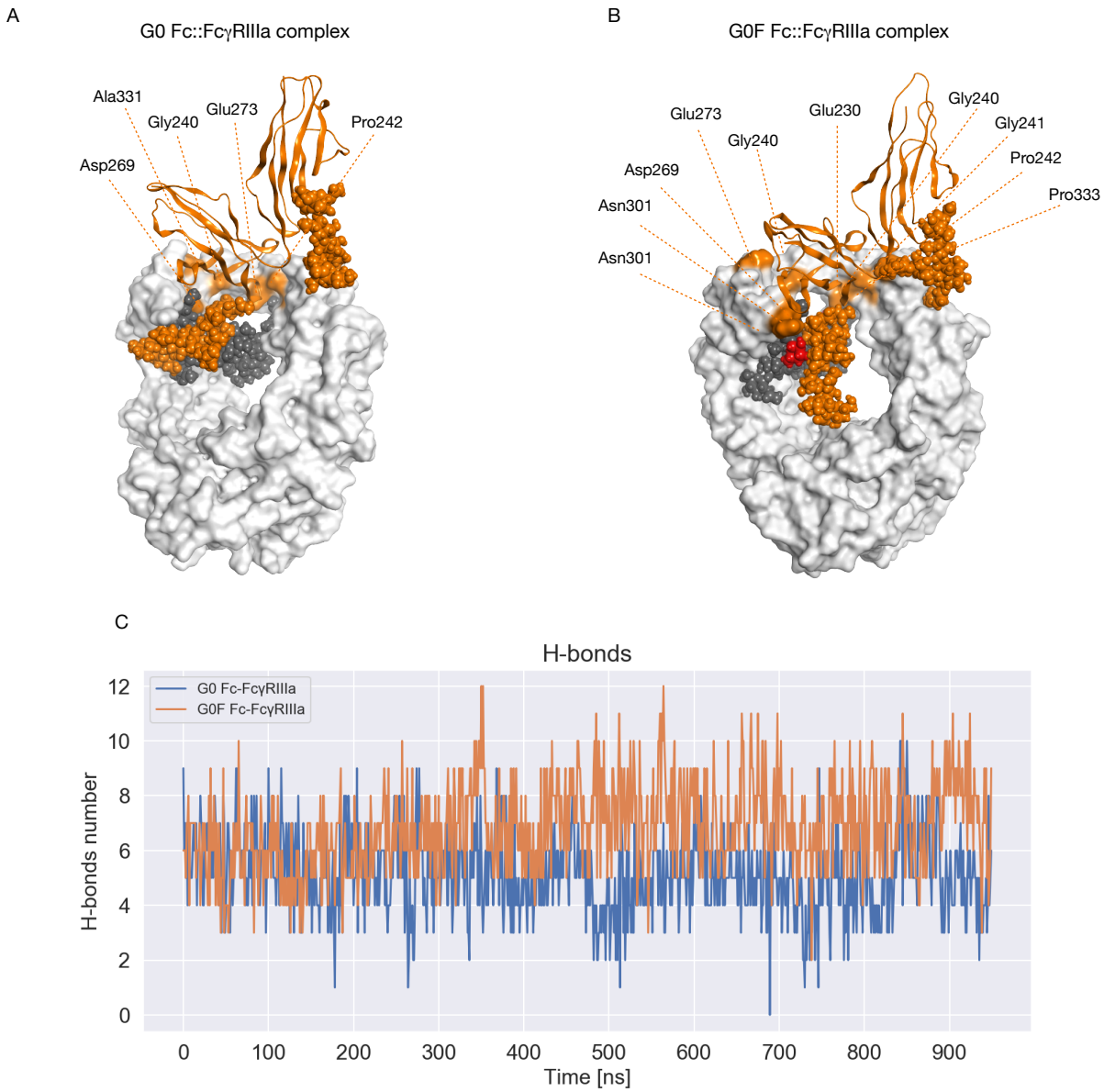

Figure 17: Fc::FcγRIIIa H-bonds network analysis. Fc residues involved in H-bonds are mapped on the molecular surface of afucosylated (A) and fucosylated (B) fragment. The receptor is represented as orange ribbons and all the glycans are shown as colored spheres: Fc glycans in grey, receptor glycans in orange and the fucose in red. (C) A plot containing the H-bonds number vs simulated time and showing comparable numbers of interactions among the two systems.

Furthermore, analyzing sugars H-bonds network, G0 and G0F chains are both involved in the same interactions, with not so relevant differences in their dynamical behavior, as already observed by dihedral angles analysis (Table 7 and Figure 18). This may suggest that in absence of hinge and Fab domains they do not act as structural modulators of antibodies.

Table 7: Glycans interaction network. In this table all the glycans interactions with G0 and G0F Fc portions are reported.

G0.A - Fc	G0.B - Fc	G0F.A - Fc	G0F.B - Fc
NAG2.O7-Arg305.NE	NAG1.O7-Ala235.N	NAG2.O7-Arg305.NE	NAG1.O7-Ala235.N
MAN4.O3-Arg305.NH2	NAG2.O7-Arg305.NH1/NH2	NAG2.O7-Arg305.NH1	NAG2.O7-Arg305.NH1/NH2
NAG5.O3-Lys250.NZ	NAG5.O3-Ser341.OG	MAN4.O3/O4-Arg305.NH1	
MAN6.O6-Lys338.NZ	NAG5.O7-Ser341.N	MAN6.O6-Lys338.NZ	
NAG7.O7-Leu246.N		NAG7.O7-Leu246.N	

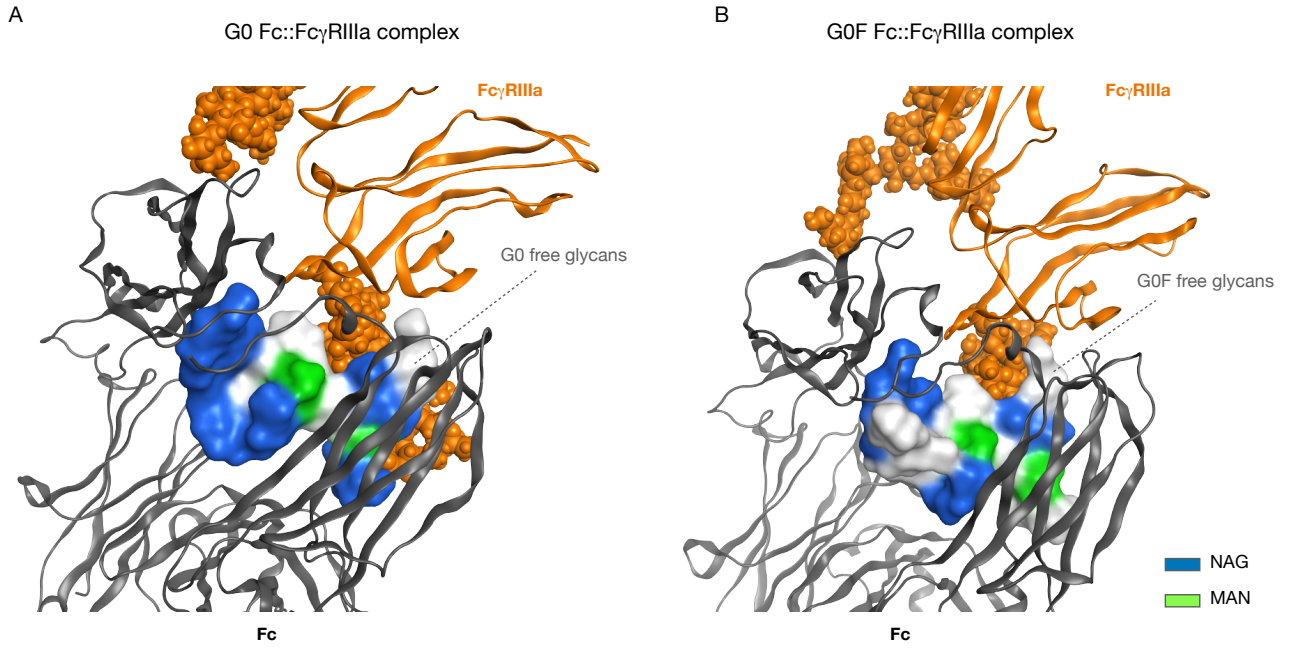

Figure 18: G0 and G0F H-bonds network analysis. Glycans units involved in H-bonds with Fc are mapped on the molecular surface according to the SNFG color system[32]. Comparing G0 (A) and G0F (B) chains residues involved in the interaction with Fc are almost the same.

As observed also for adalimumab::FcγRIIIa complexes, no H-bonds interactions among receptor and Fc sugars were detected and, as already mentioned, this is probably due to the presence of water in the interface. Moreover, as a result of the analysis of receptor glycans network, only the H-bond between Tyr300 and FUC10 (G2F2 chain, connected to Asn157) in G0 system was detected, suggesting the very low impact of receptor sugars in driving the recognition.

5.6 ΔG binding free energy calculation

The ΔG binding free energy (ΔG_{bind}) was calculated by MOE[113] for complexes formed by the whole antibody and for those including the Fc portion by using the single point energy calculation. This analysis was carried out to definitely assess which type of complex (G0 or G0F) is more favored during the dynamics and to compare the behavior of the antibody in presence and in absence of Fab domains (Table 8 and Figure 19). In particular, 21 conformations per each system, each one saved every 50 ns, were considered for the calculation. After an energy minimization run to an RMS gradient of 0.1 kcal/mol/Å^2, the interaction energy of the complex was calculated by using the 'Potential Energy' tool, considering also glycans as part of the molecules and including their contribution to the interaction. Then, $\Delta\Delta G_{bind}$ among all the states of G0 and G0F was computed. For what concern adalimumab complexes, differences up to -446 kcal/mol were observed between afucosylated and fucosylated forms, as summarized in Table 8, and both systems reach a plateau state between 350 and 700 ns of simulation (Figure 19A). Particularly in this time window, the G0 complex results to be more energetically favored than G0F one. This is likely due to the higher number of protein-protein interactions displaced by G0 complex, since the calculated energy takes into account the contribution of all the non-bonded force field energies between the antibody and the receptor.

Analyzing Fc complexes, nevertheless G0F complex shows ΔG_{bind} values slightly more negative than G0, the $\Delta\Delta G_{bind}$ calculation pointed out that the differences are not so high as for adalimumab::FcγRIIIa complexes, suggesting that energetic profiles are quite comparable.

Moreover, by comparing energy values computed for both the fucosylated forms, very similar ΔG_{bind} were observed among the adalimumab and the Fc complexes and only a slight improvement in the strength of the complex binding was recognized in presence of Fab portions.

Looking at afucosylated complexes, energy values much more negative than those observed for the Fc complex were detected for the adalimumab one, suggesting that in absence of fucose, the presence of Fab portions is decisive in stabilizing and strengthening the interaction with the receptor. On the other hand, in the fucosylated adalimumab complex the slight improvement in the binding free energy profile suggests the detrimental effect of fucose on the overall antibody molecule, since, even present, Fab portions cannot participate in the receptor recognition.

In conclusion, according to all the data shown above afucosylated and fucosylated antibodies show a different ability to recognize the FcγRIIIa that is due to the different conformational behavior of the

species, certainly influenced by the presence or absence of fucose that allosterically modulates their structure.

Table 8: ΔG_{bind} free energy computed for all G0 and G0F complexes with single point method. The values of energy correspond to specific time frames and are expressed in kcal/mol. The $\Delta\Delta G_{bind}$ computed among the afucosylated and fucosylated systems is also reported.

Simulation time (ns)	ΔG_{bind} G0 aadalimumab complex (kcal/mol)	ΔG_{bind} G0F adalimumab complex (kcal/mol)	$\Delta\Delta G_{bind\ G0\text{-}G0F}$ (kcal/mol)	ΔG_{bind} G0 Fc complex (kcal/mol)	ΔG_{bind} G0F Fc complex (kcal/mol)	$\Delta\Delta G_{bind\ G0\text{-}G0F}$ (kcal/mol)
0	-714.14	-606.18	-107.96	-661.27	-666.94	5.67
50	-971.59	-525.01	-446.58	-664.19	-622.40	-41.79
100	-624.44	-784.38	159.94	-666.22	-638.90	-27.32
150	-728.62	-756.14	27.52	-704.80	-667.59	-37.21
200	-944.93	-809.17	-135.77	-613.46	-683.046	69.59
250	-772.23	-847.55	75.31	-616.54	-654.47	37.93
300	-661.54	-798.02	136.49	-615.15	-717.50	102.34
350	-894.02	-750.72	-143.30	-554.22	-683.48	129.26
400	-914.26	-752.70	-161.56	-601.94	-690.33	88.38
450	-918.07	-809.37	-108.70	-569.08	-575.40	6.32
500	-896.27	-729.87	-166.40	-654.69	-685.35	30.66
550	-965.43	-797.60	-167.82	-500.79	-680.78	179.99
600	-940.72	-738.64	-202.09	-455.83	-687.24	231.41
650	-949.40	-745.52	-203.88	-720.48	-563.76	-156.72
700	-937.75	-824.83	-112.93	-595.42	-648.34	52.92
750	-760.93	-780.18	19.25	-550.53	-718.00	168.47
800	-770.13	-873.46	103.32	-549.27	-665.94	116.67
850	-857.79	-779.89	-77.90	-533.08	-673.04	139.96
900	-906.38	-858.00	-48.38	-645.84	-642.00	-3.84
950	-790.36	-698.11	-92.25	-512.80	-813.60	300.81
1000	-827.18	-679.38	-147.80	-541.13	-702.02	160.90

Figure 19: ΔG_{bind} free energy plot of G0 and G0F complexes vs simulation time. (A) The energetic profiles of G0 (in blue) and G0F (in orange) adalimumab::FcγRIIIa complexes suggest that the afucosylated one is more energetically favored than the fucosylated complex, since the lower ΔG_{bind} values. Both the complexes reach an energetic plateau between 350-700 ns and, considering $\Delta\Delta G_{bind}$ in this time-frame it spans from about -108 kcal/mol to -203 kcal/mol, suggesting a high discrepancy among the two systems. (B) The energetic profiles of G0 (in blue) and G0F (in orange) Fc::FcγRIIIa complexes suggest that the two systems are highly comparable and only slight differences can be observed.

5.7 Discussion

The second part of this PhD thesis has been focused on the *in silico* elucidation of recognition mechanisms that drive the triggering of FcγRIIIa by differently glycosylated IgG1. Specifically, using adalimumab as a case study and basing on data obtained from the first part of the project, four MD simulations 1 μs long were carried out in explicit solvent. First, two complexes composed of the whole adalimumab molecule, in both afucosylated and fucosylated forms, bound to the receptor were simulated. Second, two crystalized complexes formed by the glycosylated Fc part of a generic IgG1 and the FcγRIIIa were investigated to further confirm preliminary hypothesis.

The first consideration is that the conformational difference previously observed for G0 and G0F antibodies leads to a different receptor binding mode.

In fact, according to MD data shown above, the formation of the complex between the receptor and the afucosylated antibody is more favored than the complex with the fucosylated mAb. This was expected from previous analyses, by which the fucosylated mAb is blocked in a conformation apparently not suitable for the receptor, and from what is reported in literature by experimental data. The analysis of geometric parameters, like RMSD and RMSF, showed that the geometric profiles of the afucosylated adalimumab are more stable than those of fucosylated form, thus suggesting completely different behaviors in terms of conformational stability and fluctuation. The geometric parameters analysis of antibodies single domains identified the hinge region and the corresponding Fab located near to the receptor as responsible for the higher G0F mAb mobility with respect to G0 one. By structural analysis the movement that antibodies make during the MD was described. Essentially, in both complexes most of conformational exploration is localized in Fab portions, but in G0F complex, these changes in Fab orientations are definitely more marked. In fact, by cluster analysis two main conformations were isolated for each antibody and whereas in G0 system the structures are very similar, in the G0F form there is a clear distinction among them. In particular, the difference observed in G0F mAb is mainly related to the Fab portion positioned near to the receptor, that coordinated and influenced by the corresponding hinge region, explores a huge conformational space, even though it never interacts with the FcγRIIIa.

Concerning the interaction network with FcγRIIIa, the H-bonds analysis highlighted that there is a clear discrepancy among the two systems, especially in terms of protein-protein interactions between the antibody and the receptor. Specifically, the number of interactions observed for G0 complex is extremely higher than that observed for G0F one, suggesting that the conformation

adopted by G0 mAb is more able to bind the receptor than the G0F antibody. Furthermore, the G0 antibody residues involved in these bonds are mostly those reported by experimental data as key amino acids for the receptor activation, while in G0F complex, besides the low number of interactions, only two of the identified residues are recognized as critical. In addition, in G0 complex the Fab positioned in proximity of receptor is involved in the interaction, suggesting that it can have a role in recognition, or at least that a specific orientation of this domain is required to form the complex. The involvement of Fab domains in receptor binding has been already experimentally demonstrated by Yogo and colleagues[134], who recently published a work investigating the IgG1::FcγRIIIa recognition *via* hydrogen/deuterium exchange mass spectrometry. Authors demonstrated that Fab domains participate to the interaction enhancing the canonical receptor triggering mediated by Fc, thus providing experimental data supporting our findings. Concerning the G0F complex, the Fab near to the receptor does not interact with it and is always positioned far away. This different behavior is likely due to the conformation reached by the antibodies in the "*apo*" form during simulations, where the presence of fucose introduces conformational constraints that influence the dynamics of the molecule and that cannot be resolved or compensated by the presence of the receptor. Moreover, since a local asymmetry has been previously recognized for both adalimumab forms, we hypothesize that the role of two antibody halves could be inverted during time, but an extensive set of simulations would be required to definitely confirm this finding.

The analysis of glycan behavior pointed out that they act as structural modulators of antibodies and that the presence of fucose can indirectly affect the receptor recognition. In fact, by comparing these data with the previous one, both G0 and G0F sugars lose some interactions with the antibody, probably to facilitate receptor accommodation. However, in G0F antibody, glycans make H-bonds with some of the residues critical for receptor recognition, not allowing their interaction with the receptor and affecting their orientation. Moreover, both G0 and G0F sugars do not directly interact with receptor glycans and make only poor interactions with the receptor residues. This suggests that sugars definitely exert an effect on the antibody::receptor interaction, but they are not the main drivers of the receptor triggering. This hypothesis was confirmed also by the solvent analysis that predicted the presence of water in the interface among glycans and suggested that there are not direct carbohydrate-carbohydrate interactions.

Our findings are in contrast to what observed by Ferrara and colleagues[57] who solved the X-ray structure of a fucosylated IgG1 Fc portion in complex with FcγRIIIa. Authors proposed as cause of the reduced binding affinity of the G0F complex with respect to the afucosylated one, a specific steric

hindrance effect mediated by fucose in preventing a NAG-NAG interaction among antibody and receptor glycans. This effect was not observed in our simulations, that evidenced the importance of considering the whole molecular structure to describe molecular mechanisms.

However, to further confirm our findings, MD simulations of the complex solved by Ferrara *et al.*[57], in its fucosylated and afucosylated forms, were carried out. As a result, not so relevant differences were recognized among the two complexes, neither in the interaction with the receptor nor in the conformational behavior of the proteins. Also in this case, no carbohydrate-carbohydrate interactions were detected, suggesting that the differences in binding affinity of fucosylated and afucosylated antibodies to FcγRIIIa is not directly due to the fucose.

As further confirmation of data shown above, the ΔG_{bind} free energy was computed for 21 minimized conformations extracted from MD trajectories. This calculation showed that the energetic profile of G0 adalimumab complex reaches energy values more negative than those observed for the G0F one, meaning that the afucosylated system is more energetically favored than the fucosylated one. However, by comparing ΔG_{bind} free energy values of adalimumab complexes with the energetic profiles obtained for the Fc complexes, similar behaviors can be recognized for both fucosylated forms. This suggests that even in presence of Fab domains, that are potentially involved in the interaction and have an active role in stabilizing the complex, the fucose exerts a negative effect on the receptor binding. The G0F adalimumab complex, in fact, shows energy values comparable to those detected for the Fc complex, that of course is less physiologically stable. On the other hand, if we compare the ΔG_{bind} free energy profiles of afucosylated complexes a huge decrease in energy values can be detected for the adalimumab::FcγRIIIa complex, thus suggesting that in presence of Fab domains and in absence of fucose the binding is more favored and the interaction is stabilized.

In conclusion, the second part of this thesis confirmed what hypothesized before: the difference in binding mode of the FcγRIIIa to fucosylated and afucosylated IgG1 is essentially due to a different conformation of antibodies induced by the presence of fucose. In the fucosylated mAb this conformation is not suitable to perfectly bind the receptor, since antibody residues considered critical for the interaction are far away from the FcγRIIIa and partially involved in interactions with antibody glycans. Moreover, the presence of fucose inhibits the involvement of Fab portions in receptor recruiting, causing a decrease in complex stability.

Thus, according to our data, glycans act as allosteric modulators of the antibody exerting their effect on the whole antibody molecule since, in absence of Fab portions, this effect cannot be detected and both the G0 and the G0F Fc parts show a very similar conformational behavior.

Chapter 6

Conclusions

Monoclonal antibodies are the most relevant class of biopharmaceutical products on the market. Because of their high structural and functional complexity, investigating their molecular mechanisms is considered a big challenge. Moreover, their structural characterization is a key aspect in the pharmaceutical development since post-translational modifications can have a huge impact on the final product quality and on its efficacy as well as the safety of the patient.

On this basis, this PhD thesis was focused on the structural characterization and prediction of the role of N-glycosylation in IgG1 in regulating the activation of FcγRIIIa, and consequently the ADCC response, by using *in silico* approaches. Starting from published experimental data and by using adalimumab as a model antibody, we tried to elucidate which is the role of fucose in regulating IgG1 Fc effector functions.

Globally, our data suggests that:

1) N-glycans act as structural modulators of antibodies and have an effect on their conformational behavior. The presence or the absence of glycans can lead to different antibody conformations, that may influence its functions. Particularly the presence of fucose can introduce some structural constraints that force the antibody in a state not suitable for receptor triggering, where the movement of one Fab positively correlates with that of Fc. On the other hand, the lack of fucose allows the three antibody parts to move independently and to better fit to the receptor;
2) This finding was confirmed by MD simulations of afucosylated and fucosylated adalimumab forms in complex with FcγRIIIa. As a result, the afucosylated complex is more favored from both a geometrical and an energetical point of view than the fucosylated one, thus giving a structural explanation of what experimentally observed. Moreover, most of G0 mAb residues involved in the interaction with the receptor are consistent with those identified by published mutagenesis analysis, thus confirming that in the fucosylated complex the different orientation of these amino acids leads to a lower interaction with the receptor;
3) MD simulations performed on Fc::FcγRIIIa complexes pointed out that without the presence of Fab portions, there is not a conformational effect of sugars on the antibody or on the complex formation, thus highlighting that glycans do not exert a direct role in receptor triggering, but act more as allosteric modulators of the entire antibody, driving conformational changes in the molecule and making it suitable or not for receptor accommodation.

Furthermore, in this work, other two novel structural and functional aspects were elucidated. First, there is a conformational asymmetry in antibodies, especially related to Fab portions, that could be in part due to their intrinsic molecular properties and in part to the glycosylation pattern. Second, by investigating the FcγRIIIa recognition, we observed that not only hinge region and Fc portion participate in the interaction with the receptor, but also Fab arms can play a role in the recruiting, as already demonstrated by a recent published work based on experimental evaluations[134]. This means that Fab domains give a significative contribution to the complex formation and that their conformational behavior essentially depends on the presence of fucose. Based on this, next steps of this project will be focused on deeply investigating these aspects combining further *in silico* analysis and experimental procedures.

In summary, this thesis can be allocated in the wide context of pharmaceutical development and represents a starting point for improving the knowledge-base in the frame of antibody conformational behavior and the role of glycans in this, shading light on the pharmacological effects that differently glycosylated mAbs can exert and helping pharmaceutical companies to further evaluate this aspect.

Bibliography

1. MarketWatch. Monoclonal Antibodies Market demand to grow at a CAGR of 8.5% during 2019-2025 - MarketWatch. Available at: https://www.marketwatch.com/press-release/monoclonal-antibodies-market-demand-to-grow-at-a-cagr-of-85-during-2019-2025-2019-09-10. (Accessed: 16th April 2020)
2. Lu, R. M. *et al.* Development of therapeutic antibodies for the treatment of diseases. *Journal of Biomedical Science* **27**, 1–30 (2020).
3. Kaplon, H., Muralidharan, M., Schneider, Z. & Reichert, J. M. Antibodies to watch in 2020. *MAbs* **12**, (2020).
4. Mahmuda, A. *et al.* Monoclonal antibodies: A review of therapeutic applications and future prospects. *Tropical Journal of Pharmaceutical Research* **16**, 713–722 (2017).
5. Ansar, W. & Ghosh, S. Monoclonal Antibodies: A Tool in Clinical Research. *Indian J. Clin. Med.* **4**, IJCM.S11968 (2013).
6. Li, J. & Zhu, Z. Research and development of next generation of antibody-based therapeutics. *Acta Pharmacologica Sinica* **31**, 1198–1207 (2010).
7. Reff, M. E., Hariharan, K. & Braslawsky, G. Future of monoclonal antibodies in the treatment of hematologic malignancies. *Cancer Control* **9**, 152–66 (2002).
8. Singh, Surjit; Tank, Nitish K.; Dwiwedi, Pradeep; Charan, Jaykaran; Kaur, Rimplejeet; Sidhu, Preeti; Chugh, V. K. Monoclonal antibodies. A review. *Current Clinical Pharmacology* **13**, 85–99 (2018).
9. Scheid, J. F. *et al.* Broad diversity of neutralizing antibodies isolated from memory B cells in HIV-infected individuals. *Nature* **458**, 636–640 (2009).
10. Steinitz, M., Klein, G., Koskimies, S. & Makel, O. EB virus-induced B lymphocyte cell lines producing specific antibody. *Nature* **269**, 420–422 (1977).
11. Traggiai, E. *et al.* An efficient method to make human monoclonal antibodies from memory B cells: Potent neutralization of SARS coronavirus. *Nat. Med.* **10**, 871–875 (2004).
12. Lai, T., Yang, Y. & Ng, S. K. Advances in mammalian cell line development technologies for recombinant protein production. *Pharmaceuticals* **6**, 579–603 (2013).
13. Goh, J. B. & Ng, S. K. Impact of host cell line choice on glycan profile. *Crit. Rev. Biotechnol.* **38**, 851–867 (2018).
14. Hacker, D. L., De Jesus, M. & Wurm, F. M. 25 years of recombinant proteins from reactor-grown cells - Where do we go from here? *Biotechnology Advances* **27**, 1023–1027 (2009).
15. Kim, J. Y., Kim, Y. G. & Lee, G. M. CHO cells in biotechnology for production of recombinant proteins: Current state and further potential. *Applied Microbiology and Biotechnology* **93**, 917–930 (2012).
16. Butler, M. & Spearman, M. The choice of mammalian cell host and possibilities for glycosylation engineering. *Current Opinion in Biotechnology* **30**, 107–112 (2014).
17. Vidarsson, G., Dekkers, G. & Rispens, T. IgG subclasses and allotypes: From structure to effector functions. *Front. Immunol.* **5**, (2014).
18. Schur, P. H. IgG subclasses. A historical perspective. *Monographs in allergy* **23**, 1–11 (1988).
19. Ferrante, A., Beard, L. J. & Feldman, R. G. IgG subclass distribution of antibodies to bacteria and viral antigens. *Pediatr. Infect. Dis. J.* **9**, S16–S24 (1990).
20. Siber, G. R., Schur, P. H., Aisenberg, A. C., Weitzman, S. A. & Schiffman, G. Correlation between Serum IgG-2 Concentrations and the Antibody Response to Bacterial Polysaccharide Antigens. *N. Engl. J. Med.* **303**, 178–182 (1980).
21. Barrett, D. J. & Ayoub, E. M. IgG2 subclass restriction of antibody to pneumococcal polysaccharides. *Clin. Exp. Immunol.* **63**, 127–34 (1986).
22. Schauer, U. *et al.* Levels of antibodies specific to tetanus toxoid, Haemophilus influenzae type b, and pneumococcal capsular polysaccharide in healthy children and adults. *Clin. Diagn. Lab. Immunol.* **10**, 202–207 (2003).
23. Damelang, T., Rogerson, S. J., Kent, S. J. & Chung, A. W. Role of IgG3 in Infectious Diseases. *Trends in Immunology* **40**, 197–211 (2019).
24. Nirula, A., Glaser, S. M., Kalled, S. L. & Taylora, F. R. What is IgG4? A review of the biology of a unique

immunoglobulin subtype. *Curr. Opin. Rheumatol.* **23**, 119–124 (2011).
25. Hammarström, L. *et al.* Subclass restriction pattern of antigen-specific antibodies in donors with defective expression of IgG or IgA subclass heavy chain constant region genes. *Clin. Immunol. Immunopathol.* **45**, 461–470 (1987).
26. Brouwers, H. A. A. *et al.* Maternal antibodies against fetal blood group antigens A or B: Lytic activity of IgG subclasses in monocyte-driven cytotoxicity and correlation with ABO haemolytic disease of the newborn. *Br. J. Haematol.* **70**, 465–469 (1988).
27. Mawas, F., Wiener, E., Williamson, L. M. & Rodeck, C. H. Immunoglobulin G subclasses of anti-human platelet antigen la in maternal sera: relation to the severity of neonatal alloimmune thrombocytopenia. *Eur. J. Haematol.* **59**, 287–292 (2009).
28. Pollock, J. M. & Bowman, J. M. Anti-Rh(D) IgG Subclasses and Severity of Rh Hemolytic Disease of the Newborn. *Vox Sang.* **59**, 176–179 (1990).
29. Van De Veen, W., Ubeccel Akdis, M. & Davos, P. Role of IgG 4 in IgE-mediated allergic responses. (2016). doi:10.1016/j.jaci.2016.07.022
30. Salfeld, J. G. Isotype selection in antibody engineering. *Nature Biotechnology* **25**, 1369–1372 (2007).
31. Edelman, G. M. *et al.* The covalent structure of an entire gammaG immunoglobulin molecule. *Proc. Natl. Acad. Sci. U. S. A.* **63**, 78–85 (1969).
32. Varki, A. *et al.* Symbol nomenclature for graphical representations of glycans. *Glycobiology* **25**, 1323–1324 (2015).
33. Potter, M. Structural correlates of immunoglobulin diversity. *Surv. Immunol. Res.* **2**, 27–42 (1983).
34. Wu, T. Te, Johnson, G. & Kabat, E. A. Length distribution of CDRH3 in antibodies. *Proteins: Structure, Function, and Bioinformatics* **16**, 1–7 (1993).
35. Kabat, E. A., Wu, T. T. & Bilofsky, H. Variable region genes for the immunoglobulin framework are assembled from small segments of DNA - a hypothesis. *Proc. Natl. Acad. Sci. U. S. A.* **75**, 2429–2433 (1978).
36. Nimmerjahn, F. & Ravetch, J. V. Fcγ receptors as regulators of immune responses. *Nature Reviews Immunology* **8**, 34–47 (2008).
37. Meyer, S., Leusen, J. H. W. & Boross, P. Regulation of complement and modulation of its activity in monoclonal antibody therapy of cancer. *mAbs* **6**, 1133–1144 (2014).
38. Wang, X., Mathieu, M. & Brezski, R. J. IgG Fc engineering to modulate antibody effector functions. *Protein Cell* **9**, 63–73 (2018).
39. Tay, M. Z., Wiehe, K. & Pollara, J. Antibody dependent cellular phagocytosis in antiviral immune responses. *Front. Immunol.* **10**, 332 (2019).
40. Clynes, R. A., Towers, T. L., Presta, L. G. & Ravetch, J. V. Inhibitory Fc receptors modulate in vivo cytoxicity against tumor targets. *Nat. Med.* **6**, 443–446 (2000).
41. De Haij, S. *et al.* In vivo cytotoxicity of type I CD20 antibodies critically depends on Fc receptor ITAM signaling. *Cancer Res.* **70**, 3209–3217 (2010).
42. Chin, K., Chand, V. K. & Nuyten, D. S. A. Avelumab: clinical trial innovation and collaboration to advance anti-PD-L1 immunotherapy. *Annals of oncology : official journal of the European Society for Medical Oncology* **28**, 1658–1666 (2017).
43. Vivier, E. *et al.* Innate or adaptive immunity? The example of natural killer cells. *Science* **331**, 44–49 (2011).
44. Mellor, J. D., Brown, M. P., Irving, H. R., Zalcberg, J. R. & Dobrovic, A. A critical review of the role of Fc gamma receptor polymorphisms in the response to monoclonal antibodies in cancer. *Journal of Hematology and Oncology* **6**, 1 (2013).
45. Taylor, R. P. & Lindorfer, M. A. Cytotoxic mechanisms of immunotherapy: Harnessing complement in the action of anti-tumor monoclonal antibodies. *Seminars in Immunology* **28**, 309–316 (2016).
46. Melis, J. P. M. *et al.* Complement in therapy and disease. Regulating the complement system with antibody-based therapeutics. *Molecular Immunology* **67**, 117–130 (2015).
47. Schmidt, R. E. & Gessner, J. E. Fc receptors and their interaction with complement in autoimmunity. *Immunology Letters* **100**, 56–67 (2005).

48. Kuo, T. T. *et al.* Neonatal Fc receptor: From immunity to therapeutics. *J. Clin. Immunol.* **30**, 777–789 (2010).
49. Pincetic, A. *et al.* Type I and type II Fc receptors regulate innate and adaptive immunity. *Nat. Immunol.* **15**, 707–716 (2014).
50. Ben Mkaddem, S., Benhamou, M. & Monteiro, R. C. Understanding Fc Receptor Involvement in Inflammatory Diseases: From Mechanisms to New Therapeutic Tools. *Front. Immunol.* **10**, 811 (2019).
51. Bournazos, S., Woof, J. M., Hart, S. P. & Dransfield, I. Functional and clinical consequences of Fc receptor polymorphic and copy number variants. *Clin. Exp. Immunol.* **157**, 244–254 (2009).
52. Sondermann, P., Pincetic, A., Maamary, J., Lammens, K. & Ravetch, J. V. General mechanism for modulating immunoglobulin effector function. *Proc. Natl. Acad. Sci. U. S. A.* **110**, 9868–9872 (2013).
53. Sondermann, P., Huber, R., Oosthulzen, V. & Jacob, U. The 3.2-Å crystal structure of the human IgG1 Fc fragment-FcγRIII complex. *Nature* **406**, 267–273 (2000).
54. Mimoto, F. *et al.* Crystal structure of a novel asymmetrically engineered Fc variant with improved affinity for FcγRs. *Mol. Immunol.* **58**, 132–138 (2014).
55. Mimoto, F. *et al.* Engineered antibody Fc variant with selectively enhanced FcγRIIb binding over both FcγRIIa(R131) and FcγRIIa(H131). *Protein Eng. Des. Sel.* **26**, 589–98 (2013).
56. Kiyoshi, M. *et al.* Structural basis for binding of human IgG1 to its high-affinity human receptor FcγRI. *Nat. Commun.* **6**, (2015).
57. Ferrara, C. *et al.* Unique carbohydrate-carbohydrate interactions are required for high affinity binding between FcgammaRIII and antibodies lacking core fucose. *Proc. Natl. Acad. Sci.* **108**, 12669–12674 (2011).
58. Woof, J. M. & Burton, D. R. Human antibody-Fc receptor interactions illuminated by crystal structures. *Nature Reviews Immunology* **4**, 89–99 (2004).
59. Lu, J. *et al.* Structure of FcγRI in complex with Fc reveals the importance of glycan recognition for high-affinity gG binding. *Proc. Natl. Acad. Sci. U. S. A.* **112**, 833–838 (2015).
60. Bolland, S. & Ravetch, J. V. Inhibitory pathways triggered by itim-containing receptors. *Adv. Immunol.* **72**, 149–177 (1999).
61. Da Silva, F. P. *et al.* CD16 promotes Escherichia coli sepsis through an FcRγ inhibitory pathway that prevents phagocytosis and facilitates inflammation. *Nat. Med.* **13**, 1368–1374 (2007).
62. Pasquier, B. *et al.* Identification of FcαRI as an inhibitory receptor that controls inflammation: Dual role of FcRγ ITAM. *Immunity* **22**, 31–42 (2005).
63. Kanamaru, Y. *et al.* Inhibitory ITAM Signaling by FcαRI-FcRγ Chain Controls Multiple Activating Responses and Prevents Renal Inflammation. *J. Immunol.* **180**, 2669–2678 (2008).
64. Aloulou, M. *et al.* IgG1 and IVIg induce inhibitory ITAM signaling through FcγRIII controlling inflammatory responses. *Blood* **119**, 3084–3096 (2012).
65. Mkaddem, S. Ben *et al.* Shifting FcγRIIA-ITAM from activation to inhibitory configuration ameliorates arthritis. *J. Clin. Invest.* **124**, 3945–3959 (2014).
66. Iborra, S. *et al.* Leishmania Uses Mincle to Target an Inhibitory ITAM Signaling Pathway in Dendritic Cells that Dampens Adaptive Immunity to Infection. *Immunity* **45**, 788–801 (2016).
67. Getahun, A. & Cambier, J. C. Of ITIMs, ITAMs, and ITAMis: Revisiting immunoglobulin Fc receptor signaling. *Immunological Reviews* **268**, 66–73 (2015).
68. Blank, U., Launay, P., Benhamou, M. & Monteiro, R. C. Inhibitory ITAMs as novel regulators of immunity. *Immunological Reviews* **232**, 59–71 (2009).
69. Hossler, P., Khattak, S. F. & Li, Z. J. Optimal and consistent protein glycosylation in mammalian cell culture. *Glycobiology* **19**, 936–949 (2009).
70. Raju, T. S. Terminal sugars of Fc glycans influence antibody effector functions of IgGs. *Curr. Opin. Immunol.* **20**, 471–478 (2008).
71. Jefferis, R. Glycosylation as a strategy to improve antibody-based therapeutics. *Nat. Rev. Drug Discov.* **8**, 226–234 (2009).
72. Hart, G. Glycosylation. *Curr. Opin. Cell Biol.* **4**, 1017–1023 (1992).
73. Jefferis, R. Glycosylation of recombinant antibody therapeutics. *Biotechnology Progress* **21**, 11–16

(2005).
74. Shantha Raju, T. Glycosylation variations with expression systems and their impact on biological activity of therapeutic immunoglobulins. *Bioprocess int* **1**, 44–53 (2003).
75. Yoo, E. M., Chintalacharuvu, K. R., Penichet, M. L. & Morrison, S. L. Myeloma expression systems. *Journal of Immunological Methods* **261**, 1–20 (2002).
76. Liu, L. Antibody Glycosylation and Its Impact on the Pharmacokinetics and Pharmacodynamics of Monoclonal Antibodies and Fc-Fusion Proteins. *J Pharm Sci* **104**, 1866–1884 (2015).
77. Kornfeld, R., Keller, J., Baenziger, J. & Kornfeld, S. The structure of the glycopeptide of human gamma G myeloma proteins. *J. Biol. Chem.* **246**, 3259–3268 (1971).
78. Kornfeld, R. & Kornfeld, S. *COMPARATIVE ASPECTS OF GLYCOPROTEIN STRUCTURE*. (1976).
79. Kornfeld, R. & Kornfeld, S. Assembly of Asparagine-Linked Oligosaccharides. *Annu. Rev. Biochem.* **54**, 631–664 (1985).
80. Hayes, J. M. *et al.* Glycosylation and Fc Receptors. *Curr. Top. Microbiol. Immunol.* **382**,
81. Mimura, Y. *et al.* The influence of glycosylation on the thermal stability and effector function expression of human IgG1-Fc: Properties of a series of truncated glycoforms. *Mol. Immunol.* **37**, 697–706 (2000).
82. Zheng, K., Bantog, C. & Bayer, R. The impact of glycosylation on monoclonal antibody conformation and stability. *MAbs* **3**, 568 (2011).
83. Malhotra, R. *et al.* Glycosylation changes of IgG associated with rheumatooid arthritis can activate complement via the mannose-binding protein. *Nat. Med.* **1**, 237–243 (1995).
84. Simister, N. E. Placental transport of immunoglobulin G. in *Vaccine* **21**, 3365–3369 (Elsevier BV, 2003).
85. Kaneko, Y., Nimmerjahn, F. & Ravetch, J. V. Anti-Inflammatory Activity of Immunoglobulin G Resulting from Fc Sialylation. *Science (80-.).* **313**, 670–673 (2006).
86. Rothman, R. J., Perussia, B., Herlyn, D. & Warren, L. Antibody-dependent cytotoxicity mediated by natural killer cells is enhanced by castanospermine-induced alterations of IgG glycosylation. *Mol. Immunol.* **26**, 1113–1123 (1989).
87. Shields, R. L. *et al.* Lack of fucose on human IgG1 N-linked oligosaccharide improves binding to human FcγRIII and antibody-dependent cellular toxicity. *J. Biol. Chem.* **277**, 26733–26740 (2002).
88. Wu, J. *et al.* A novel polymorphism of FcγRIIIa (CD16) alters receptor function and predisposes to autoimmune disease. *J. Clin. Invest.* **100**, 1059–1070 (1997).
89. H R Koene, M Kleijer, J Algra, D Roos, A E von dem Borne, M. de H. Fc gammaRIIIa-158V/F Polymorphism Influences the Binding of IgG by Natural Killer Cell Fc gammaRIIIa, Independently of the Fc gammaRIIIa-48L/R/H Phenotype. *Blood* **90**, 1109–1114 (1997).
90. Shields, R. L. *et al.* High Resolution Mapping of the Binding Site on Human IgG1 for Fc$γ$RI, Fc$γ$RII, Fc$γ$RIII, and FcRn and Design of IgG1 Variants with Improved Binding to the Fc$γ$R. *J. Biol. Chem.* **276**, 6591–6604 (2001).
91. Shinkawa, T. *et al.* The Absence of Fucose but Not the Presence of Galactose or Bisecting N -Acetylglucosamine of Human IgG1 Complex-type Oligosaccharides Shows the Critical Role of Enhancing Antibody-dependent Cellular Cytotoxicity. *J. Biol. Chem.* **278**, 3466–3473 (2003).
92. Li, H. *et al.* Optimization of humanized IgGs in glycoengineered Pichia pastoris. *Nat. Biotechnol.* **24**, 210–215 (2006).
93. Iida, S. *et al.* Nonfucosylated therapeutic IgG1 antibody can evade the inhibitory effect of serum immunoglobulin G on antibody-dependent cellular cytotoxicity through its high binding to FcγRIIIa. *Clin. Cancer Res.* **12**, 2879–2887 (2006).
94. Masuda, K. *et al.* Enhanced binding affinity for FcγRIIIa of fucose-negative antibody is sufficient to induce maximal antibody-dependent cellular cytotoxicity. *Mol. Immunol.* **44**, 3122–3131 (2007).
95. Liu, L. Antibody Glycosylation and Its Impact on the Pharmacokinetics and Pharmacodynamics of Monoclonal Antibodies and Fc-Fusion Proteins. *J. Pharm. Sci.* **104**, 1866–1884 (2015).
96. Pereira, N. A., Chan, K. F., Lin, P. C. & Song, Z. The “less-is-more” in therapeutic antibodies: Afucosylated anti-cancer antibodies with enhanced antibody-dependent cellular cytotoxicity. *mAbs* **10**, 693–711 (2018).

97. Ferrara, C. *et al.* The Carbohydrate at FcRIIIa Asn-162 AN ELEMENT REQUIRED FOR HIGH AFFINITY BINDING TO NON-FUCOSYLATED IgG GLYCOFORMS * EXPERIMENTAL PROCEDURES Downloaded from. *J. Biol. Chem.* **281**, 5032–5036 (2006).
98. Yamaguchi, Y. & Barb, A. W. A Synopsis of Recent Developments Defining How N-glycosylation Impacts Immunoglobulin G Structure and Function. *Glycobiology* **30**, 214–225 (2020).
99. Borrok, M. J., Jung, S. T., Kang, T. H., Monzingo, A. F. & Georgiou, G. Revisiting the role of glycosylation in the structure of human IgG Fc. *ACS Chem. Biol.* **7**, 1596–1602 (2012).
100. Feige, M. J. *et al.* Structure of the Murine Unglycosylated IgG1 Fc Fragment. *J. Mol. Biol.* **391**, 599–608 (2009).
101. Baruah, K. *et al.* Selective deactivation of serum IgG: A general strategy for the enhancement of monoclonal antibody receptor interactions. *J. Mol. Biol.* **420**, 1–7 (2012).
102. Subedi, G. P. P. & Barb, A. W. W. The Structural Role of Antibody N-Glycosylation in Receptor Interactions. *Structure* **23**, 1573–1583 (2015).
103. Davies, A. M., Jefferis, R. & Sutton, B. J. Crystal structure of deglycosylated human IgG4-Fc. *Mol. Immunol.* **62**, 46–53 (2014).
104. Mizushima, T. *et al.* Structural basis for improved efficacy of therapeutic antibodies on defucosylation of their Fc glycans. *Genes to Cells* **16**, 1071–1080 (2011).
105. Falconer, D. J., Subedi, G. P., Marcella, A. M. & Barb, A. W. Antibody Fucosylation Lowers the FcγRIIIa/CD16a Affinity by Limiting the Conformations Sampled by the N162-Glycan. *ACS Chem. Biol.* **13**, 2179–2189 (2018).
106. Sakae, Y. *et al.* Conformational effects of N-glycan core fucosylation of immunoglobulin G Fc region on its interaction with Fcγ receptor IIIa. *Sci. Rep.* **7**, (2017).
107. Brandt, J. P., Patapoff, T. W. & Aragon, S. R. Construction, MD simulation, and hydrodynamic validation of an all-atom model of a monoclonal IgG antibody. *Biophys. J.* **99**, 905–913 (2010).
108. Kortkhonjia, E. *et al.* Probing antibody internal dynamics with fluorescence anisotropy and molecular dynamics simulations. *MAbs* **5**, 306–322 (2013).
109. Harbison, A. M., Brosnan, L. P., Fenlon, K. & Fadda, E. Sequence-to-structure dependence of isolated IgG Fc complex biantennary N-glycans: a molecular dynamics study. *Glycobiology* **29**, 94–103 (2019).
110. *Guidance for Industry Q8(R2) Pharmaceutical Development*. (2009).
111. Yu, L. X. *et al.* Understanding pharmaceutical quality by design. *AAPS Journal* **16**, 771–783 (2014).
112. Alt, N. *et al.* Determination of critical quality attributes for monoclonal antibodies using quality by design principles. *Biologicals* **44**, 291–305 (2016).
113. MOE. Molecular Operating Environment (MOE), 2019.01; Chemical Computing Group ULC, 1010 Sherbrooke St. West, Suite #910, Montreal, QC, Canada, H3A 2R7, 2019. (2019).
114. Hu, S. *et al.* Comparison of the inhibition mechanisms of adalimumab and infliximab in treating tumor necrosis factor α-associated diseases from a molecular view. *J. Biol. Chem.* **288**, 27059–67 (2013).
115. Saphire, E. O. *et al.* Crystal structure of a neutralizing human IGG against HIV-1: a template for vaccine design. *Science* **293**, 1155–1159 (2001).
116. Labute, P. The generalized born/volume integral implicit solvent model: Estimation of the free energy of hydration using London dispersion instead of atomic surface area. *J. Comput. Chem.* **29**, 1693–1698 (2008).
117. McGibbon, R. T. *et al.* MDTraj: A Modern Open Library for the Analysis of Molecular Dynamics Trajectories. *Biophys. J.* **109**, 1528–1532 (2015).
118. Case, D. A. et al. AMBER 10. (2008).
119. Barker, J. A. & Watts, R. O. Monte carlo studies of the dielectric properties of water-like models. *Mol. Phys.* **26**, 789–792 (1973).
120. Watts, R. O. Monte carlo studies of liquid water. *Mol. Phys.* **28**, 1069–1083 (1974).
121. Phillips, J. C. *et al.* Scalable molecular dynamics with NAMD. *J. Comput. Chem.* **26**, 1781–1802 (2005).
122. Martyna, G. J., Tobias, D. J. & Klein, M. L. Constant pressure molecular dynamics algorithms. *J. Chem. Phys.* **101**, 4177–4189 (1994).
123. Feller, S. E., Zhang, Y., Pastor, R. W. & Brooks, B. R. Constant pressure molecular dynamics simulation:

The Langevin piston method. *J. Chem. Phys.* **103**, 4613–4621 (1995).
124. Van Der Spoel, D. *et al.* GROMACS: Fast, flexible, and free. *J. Comput. Chem.* **26**, 1701–1718 (2005).
125. Kirschner, K. N. *et al.* GLYCAM06: A generalizable biomolecular force field. carbohydrates. *J. Comput. Chem.* **29**, 622–655 (2008).
126. Gerber, P. R. & Müller, K. MAB, a generally applicable molecular force field for structure modelling in medicinal chemistry. *J. Comput. Aided. Mol. Des.* **9**, 251–268 (1995).
127. Erbel, P. J. A. *et al.* Effects of the N-linked glycans on the 3D structure of the free α- subunit of human chorionic gonadotropin. *Biochemistry* **39**, 6012–6021 (2000).
128. Ferrara, C., Stuart, F., Sondermann, P., Brünker, P. & Umaña, P. The carbohydrate at FcγRIIIa Asn-162: An element required for high affinity binding to non-fucosylated IgG glycoforms. *J. Biol. Chem.* **281**, 5032–5036 (2006).
129. Zeck, A., Pohlentz, G., Schlothauer, T., Peter-Katalinić, J. & Regula, J. T. Cell type-specific and site directed N-glycosylation pattern of Fc RIIIa. *J. Proteome Res.* **10**, 3031–3039 (2011).
130. Shields, R. L. *et al.* High Resolution Mapping of the Binding Site on Human IgG1 for FcγRI, FcγRII, FcγRIII, and FcRn and Design of IgG1 Variants with Improved Binding to the FcγR. *J. Biol. Chem.* **276**, 6591–6604 (2001).
131. Jean-Pierre Hansen, I. R. M. *Theory of Simple Liquids: with Applications to Soft Matter*. (Elsevier, 2006).
132. Beglov, D. & Roux, B. An integral equation to describe the solvation of polar molecules in liquid water. *J. Phys. Chem. B* **101**, 7821–7826 (1997).
133. Kovalenko, A. & Hirata, F. Self-consistent description of a metal-water interface by the Kohn-Sham density functional theory and the three-dimensional reference interaction site model. *J. Chem. Phys.* **110**, 10095–10112 (1999).
134. Yogo, R. *et al.* The Fab portion of immunoglobulin G contributes to its binding to Fcγ receptor III. *Sci. Rep.* **9**, 11957 (2019).